# UNIVERSITÀ DEGLI STUDI DI MILANO

*DEPARTMENT OF PHARMACEUTICAL SCIENCES*

*Doctoral School in Pharmaceutical Sciences*

XXX Cycle

## MASS SPECTROMETRIC STRATEGIES FOR THE STUDY OF PLANT EXTRACTS BIOAVAILABILITY, BIOACTIVITY AND MECHANISMS OF ACTION

SECTOR CHIM/08 – PHARMACEUTICAL CHEMISTRY

Dr. Baron Giovanna

R10906

**Tutor:** Prof. Giancarlo Aldini

**PhD coordinator:** PROF. GIANCARLO ALDINI

**Academic year 2016/2017**

# I

# General introduction

## 1. Natural products as pharmaceutical source

Natural products have been used since ancient times as a pharmacological source. Medicinal plant therapy has been based on empirical findings for thousands of years, leading to the birth of several traditional systems of medicine (e.g. Chinese Traditional Medicine, European Medicine, American Traditional Medicine, etc.). However, since from the end of XVIII century, the concept of finding the single active principle of plants began to have an important role in drug discovery. Moreover, the Industrial Revolution and the development of organic chemistry moved the attention to synthetic compounds in pharmacological therapies. However, there has recently been a shift in the research from the single active principle to a multidrug treatment, which is on-going. The reason could be found in the increased inefficacy and side effects shown by monodrug therapies. These complications have been mainly observed in chronic disease treatments such as antiinflammatory and anticarcenogenic drugs [2]. The inefficacy could also be related to different targets involved in these kinds of diseases. In light of all these considerations, a mixture of several active molecules (*Par. 1 - Appendix*), such as those present in natural products, could lead to more therapeutic effects and improve the health status of patients. These results can be obtained by the synergy of plant extract components. Wagner H. and Ulrich-Merzenich G. [1] described different mechanisms of synergy effects : the “synergistic multi-target effects” (*Figure 1*) which means that the single constituents of the extract affect several targets, thus cooperating in an agonistic way ;

“Pharmacokinetic effects based on improved solubility, resorption rate and enhanced bioavailability” which indicates that some extract components, even if they themselves don’t possess an activity, can act as enhancer of the bioavailability of the other compounds ; the inhibition of bacteria resistance through antibiotics ; and the respective elimination or neutralization of side effects by compounds contained in the extract.

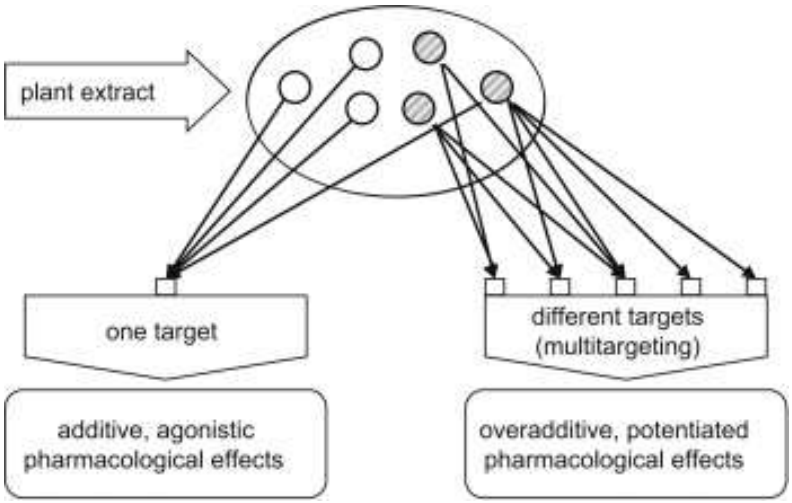


***Figure 1*** *– Synergistic multi-target effects graphic description [1]*

## 2. Importance of phytomedicines mechanisms of action and ADME profiles elucidation

There are new forms of registered plant-derived medicines (phytomedicines) that are not single chemical entities but a complex mixture of active and inert ingredients derived form a crude extraction. However the development of these kinds of products have long been limited since adequate methods to standardize complex plant mixtures as well as to rationalize complex modes of actions were lacking.

The standardization of phytomedicine is important to guarantee a specific concentration range of the bioactive components [3]. Since plant composition is influenced by different factors, such as origin, growth, storage and processing conditions, standardization processes should include all these steps [3]. In this way, a higher level of quality, safety and efficacy of plant based products can be achieved.

Moreover, ADMET studies were limited due to the complexity of the phytomedicines. Hence, most of the information that is usually retrieved for NCE during the drug discovery stage, such as the ADME profile and the mechanism of action, was often not obtained for such complex natural derivatives, limiting their efficacy and application in therapy. Although many answers have now been provided on some bioactive components of plants (*Par. 2 - Appendix*), this issue is still far from established.

In fact only recently, thanks to the advent of novel MS techniques and to the commercial availability of high resolution MS analyzers, the opportunity to determine the ADME profiles of plant extracts and to explore their mode of action has become possible [4]. Advanced analytical techniques play an increasingly important role in the characterization, identification and quantification of plant extract compounds, not only in the context of their natural source but also in biological fluids to study their bioavailability and to discover the active compounds (*Par 3 – Appendix*). Mass spectrometry has become one of the main standard techniques in this field because of the high sensitivity and specificity of the available mass analyzers.

## References

[1] H. Wagner, G. Ulrich-Merzenich, Synergy research: approaching a new generation of phytopharmaceuticals, Phytomedicine 16(2-3) (2009) 97-110.
[2] J.B. Calixto, Efficacy, safety, quality control, marketing and regulatory guidelines for herbal medicines (phytotherapeutic agents), Braz J Med Biol Res 33(2) (2000) 179-89.
[3] V. Garg, V.J. Dhar, A. Sharma, R. Dutt, Facts about standardization of herbal medicine: a review, Zhong Xi Yi Jie He Xue Bao 10(10) (2012) 1077-83.
[4] H. Wu, J. Guo, S. Chen, X. Liu, Y. Zhou, X. Zhang, X. Xu, Recent developments in qualitative and quantitative analysis of phytochemical constituents and their metabolites using liquid chromatography-mass spectrometry, J Pharm Biomed Anal 72 (2013) 267-91.

# II

# Aim of the work

The aim of the present work has been to set-up and apply state of the art MS strategies to better understand the bioavailability, bioatcivity and mechanisms of action of some plant extracts.

In the first part, attention was focused on the set-up and application of MS methods to elucidate biological activities and mechanisms of action of plant extracts and in particular on two studies regarding:

- The elucidation of the ability of different rice extracts to inhibit protein carbonylation by reactive carbonyl species. Based on the knowledge that rice extracts have antioxidant properties, the screening of different types of rice extract was performed to select the most active. A strategy based on a isotopic labelling of the reactive carbonyl species was set up to get a specific mass pattern of the bioactive components present in the most active rice extract selected.

- The evaluation of tannin capacity to precipitate bradykinin, a proline rich peptide involved in the inflammatory cascade. Tannins are widely distributed in plant extracts and their interaction with proline rich proline has long been studied, but the extent of the protein precipitation was only quantified by low precision methods. The ESI-MS method developed and the fast sample preparation aimed at obtaining suitable, accurate and easily comparable results.

Considering that ADME profile of plant extracts is a quite challenging approach, in the second part of this thesis I applied MS strategies based on targeted and untageted analyses to overcome these limits. In particular I studied the ADME profile of two standardized berry extracts in humans and rodents:

- Since there are controversial hypotheses as to the identity of the bioactive components of cranberry used in the prevention of urinary tract infections, the purpose was to set up a HRMS method able to detect known and unknown metabolites in urine. An on target and an off target data analysis methods were used to identify cranberry (*Vaccinium macrocarpon*) components and metabolites in human urine after the assumption of a standardized cranberry extract (Anthocran™) for 7 days. The dosage used was the same as found to be active in human studies in order to replicate real life conditions. Urine fractions were also tested on *C. albicans* adhesion in order to obtain the active fractions and thus a list of possible bioactive components.

- Anthocyanin bioavailability is known to be low, but less is known about the mechanism of absorption. In the present work the research was focused on the evaluation of the role of GLUT transporters (GLUT2 and sGLT1) in anthocyanins absorption. A quantitative HPLC-MS/MS method was set up to determine the absorption of 15 anthocyanins

present in a standardized bilberry extract (Mirtoselect®, 36% anthocyanins) in rats. The investigation was performed under fasted and fed conditions and, in fasting conditions with the co-somministration of glucose. The pharmacokinetic results were associated with docking studies on the two transporters to obtain the final evidence of GLUT transporters involvement.

# III

# Set-up and application of MS methods to elucidate biological activities and mechanisms of action of plant extracts

# Study 1

**Set-up of an isotopic labelling procedure for the characterization of HNE-sequestering agents in natural extracts and its application for the identification of anthocyanidins in black rice giant germ**

**Abstract**

Reactive carbonyl species (RCS) are cytotoxic molecules originating from lipid peroxidation and sugar oxidation. Due to their involvement in the onset and propagation of different oxidative based diseases, RCS are not only considered as biomarkers of oxidative stress, but also as promising drug targets. Natural derivatives represent a very interesting source of potential RCS scavenging molecules but their investigation is limited, mainly by the lack of analytical methods able to screen and identify the bioactive compounds contained in complex matrices.

In the present work, we test the ability of water-soluble rice extracts to act as inhibitors of RCS-induced protein carbonylation. The method was based on ubiquitin as protein model and HNE as RCS. Black rice with giant germ extract was found to be the most active. Identification of bioactive compounds was then carried out by an isotopic signature profile method using the characteristic isotopic ion cluster generated by the mixture of HNE:$^{2}H_{5}$-HNE mixed at a 1:1 stoichiometric ratio. Available databases were used to obtain the structures of the possible bioactive components. The identified compounds were tested as HNE sequestering agent by using a HPLC-UV analysis.

## 1. Introduction

Reactive carbonyl species (RCS) are a class of breakdown products arising from the oxidation of sugars and lipids which can be formed either exogenously, for instance during food processing or cooking, and endogenously, in different physio-pathological conditions. RCS are chemically quite heterogeneous, belonging to different classes, including di-aldehydes, cheto-aldehydes and alfa,beta-unsaturated aldehydes. RCS have the common property of covalently reacting with nucleophilic substrates such as proteins, leading to the formation of covalent adducts which are named ALEs, when RCS originate from lipids, and AGEs when the precursors are from sugars [1]. Since the 1980s, RCS and the corresponding reaction products have been widely used as markers of oxidative stress and several analytical methods for their measurements have been set-up and widely applied. More recently, due to growing literature reporting the involvement of AGEs and ALEs in the onset and propagation of some human diseases, RCS have been considered not only as biomarkers but also as potential drug targets [2, 3]. Among the damaging RCS, HNE is one of the most studied since its discovery by Hermann Esterbauer in 1964 and this due to its abundance, reactivity, and biological effects. The strict link between HNE tissue/blood levels and some human diseases suggested the HNE involvement in this kind of diseases. Several studies based on cell signalling and protein covalent modification have since reported the molecular mechanisms involved in the cytotoxic effect of HNE [4].

Different molecular approaches for reducing the overproduction of HNE and in general of RCS have been reported and summarized in some recent reviews. Among the proposed approaches, the most promising is based on small nucleophilic molecules (RCS sequestering agents) which covalently react with RCS, forming unreactive adducts which are then metabolized and excreted. Several RCS sequestering agents have been proposed such as aminoguanidine, pyridoxamine, hydralazine and carnosine and their protective effects in animal models, as confirmed by several independent labs, further underline the promising therapeutic efficacy of targeting HNE [5]. Carnosine has recently been reported as the most efficient and selective sequestering agent of HNE and its promising activity has been demonstrated in animal models and most recently in obese subjects [6]. However, the application of carnosine as HNE sequestering agent in humans is limited because of its poor bioavailability, due to the presence of serum carnosinases which catalyze the hydrolytic cleavage of the dipeptide. Nowadays there is great interest in the discovery of novel HNE sequestering agents such as carnosine derivatives resistant to carnosinases.

Among others, an interesting discovery approach to identify novel HNE sequestering agents is that based on searching for bioactive compounds in plant extracts. Plants are also subject to RCS stress, in particular mediated by alfa,beta-unsaturated aldehydes, HNE being the most abundant and toxic carbonyl compound formed in stress conditions. Because plants are subject to RCS and protein carbonylation damage [7], they have developed efficient

enzymatic and non-enzymatic detoxification pathways. Hence, besides detoxifying enzymes, it is reasonable to consider the presence of secondary metabolites acting as RCS sequestering agents. Such a hypothesis has been partially confirmed by previous studies which have reported that EGCG and other polyphenols are effective as sequestering agents of HNE [8] and of other RCS, including acrolein and MGO. These results prompted scientists to screen the sequestering activity of different plant metabolites and in particular polyphenol class. As an example, Zhu et al compared 21 natural polyphenols with diverse structural characteristics for their ACR-/HNE-trapping capacities under simulated physiological conditions [9].

To our knowledge, the search for a potential RCS natural sequestering agent has been carried out by using isolated molecules or highly purified extracts and not applying off-target methods involving crude extracts. One reason is the lack of analytical methods able to test the sequestering activity of complex matrices and to fish out the bioactive compounds. As an example, one of the most used methods to evaluate HNE sequestering efficacy is based on a HPLC-UV method for measuring the residual amount of HNE. Such an approach is clearly suitable for testing single molecules and not mixtures, which would interfere with HNE analysis.

We recently reported an in vitro high resolution mass spectrometry (MS) method to test the ability of compounds, mixtures and extracts to trap RCS by measuring their efficacy in inhibiting ubiquitin carbonylation induced by reactive carbonyl species including HNE [10]. Such a method was found

suitable to evaluate the overall quenching activity of extracts but it does not permit the identification of the active components.

In the present paper, we report an LC-ESI-MS method based on an isotopic labelling procedure, which permits the identification of the HNE sequestering agents contained in a crude mixture. Together with the ubiquitin method, it was applied to search for HNE sequestering agents contained in rice extracts prepared from different varieties.

## 2. Materials and Methods

### *2.1 Chemicals*

Formic acid (HCOOH), sodium dihydrogen phosphate ($NaH_2PO_4 \cdot H_2O$), sodium hydrogen phosphate ($Na_2HPO_4 \cdot 2.H_2O$), phenylalanine, gamma-aminobutyric acid, histidine, lyophilized ubiquitin from bovine erythrocytes (BioUltra, ≥98%) and LC–MS grade solvents were purchased from Sigma–Aldrich (Milan, Italy). Peonidin-glucoside, malvidin, peonidin, pelargonidin and tricin-glucoside were from Extrasynthese (Genay, France). Carnosine (beta-alanyl-L-histidine) was a generous gift from Flamma S.p.A (Chignolo d'Isola, Bergamo, Italy). LC-grade $H_2O$ (18 MΩ cm) was prepared with a Milli-Q $H_2O$ purification system (Millipore, Bedford, MA, USA). All other reagents were of analytical grade. 4-Hydroxy-2-nonenal diethylacetal (HNE-DEA) and $^2H_5$-4-Hydroxy-2-nonenal diethylacetal ($^2H_5$-HNE-DEA) were synthesized according to the literature [11] and stored at −20 °C. For each experiment, fresh 4-hydroxy-2-nonenal (HNE) was prepared starting from stored HNE-DEA, which

was evaporated under nitrogen stream and hydrolyzed with 1 mM HCl, pH 3 for 1 h at room temperature to obtain HNE. The concentration of HNE was estimated by measuring the absorbance at λ = 224 nm (molar extinction coefficient = 13,750 $M^{-1} \times cm^{-1}$).

*2.2 Plant material*

Rice (Oryza sativa L.) seeds were stored at 4 °C in a cold room before their use. Rice extract preparation: the seeds were manually dehulled with a wooden rice dehuller and ground to a powder by using a mortar and pestle. The milled rice powders were stored at −80 °C until further use. Rice powders were extracted in water by using a thermomixer (Eppendorf AG, Germany) at 700 rpm for 30 min at 37 °C. After centrifugation, the water extract was collected into a new tube and then dried in a speed vacuum concentrator. Rice extract filtration: for the ubiquitin assay as well as for the isotopic labelling procedure, rice powder extract were the dissolved in water and ultrafiltered by using a 3 kDa ultrafilters so to remove proteins and high MW components. The yield of the low molecular fraction after 3 kDa ultrafiltration was ≈ 10% of the starting sample for all the rice varieties tested.

*2.3 Ubiquitin carbonylation assay*

The effect of rice extracts on HNE-induced protein carbonylation was tested by using the ubiquitin assay as previously reported. Briefly, ubiquitin (10 μM final concentration) chosen as protein target of HNE induced protein adduction, was incubated for 24 h at 37°C in 10 mM phosphate buffer in the presence of 500 μM HNE, together with the rice extracts at increasing concentrations (10, 25 and 50 mg/mL). To remove high molecular components which could interfere with the assay, the rice extracts were filtered by using Amicon YM3 filters (Millipore, Milan, Italy) and the filtered fractions were then used for the assay. After an incubation time of 24 hours, the reactions were stopped by centrifugation using Amicon YM3 filters and the extent of ubiquitin carbonylation was determined by MS intact protein analysis using the microflow automated loop injection procedure as already described [10].

*2.4 Identifying the HNE sequestering agents by an isotopic labelling procedure*

After filtration by using Amicon YM3 filters, the black rice giant germ extract (BRGE) was dissolved in PBS at a final concentration of 50 mg/mL and was then incubated in the absence and in the presence of HNE or deuterium labelled HNE ($^{2}H_{5}$-HNE). After 24 hours the samples were analyzed individually by LC-MS together with a sample prepared by mixing in a 1:1 v:v ratio the samples incubated with HNE and $^{2}H_{5}$-HNE .

Chromatographic separation was performed on a reversed-phase Agilent Zorbax SB-C18 column (150 x 2.1 mm, i.d. 3.5 µm, CPS analitica, Milan, Italy), protected by an Agilent Zorbax guard column, by an UltiMate 3000 system (Dionex) equipped with an autosampler kept at 4°C working at a constant flow rate (200 µL/min). 10 µL of sample was injected into the column and the analytes were eluted with a 45 min multistep gradient of phase A $H_2O$/HCOOH (100/0.1 % v/v) and phase B $CH_3CN$/HCOOH (100/0.1 % v/v): 0-5 min, isocratic of 1% B; 5-15 min, from 1% B to 25% B; 15-30 min, from 25% B to 65% B; 30-32 min, from 65% B to 80% B; 32-36 min, isocratic of 80% B; 36-36.1 min, from 80% B to 1 % B, and then 36.1-45 min of isocratic 1% B. The acquisitions were performed on a LTQ-Orbitrap XL mass spectrometer using an ESI source, acquiring in positive and in negative ion mode. A real-time mass calibration was obtained by using a list of 20 background ions [12]. The source parameters used for the positive mode are: spray voltage 3 kV, capillary temperature 275 °C, capillary voltage 49 V, sheath gas flow 15 units, auxiliary gas flow 5 units, tube lens offset 130 V; for the negative ion mode: spray voltage 3.5 kV, capillary temperature 275 °C, capillary voltage -17 V, sheath gas flow 15 units, auxiliary gas flow 5 units, tube lens offset -100 V. The instrument was set up to work in a data-dependent scan mode to acquire both full MS and MS/MS spectra. Full MS spectra were acquired in profile mode by the FT analyzer in a scan range of 100-1000 m/z, using AGC scan target 5 x $10^5$ and resolution 100000 FWHM at 400 m/z. Tandem mass spectra were acquired by the linear ion trap (LTQ) that was set

up to fragment the 3 most intense ions exceeding 1 x $10^3$ counts. Mass acquisition settings were: centroid mode, AGC scan target 1 x $10^4$, precursor ion isolation width of 2.5 *m/z*, and collision energy (CID) of 30 eV. Dynamic exclusion was enabled to reduce redundant spectra acquisition: 2 repeat counts, 20 sec repeat duration, 30 sec of exclusion duration. Moreover, quaternary and more charged ions were not fragmented. Instrument control and spectra analysis were provided by the software Xcalibur 2.0.7 and Chromeleon Xpress 6.80.

### *2.5 HPLC-UV HNE sequestering assay*

The compounds identified as putative HNE binders with the method described in section 2.4 were purchased as pure standards and tested individually for their HNE sequestering ability. The assay was a three-hour time course experiment at pH 7.4 and 37 °C, in the presence of 50 µM HNE and 1 mM of the tested compound. The residual HNE was measured hourly within a three-hour reaction time by using the HPLC-UV assay described by Vistoli et al. [13] with some minor modifications. Briefly, HNE concentration was determined by a Surveyor HPLC platform (ThermoScientific, Milan, Italy) setting the UV detector at 224 nm. HNE elution was performed in 6 minutes by reverse phase chromatography at 37 °C and flow rate of 0.3 mL/min. A Kinetex column (75 mm x 2.1 mm i.d., 2.6 µm particle size, 100 Å porosity, Phenomenex, Castel Maggiore, Italy) was used as stationary phase, while mobile phase consisted of $H_2O$/$CH_3CN$/ HCOOH, 80/20/0.1 (% v/v/v).

The amount of reacted HNE was calculated by the following formula:

$$reacted\ HNE\ (\%) = \frac{[HNE]_{t0} - [HNE]_{t3}}{[HNE]_{t0}} \times 100$$

$[HNE]_{t0}$ being the concentration of HNE at the beginning of the incubation and $[HNE]_{t3}$ being the concentration of HNE at the end of the incubation. Carnosine, which is a HNE sequestering agent not containing a thiol moiety, was used as positive control to assess the assay reproducibility. To demonstrate that HNE consumption over time is not caused by auto-oxidation, an incubation in pure phosphate buffer was performed as negative control.

The activity of each compound was also given as Carnosine Units (i.e. the ratio between the % of HNE reacted with the compound at a given time and the % of HNE reacted with carnosine in the same span of time).

## 3. Results and discussion

### *3.1 Overview of the approach*

RCS are well known pathogenetic factors of various oxidative based diseases and recently molecular approaches based on their detoxification have been found effective in preventing the onset and progression of some diseases in different animal models. Among the different strategies aimed at detoxifying RCS, that based on small nucleophilic compounds capable of trapping and detoxify RCS is receiving a wide scientific interest. Several synthetic and natural RCS sequestering agents have so far been reported to be effective in

several animal models but for many of these compounds a clinical application is limited due to their promiscuous activity, lack of selectivity and of a suitable bioavailability. Hence, a discovery approach aimed at identifying novel RCS sequestering agents is welcome. In the present paper, we report a discovery approach aimed at identifying RCS sequestering agents in crude mixtures such as natural extracts. Natural sources and, in particular, plant extracts can represent a potential source of RCS sequestering agents, due to the fact that plants are also subject to RCS stress, in particular mediated by $\alpha,\beta$-unsaturated aldehydes, and that they have developed efficient enzymatic and non-enzymatic detoxification pathways. Many non-enzymatic pathways and, in particular, those based on small nucleophilic agents are still unexplored and they would represent an interesting potential source of novel bioactive compounds.

Searching for RCS sequestering agents in a crude mixture is quite a challenging process because they are usually present as minor components in respect to the complex matrix, making their identification and characterization a quite complex analytical challenge. Moreover, a robust method capable of measuring the overall RCS sequestering activity is needed in order to have an analytical tool able to select the most effective plant extracts where the bioactive components might be found.

The approach here reported addresses this challenge and is based on the following steps: i) the RCS sequestering activity of the tested extracts is firstly

assayed by using the ubiquitin assay as previously reported; ii) the most active extracts are then selected for the second step which consists of identifying the sequestering agents by using an innovative isotopic labelling procedure, iii) the RCS sequestering activities of the identified compounds are then validated by using standard compounds and using an HPLC-UV method.

The method proposed has been applied by using HNE as target aldehyde and eight rice extracts as potential sources of RCS sequestering agents. HNE is an α,β-unsaturated aldehyde generated endogenously and exogenously (it is present in food) by the radical-mediated peroxidation of ω-6 polyunsaturated fatty acids. Since its identification, 4-hydroxy-nonenal (HNE), an autoxidation product of unsaturated fats and oils, (at first erroneously described as 4-hydroxy-octenal) [14] has attracted great scientific interest, as demonstrated by the publication of more than 4200 papers since 1980. Compared to other 4-hydroxyalkenals, HNE is the most extensively studied and reviewed as it was the first one discovered [14], it represents the main 4-hydroxyalkenal formed during the autoxidation of unsaturated fatty acids [15], it is highly reactive [16] and numerous biological effects have been demonstrated [15], leading HNE being considered as a promising drug target.

Rice (*Oryza sativa*) is one of the five different cereal grains, which are the most commonly consumed throughout the world and are functionally reported to have antioxidant activity. Bioactive components of rice, have demonstrated antioxidant and anti-inflammatory activities in cells and animals [17, 18]. However, although the direct and indirect antioxidant activity of rice has been

demonstrated in different *in vitro* and also *in vivo* models, no data to our knowledge have so far been reported regarding the efficacy of rice towards protein carbonylation and in particular on its effect to sequester RCS. We then decided to apply the proposed method to test the RCS sequestering capability of rice and for this we evaluated the water extracts of white, brown and black rice.

### 3.2 *HNE sequestering activity of rice extracts*

The overall HNE sequestering activity of eight rice extracts was studied using the ubiquitin assay as previously reported. The method consists of incubating ubiquitin as protein target with HNE at a specific molar ratio and incubation time, thus inducing ubiquitin covalent modification of almost 50%. The protein carbonylation was monitored by measuring the ratio of the areas of two peaks: one at *m/z* 779.61239 relative to the 11-charged peak (named z11) of native ubiquitin and the second at *m/z* 793.80415 corresponding to the 11-charged peak of ubiquitin covalently modified by HNE. *Figure 1* shows the MS spectra of ubiquitin incubated in the absence and in the presence of HNE. When ubiquitin incubated with HNE was spiked with rice extracts, a dose-dependent reduction of the peak area relative at *m/z* 793.80415 was observed. The $IC_{50}$ value, which is the rice extract concentration able to decrease by 50% the level of protein carbonylation, was determined. *Table 1* summarizes the $IC_{50}$ of the tested rice extracts. White rice extract was found less effective in

respect to colored rice and of these, black rice with giant embryo was the most effective and for this reason, it was selected for the next step aimed at identifying the compounds responsible for the sequestering effect of the extract.

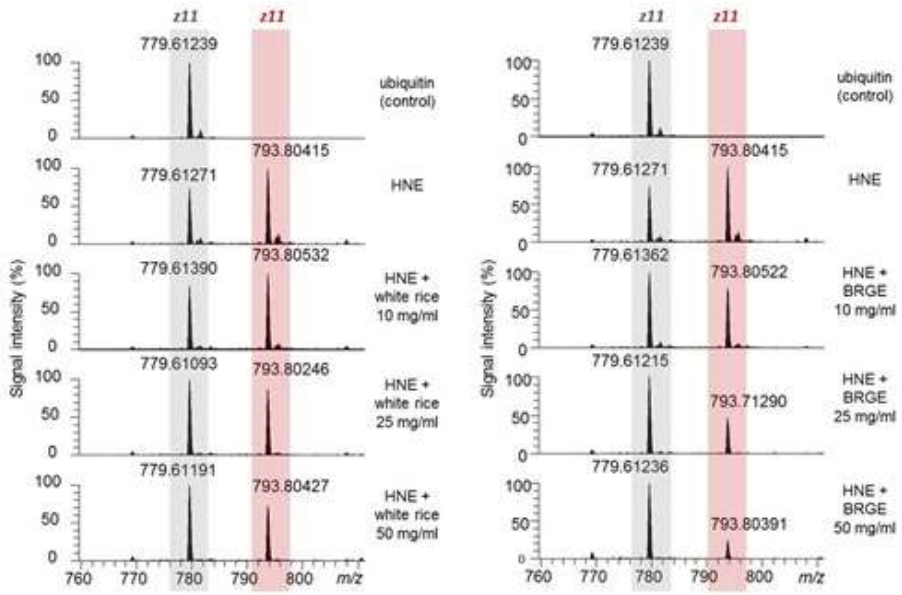


***Figure 1*** *– 11-charged MS peaks of ubiquitibìn incubated in the absence and in the presence of HNE and increasing concentration of two extract: white rice extract (panel on the left) and BRGE (panel on the right).*

| | Average $IC_{50}$ (mg/ml) | St. dev. | CV% |
|---|---|---|---|
| Black rice giant germ (BRGE) | **29.1** | 0.79 | 2.7 |
| Black rice giant germ bran | **30.63** | 3.70 | 12.4 |
| Miryang282 | **39.32** | 2.48 | 6.3 |
| White rice (brown) | **45.46** | 2.29 | 5.0 |
| Black rice | **≈ 52.04** | 8.34 | 16.0 |
| Black rice giant germ 2 (BRGE2) | **≈ 65.92** | 2.13 | 3.2 |
| Red rice | **≈ 71.32** | 4.04 | 5.7 |
| White rice | **≈ 151.0** | 17.7 | 11.7 |

***Table 1*** *- HNE sequestering activity of rice extracts. Activities are reported as $IC_{50}$ which represents the concentration of the tested compound able to reduce by 50% HNE-induced ubiquitin carbonylation.*

### *3.3 Set-up of an isotopic labelling procedure for the identification of HNE-sequestering agents*

An off-target approach based on isotopic signature was then set-up to identify HNE adducted compounds when present in complex matrices such as plant extracts. As summarized in *Figure 2*, the method consists of the following steps: i) the plant extract is spiked with HNE (156.11502 Da) and $^{2}H_{5}$-HNE (161.07590 Da) mixed at the same molar ratio. Compounds which are reactive towards HNE, react with both the isotopes at the same rate forming reaction products which have a specific isotopic pattern, a pair of peaks with a similar intensity spaced by the delta mass corresponding to the incremental mass of $^{2}H_{5}$-HNE in respect to HNE (5.03088 Da ± 10 ppm).

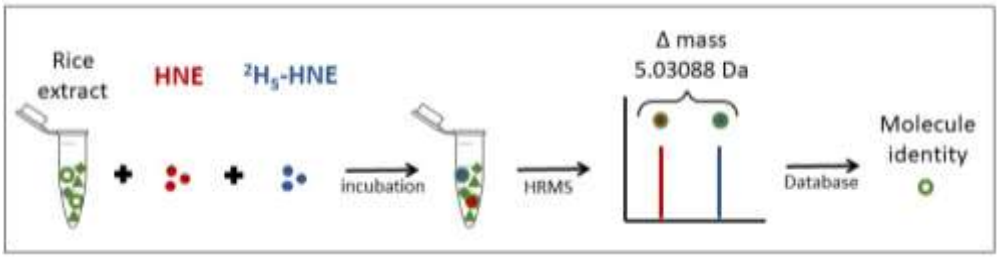


***Figure 2*** *– Graphic representation of the method*

The second step consists of extracting the m/z values relative to the ions of the HNE adducts. This is automatically carried out by Compound Discoverer™ on the basis of the specific isotopic pattern characterized by the two peaks with the same intensity and with a delta mass corresponding to five deuterium atoms. *Figure 3* shows in more detail the specific workflow generated to extract the peak lists from the mass spectra. By setting the "Pattern Tracer" node with a delta mass of 5.03088 Da, a chromatogram of the peak pairs characterized by the set delta mass was obtained. Elution times of the most abundant peaks were then extracted and the m/z values of each peak pair were then obtained by the TIC chromatogram. HNE adducts were then confirmed by manually inspecting the characteristic relative abundance and mass shift of the isotopic pattern.

Further confirmation of the identity of the HNE adducts was given by the Unknown Detector node which checks for the absence of the detected peaks as above reported in non-spiked samples.

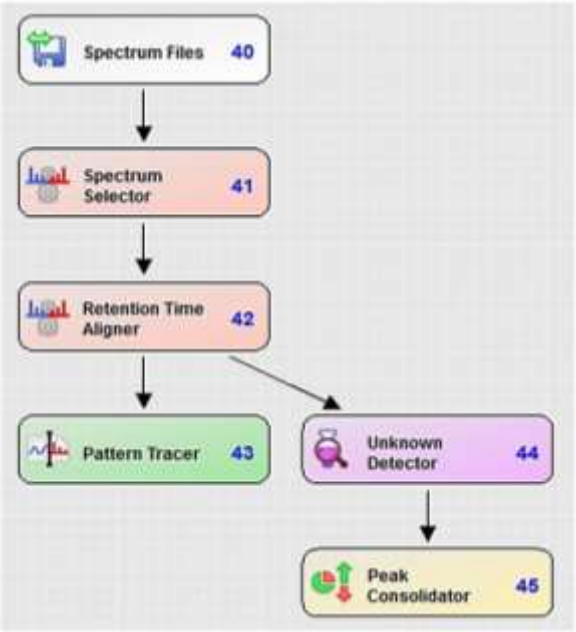


***Figure 3*** *- Workflow's nodes used in Compound Discoverer.*

As a final confirmation of the adduct, the MS/MS spectra of each ion of the isotopic pattern (non deuterated and deuterated ions) were checked in order to verify the overlap between the spectra, thus confirming the same structures and avoiding false positives. The M.W of the bioactive compounds were then calculated by subtracting the M.W. of the HNE molecule (156.11502 Da) from the masses of the identified compounds, and assuming that the detected ions are attributed to the Michael adduct between HNE and the bioactive molecule (as reported for a series of bioactive molecules able to quench HNE [19]).

*3.4 Identification of sequestering components in black rice with giant embryo*

*Figure 4* shows the pattern trace of BRGE incubated in the presence of HNE and $^{2}H_{5}$-HNE mixed at the same molar ratio. Eleven peaks over the threshold intensity were easily identified and their HNE adducted nature was confirmed by manual inspection taking into account the mass shift between the ion pairs, their relative abundances and the overlapping MS/MS fragmentation pattern.

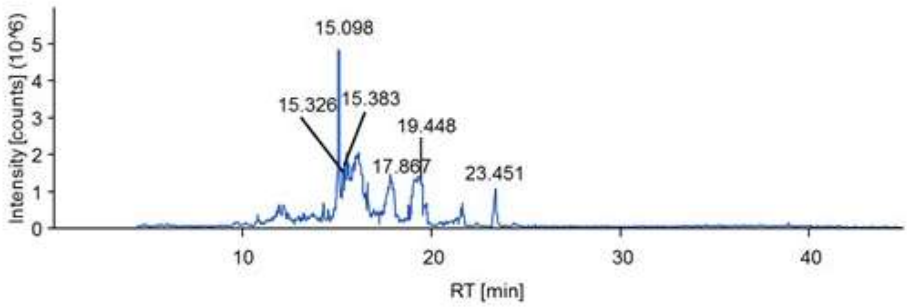


***Figure 2** - The "pattern tracer" chromatogram obtained by Compound Discoverer of BRGE + HNE + $^{2}H_{5}$-HNE (negative ion mode).*

The MW of the sequestering agents were then determined by subtracting the MW of the adducts from that of HNE. The identity of the parent compounds was then assigned by matching the experimental accurate masses and MS/MS fragment ions with those contained in a database of compounds present in plants by using VEGA ZZ software (http://www.vegazz.net/). The database contained 6584 entries. Moreover the research was also performed on ChemSpider. A list of nine compounds with a MW lower than 350 Da was then obtained and listed in *Table 2*.

| Quencher monoisotopic MW | Calculated MW | Δppm | Possible structure |
|---|---|---|---|
| 103.06336 | 103.06333 | 0.304 | γ-Aminobutirric acid |
| 155.06950 | 155.06948 | 0.151 | Histidine |
| 165.07922 | 165.07898 | 1.462 | Phenylalanine |
| 271.06133 | 271.06064 | 2.514 | Pelargonidin |
| 301.07236 | 301.07121 | 3.809 | Peonidin |
| 317.06864 | 317.06612 | 7.923 | Petunidin |
| 317.12164 | 317.12229 | -2.082 | Asp-Ser-Pro |
| 330.07634 | 330.07395 | 7.232 | Tricin |
| 331.08361 | 331.08177 | 5.533 | Malvidin |

***Table 2** - HNE quenchers identified in rice extract BRGE by using the isotopic labelling procedure.*

Five out of 9 compounds were flavonoids, four of them belonging to the anthocyanins class, three compounds were aminoacids, two of them proteogenic, while one a peptide.

### *3.5 HNE sequestering activity*

The commercially available compounds identified as described in section 3.4 were then tested as HNE sequestering agent by using an HPLC-UV test. The test is based on measuring free HNE after incubating the tested compound with HNE. *Table 3* reports the percentage of HNE sequestered by the active compounds identified in BRGE extract. Results are reported either as % of HNE consumption at 1 and 3 hours and as carnosine units at 1 and 3 hours, setting as 1 the value of carnosine activity for both the time points. Histidine,

phenylalanine and aminobutyric acid were the aminoacids identified as having HNE sequestering activity. The reactivity for histidine is due to the imidazole ring as has already been reported, together with the full elucidation of the reaction adduct by NMR. The activity of histidine is increased when bonded to specific aminoacids such as beta-alanine as in the case of carnosine or analogues which are histidine peptides found in mammals. However, no histidine peptides were detected as HNE adducts in the rice extract. The HNE sequestering activity of GABA and phenylalanine, which is more likely due to their primary amino group, is very weak and much lower in respect to that of carnosine (the HNE sequestering activity was under the detection limit as determined by using the HPLC-UV assay). However, even if these two compounds are characterized by a very low potency as HNE sequestering agents in comparison to that of carnosine, they act as HNE sequestering agents in the crude mixture. This apparent contradiction could be explained by considering that they are probably contained in high concentrations in the extract or could be explained by the specific milieu which catalyses their reactions. In other words, it should be considered that the overall sequestering efficacy of compounds in plant extracts is not only due to their intrinsic nucleophilic reactivity but also to their relative concentration as well as to the matrix which could affect the intrinsic activity itself.

A set of polyphenols were then identified as HNE sequestering agents, four anthocyanidins and one flavone (tricin). All the identified compounds were found less effective than carnosine but they were characterized by a well

detectable activity in the HPLC-UV assay. Among these polyphenols, pelargonidin was the most potent, followed by tricin, peonidin and malvidin. The activity of anthocyanindins as HNE sequestering agents which are characteristic components of black rice can also explain the higher overall activity of black rice in respect to white rice and to the other rice varieties.

| | ACTIVITY (CARNOSINE UNITS) | | HNE CONSUMPTION (%) | |
|---|---|---|---|---|
| | 1h | 3h | 1h | 3h |
| **REFERENCE COMPOUNDS** | | | | |
| **BUFFER** | <0.1 | <0.1 | 0.17±0.31 | 0.71±0.67 |
| **CARNOSINE** | 1.00 | 1.00 | 13.78±2.34 | 36.06±4.98 |
| **POLYPHENOLS** | | | | |
| **PEONIDIN-GLUCOSIDE** | 0.29 | 0.20 | 4.00±1.39 | 7.27±2.42 |
| **MALVIDIN (anthocyanidin)** | <0.1 | <0.1 | 1.15±1.10 | 1.87±1.35 |
| **PEONIDIN (anthocyanidin)** | <0.1 | 0.12 | 1.02±0.47 | 4.31±0.92 |
| **PELARGONIDIN (anthocyanidin)** | 0.57 | 0.35 | 7.81±0.49 | 12.60±1.99 |
| **TRICIN-GLUCOSIDE (o-methylated flavone)** | 0.30 | 0.20 | 5.03±2.58 | 8.31±2.91 |
| **AMINOACIDS** | | | | |
| **PHENYLALANINE** | <0.1 | <0.1 | 0.84±0.78 | 1.28±0.47 |
| **GABA** | <0.1 | <0.1 | 0.34±0.59 | 0.35±0.62 |
| **HISTIDINE** | 0.12 | 0.17 | 1.77±1.82 | 6.26±2.69 |

***Table 3** - HNE sequestering activity of standard compounds identified in rice extract BRGE. The activity was determined by measuring free HNE by HPLC-UV analysis*

## 4. Conclusions

In conclusion, we here report a novel approach which permits the screening of plant extracts and in general complex matrices for their overall activity as HNE sequestering agents and the identification of small molecules responsible for the sequestering effects. The approach could be applied to screen a variety of plant extracts with the final aim of identifying novel and potent HNE sequestering agents. The methods can also be easily adapted to other cytotoxic RCS compounds such as MDA, glyoxal and methylglyoxal for which potent sequestering agents are yet to be found.

By using this assay, we also found that rice and in particular black rice is a valuable source of detoxifying agents of HNE which is known to be formed during food digestion and has a role in the promotion of colon cancer (Bastide et al., 2015). HNE derived from food is estimated to be 16 μg $day^{-1}$ as daily exposure in korean food for a 60 Kg korean adult (Surh and Kwon, 2005). Based on the fact that 29.1 mg, corresponding to 673 mg black rice, inhibits 50% of protein carbonylation induced by 78.0 μg $ml^{-1}$ of HNE we can easily conclude that the HNE daily exposure of 16 μg $day^{-1}$ should be easily detoxified by a serving portion of 75 gr.

**Abbreviations:** RCS, reactive carbonyl species; AGEs, advanced glycation end-products; ALEs, advanced lipoxidation end-products; HNE, 4-Hydroxy-2-nonenal; ACR, acrolein; EGCG, epigallocatechin-gallate; MGO, methylglyoxal; MDA, malondialdehyde; BRGE, black rice with giant germ extract; HNE-DEA, 4-Hydroxy-2-nonenal diethylacetal; $^{2}H_{5}$-HNE-DEA, $^{2}H_{5}$-4-Hydroxy-2-nonenal diethylacetal.

## References

[1] G. Vistoli, D. De Maddis, A. Cipak, N. Zarkovic, M. Carini, G. Aldini, Advanced glycoxidation and lipoxidation end products (AGEs and ALEs): an overview of their mechanisms of formation, Free Radic Res 47 Suppl 1 (2013) 3-27.
[2] G. Aldini, I. Dalle-Donne, R.M. Facino, A. Milzani, M. Carini, Intervention strategies to inhibit protein carbonylation by lipoxidation-derived reactive carbonyls, Med Res Rev 27(6) (2007) 817-68.
[3] G. Aldini, I. Dalle-Donne, R. Colombo, R. Maffei Facino, A. Milzani, M. Carini, Lipoxidation-derived reactive carbonyl species as potential drug targets in preventing protein carbonylation and related cellular dysfunction, ChemMedChem 1(10) (2006) 1045-58.
[4] G. Poli, R.J. Schaur, W.G. Siems, G. Leonarduzzi, 4-hydroxynonenal: a membrane lipid oxidation product of medicinal interest, Med Res Rev 28(4) (2008) 569-631.
[5] M. Colzani, D. De Maddis, G. Casali, M. Carini, G. Vistoli, G. Aldini, Reactivity, Selectivity, and Reaction Mechanisms of Aminoguanidine, Hydralazine, Pyridoxamine, and Carnosine as Sequestering Agents of Reactive Carbonyl Species: A Comparative Study, ChemMedChem 11(16) (2016) 1778-89.
[6] G. Aldini, M. Orioli, G. Rossoni, F. Savi, P. Braidotti, G. Vistoli, K.J. Yeum, G. Negrisoli, M. Carini, The carbonyl scavenger carnosine ameliorates dyslipidaemia and renal function in Zucker obese rats, J Cell Mol Med 15(6) (2011) 1339-54.

[7] M.S. Biswas, J. Mano, Reactive Carbonyl Species Activate Caspase-3-Like Protease to Initiate Programmed Cell Death in Plants, Plant Cell Physiol 57(7) (2016) 1432-1442.
[8] G. Beretta, S. Furlanetto, L. Regazzoni, M. Zarrella, R.M. Facino, Quenching of alpha,beta-unsaturated aldehydes by green tea polyphenols: HPLC-ESI-MS/MS studies, J Pharm Biomed Anal 48(3) (2008) 606-11.
[9] Q. Zhu, Z.P. Zheng, K.W. Cheng, J.J. Wu, S. Zhang, Y.S. Tang, K.H. Sze, J. Chen, F. Chen, M. Wang, Natural polyphenols as direct trapping agents of lipid peroxidation-derived acrolein and 4-hydroxy-trans-2-nonenal, Chem Res Toxicol 22(10) (2009) 1721-7.
[10] M. Colzani, A. Criscuolo, D. De Maddis, D. Garzon, K.J. Yeum, G. Vistoli, M. Carini, G. Aldini, A novel high resolution MS approach for the screening of 4-hydroxy-trans-2-nonenal sequestering agents, J Pharm Biomed Anal 91 (2014) 108-18.
[11] M.S. Rees, F.J.G.M. van Kuijk, A.N. Siakotos, B.P. Mundy, Improved synthesis of various isotope labeled 4-hydroxyalkenals and peroxidation intermediates, Synthetic Communications 25(20) (1995) 3225-3236.
[12] B.O. Keller, J. Sui, A.B. Young, R.M. Whittal, Interferences and contaminants encountered in modern mass spectrometry, Anal Chim Acta 627(1) (2008) 71-81.
[13] G. Vistoli, M. Orioli, A. Pedretti, L. Regazzoni, R. Canevotti, G. Negrisoli, M. Carini, G. Aldini, Design, synthesis, and evaluation of carnosine derivatives as selective and efficient sequestering agents of cytotoxic reactive carbonyl species, ChemMedChem 4(6) (2009) 967-75.
[14] R.J. Schaur, W. Siems, N. Bresgen, P.M. Eckl, 4-Hydroxy-nonenal-A Bioactive Lipid Peroxidation Product, Biomolecules 5(4) (2015) 2247-337.
[15] A. Catalá, Lipid peroxidation of membrane phospholipids generates hydroxy-alkenals and oxidized phospholipids active in physiological and/or pathological conditions, Chem Phys Lipids 157(1) (2009) 1-11.
[16] G. Poli, R.J. Schaur, 4-Hydroxynonenal in the pathomechanisms of oxidative stress, IUBMB Life 50(4-5) (2000) 315-21.
[17] Y.M. Lee, S.I. Han, B.C. Song, K.J. Yeum, Bioactives in Commonly Consumed Cereal Grains: Implications for Oxidative Stress and Inflammation, J Med Food 18(11) (2015) 1179-86.
[18] K. Masisi, T. Beta, M.H. Moghadasian, Antioxidant properties of diverse cereal grains: A review on in vitro and in vivo studies, Food Chem 196 (2016) 90-7.

[19] G. Aldini, R.M. Facino, G. Beretta, M. Carini, Carnosine and related dipeptides as quenchers of reactive carbonyl species: from structural studies to therapeutic perspectives, Biofactors 24(1-4) (2005) 77-87.

# Study 2

**Development of a direct ESI-MS method to measure the tannin precipitation effect of proline rich peptides**

## Abstract

Tannins are a heterogeneous class of polyphenols that are present in several plants and foods. The ability of such molecules to interact and precipitate proline-rich proteins leads to different effects such as astringency or antidiarrheal activity. Thus, it is important to evaluate tannin content in plant extracts to evaluate their potential use as pharmaceutical and nutraceuticals. Several methods have been proposed to study tannin-protein interaction but few of them are focused on quantification. The purpose of the present work is to set up a suitable and time efficient method able to quantify the extent of tannin protein precipitation. Bradykinin, chosen as a model, was incubated with increasing concentrations of 1,2,3,4,6-pentagalloyl β-D-glucose and tannic acid chosen as reference of tannic compounds. Bradykinin not precipitated by tannins was determined by a mass spectrometer TSQ Quantum Triple Quadrupole equipped with an ESI source (direct infusion analysis). The results were expressed as $PC_{50}$, which is the concentration able to precipitate 50% of the target protein. The type of tannin-protein interaction was also evaluated after precipitate solubilization. The involvement of proline residue in tannin-protein interaction was confirmed by repeating the experiment using a synthesized peptide (RR-9) characterized by the same bradykinin sequence, but having proline residues replaced by glycine residues: no interaction occurred between the peptide and the tannins.

## 1. Introduction

Tannins are a heterogeneous class of polyphenols that are present in several plants and foods, such as fruits, cereals, wine, tea, cocoa and vegetables [1]. According to Bate-Smith and Swain, tannins are water-soluble phenolic compounds with a molecular weight between 500 and 3000 Da, characterized by many hydroxyl groups and capable of forming cross-linkages with proteins. These compounds are classified as hydrolysable and condensed tannins. Hydrolysable tannins are made of a monosaccharide core, such as glucose, partially or completely esterified with an organic acid, such as gallic acid (gallotannins) or ellagic acid (ellagitannins) [2]. Condensed tannins are more complex than hydrolysable tannins: they are polymers of flavan-3-ols linked through acid-labile carbon-carbon bonds [3].

As secondary metabolites of plants, tannins have a role in plant defense, discouraging herbivores from feeding on the plant. These compounds are also used in the production of leather and their level needs to be controlled in wine production to reduce astringency. All these actions are related to the effect of tannins in inducing protein precipitation. In particular, the interaction is known to occur between tannins and proteins rich in proline residues (PRPs) [4].

More recently, the protein precipitation effects induced by some plant components has also been considered to explain some bioactive actions. Such effects occur when the precipitating protein (protein target) has a damaging effect or is contained in infectious organisms. Based on such a

mechanism, tannins and plant extracts rich in tannins have been proposed as antidiarrheal [5], antiviral [6, 7], antibacterial agents [8-10] and to neutralize the toxic activities of snake venoms [11]. Moreover, a fully detailed study on the molecular interaction of tannin and in particular of penta-O-galloyl-d-glucopyranose with bradykinin has been carried out by NMR. Bradykinin is a proline-rich peptide (Pro residues accounting for 30% of the residues) which acts as an inflammatory mediator and its complexing by tannin can partially explain the well-known anti-inflammatory properties of such a class of compounds. More recently, the molecular interaction between tannin and different wheat-derived peptidic fractions which contain a high content of proline residues and which are responsible for the onset of celiac disease has been studied. This study indicates that the aggregation between tannins and immunoreactive peptides could represent an important field in the potential protective effect of tannins on the cytotoxicity and/or the immunogenicity of gluten peptides.

Based on these recent findings it seems that beside salivary rich peptides such histatins, interaction of tannins with bioactive proline rich peptides deserves some interest; in particular a valuable method able to measure the precipitating effect of tannins towards damaging peptides could be useful in order to identify potential bioactive compounds and/or plant extracts containing them.

The aim of the present work is to set-up an analytical method able to measure the ability of tannins and/or plant extracts to interact with and precipitate

peptides rich in proline. Bradykinin was chosen as a target for tannin binding not only because it is a peptide rich in proline residues, but also due to its involvement in inflammatory disorders such allergies and the common cold, hence representing a potential target peptide of the tannin precipitation effect. Tannic acid (TA) and penta-O-galloyl-β-D-glucose (PGG) were used as reference compounds of tannins.

## 2. Materials and Methods

### *2.1 Chemicals and reagents*

HPLC-grade water was prepared with a Milli-Q water purification system (Millipore, Milan, Italy). Ammonium acetate was from Riedel-de Haën (Seelze, Germany). Bradykinin acetate, tannic acid (TA), penta-O-galloyl-β-D-glucose (PGG), formic acid and LC-grade and analytical-grade organic solvents were from Sigma-Aldrich (Milan, Italy). The internal standard peptide LVNEVTEF was custom synthesized by Sigma-Aldrich (Milan, Italy). The peptide RR-9 RGGGFSGFR was synthesized by PRIMM (Milan, Italy).

### *2.2 Bradykinin-tannin co-precipitation assay*

Bradykinin 100 μM was dissolved in 50 mM acetate buffer pH 7.4 and 25 μL samples were spiked with of PGG or TA at the following concentrations: 10

(only for PGG), 50, 100, 150, 200, 250, 500, 1000 (only for TA) µM performed in 3 replicates. The mixtures were incubated for 10 minutes at 37°C under gentle shaking (1400 rpm on a Thermomixer) and then centrifuged for 10 minutes at 14000 rpm. The supernatant (25 µL) was diluted 1:10 with $H_2O$/$CH_3CN$/HCOOH (70/30/0.1, % v/v), spiked with the peptide LVNEVTEF as internal standard (10 µM final concentration) and analysed by direct infusion MS as below detailed in order to quantify the amount of bradykinin not precipitated by tannins. The precipitates were then dried, dissolved in $H_2O$/$CH_3CN$/HCOOH (70/30/0.1, % v/v) and analysed by MS in order to verify the presence of bradykinin.

*2.3 Supernatant and precipitate analyses by mass spectrometry*

30 µL of the supernatant was injected by an automated sample injection into a TSQ Quantum Ultra Triple Quadrupole (Thermo Finnigan, Milan, Italy) equipped with an ESI-source. An HPLC Surveyor MS Pump (Thermo Finnigan, Milan, Italy) pumped the sample at 25 µL/min with an isocratic phase $H_2O$/$CH_3CN$/HCOOH (70/30/0.1, % v/v). The analyses were performed in positive ion mode and with the following ion source parameters: capillary temperature 270° C; spray voltage 4.5 kV; capillary voltage 35 V; tube lens voltage 114 V. The flow rate of the nebulizer gas (nitrogen) was 15 a.u. The mass spectrometer operated in full mass scan and the Q3 was used as detector with a scan range 450-1300 *m/z*.

Xcalibur 2.0.7 version was used for the relative quantification of bradykinin. A processing method was set up in order to obtain an automated integration of the areas of the z = 2 (*m/z* 530.9) and z = 1 (*m/z* 1060.6) peak of bradykinin and z = 1 (950.5 *m/z*) peak of the internal standard. The ICIS peak integration parameters set were: smoothing points 7; baseline window 40; area noise factor 5; peak noise factor 10; minimum peak high (S/N) 3. This processing method was applied in the Quan Browser window of Xcalibur for the analysis of all the samples. The results were verified and manually corrected where the integrations were not appropriate.

20 µL of the precipitate dissolved was injected by an automated sample injection into a LTQ -Orbitrap XL mass spectrometer (Thermo Scientific, Milan, Italy) equipped with an ESI-source. An HPLC UltiMate 3000 (Thermo Scientific, Milan, Italy) pumped the sample at 25 µL/min with an isocratic phase $H_2O/CH_3CN/HCOOH$ (70/30/0.1, % v/v). The analyses were performed in positive ion mode and with the following ion source parameters: capillary temperature 270° C; spray voltage 4.5 kV; capillary voltage 35 V; tube lens voltage 114 V. The flow rate of the nebulizer gas (nitrogen) was 15 a.u. After mass spectrometry analysis, the deconvolution was carried out with MagTran 1.02 software.

## 3. Results

### *3.1 Set-up of a ESI-MS method to measure the tannin precipitation effect*

Several ESI-MS approaches have been reported to better understand the non-covalent interaction between tannins and peptides, which in particular have been found suitable for the study of the (1) molecular interactions, (2) the binding stoichiometry and (3) the evaluation of the complex stability.

To our knowledge, no studies based on MS have been reported for the measurement of the precipitating effect of tannins towards proline rich peptides, which is the aim of this paper. Bradykinin was selected as target peptide and tannic acid (TA) and penta-O-galloyl-β-D-glucose (PGG) as reference compounds of tannins.

*Figure 1* summarizes the assay. After incubating the target peptide with tannin at different final concentrations, the sample is centrifuged and the relative content of the target peptide in the supernatant determined by ESI-MS using LVNEVTEF as internal stdandard. The precipitating effect is determined by calculating the residual amount of the target peptide in the supernatant in relation to a sample containing the target peptide and prepared in absence of tannins (100% of the peptide).

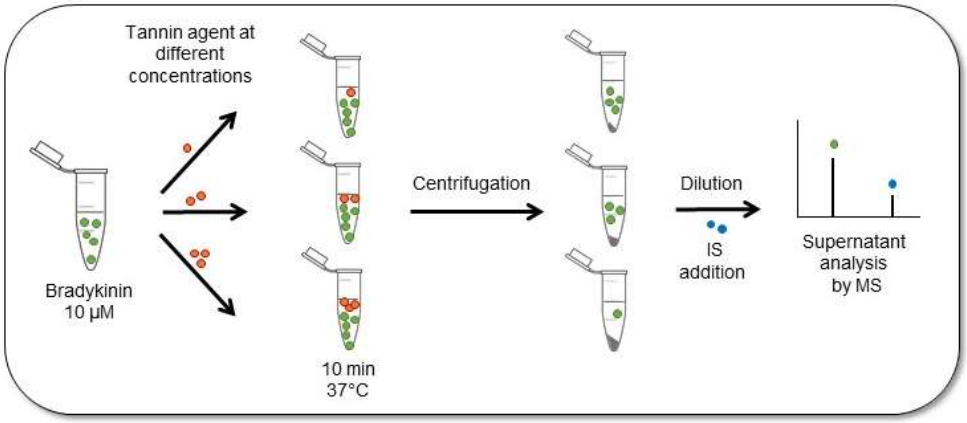


***Figure 1*** *– Graphic representation of the bradykinin precipitation assay*

*Figure 2* shows the ESI-MS spectra of bradykinin spiked with the internal standard. The ions at *m/z* 530.9 and *m/z* 1060.6 refer to the $[M+2H]^{2+}$ and $[M+H]^{+}$ of bradykinin, respectively, while the ion at *m/z* 950.5 is attributed to the $[M+H]^{+}$ of the internal standard.

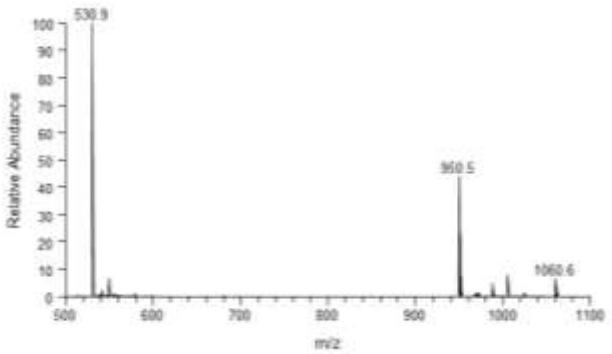


***Figure 2*** *– ESI-MS spectrum of a solution of bradykinin (10 µM) spiked with the IS. Ions at 530.9 m/z and 1060.6 m/z are the $[M+2H]^{2+}$ and $[M+H]^{+}$ of bradykinin, respectively. The ion at 950.5 m/z refers to the $[M+H]^{+}$ of the internal standard.*

In preliminary experiments carried out by LC-ESI-MS/UV, both TA and PGG up to a concentration of 1 mM did not significantly precipitate the IS. As shown in *Figure 3A,* the intensity of bradykinin peaks (but not that of the internal std.) decreases as the concentration of TA increases. *Figure 3B* shows the dose dependent precipitating effect of TA which started at 50 µM (% of residual bradykinin = 87.88±12.52) and reached a plateau at 500 µM (13.00±12.36%).

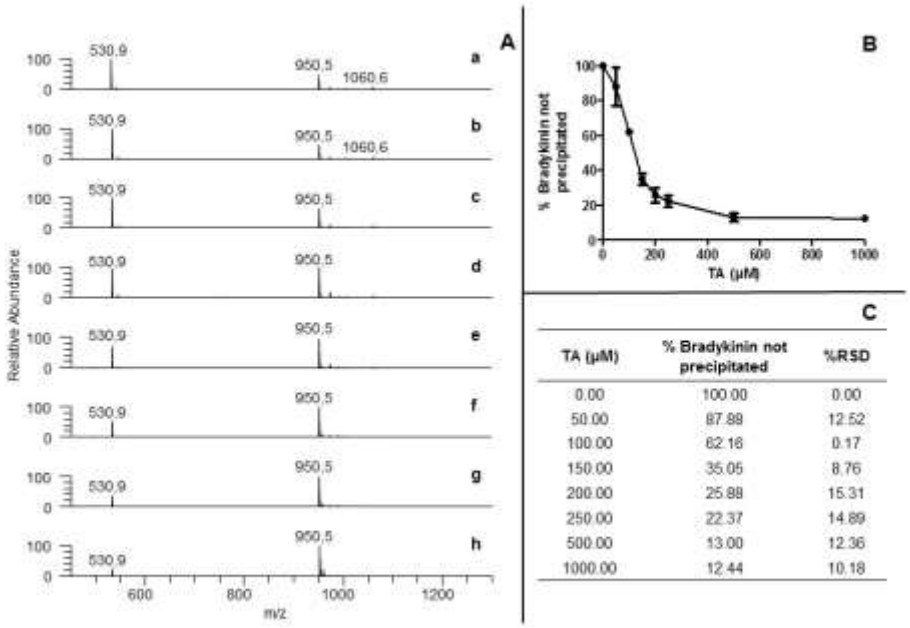


| TA (µM) | % Bradykinin not precipitated | %RSD |
|---|---|---|
| 0.00 | 100.00 | 0.00 |
| 50.00 | 87.88 | 12.52 |
| 100.00 | 62.16 | 0.17 |
| 150.00 | 35.05 | 8.76 |
| 200.00 | 25.88 | 15.31 |
| 250.00 | 22.37 | 14.89 |
| 500.00 | 13.00 | 12.36 |
| 1000.00 | 12.44 | 10.18 |

***Figure 3*** *- Dose-dependent precipitating effect of Bradykinin induced by TA. A) Tannic Acid dose-dependently reduces the relative abundance of the ion at m/z 530.9 refers to bradykinin* $[M+2H]^{2+}$ *in respect to the abundance of the ion at m/z 950.5 attributed to the internal standard (LVNEVTEF). TA concentrations: 0 µM (a), 50 µM (b), 100 µM (c), 150 µM (d), 200 µM (e), 250 µM (f), 500 µM (g), 1000 µM (h). B) Plot showing the residual bradykinin in respect to TA concentration. Values are mean ± SD of three replicates. C) Mean % of residual bradykinin for each concentration tested.*

Figure 3C reports the % of residual bradykinin values for each concentration tested. A similar precipitating effect was observed for PGG (*Figure 4A, B* and *C*).

The protein precipitation potency for each tannin was then quantified as the concentration able to precipitate the 50% of bradykinin (100μM) ($PC_{50}$). The calculated values are 112.3 μM and 84.6 μM for TA and PGG, respectively.

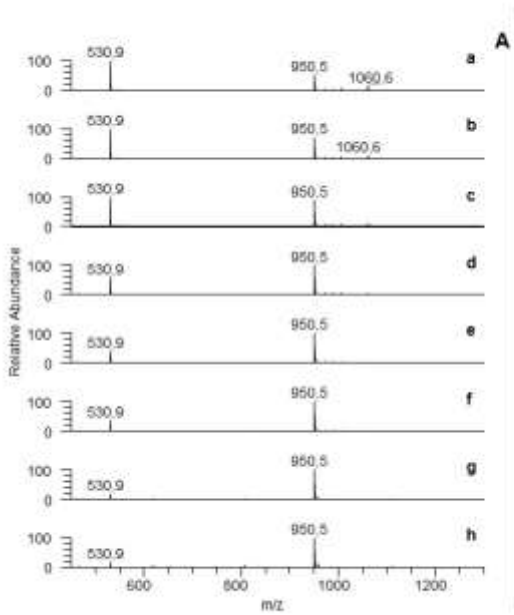


C

| PGG (μM) | % Bradykinin not precipitated | % RSD |
|---|---|---|
| 0.00 | 100.00 | 0.00 |
| 10.00 | 100.46 | 8.82 |
| 50.00 | 87.76 | 2.34 |
| 100.00 | 43.68 | 4.82 |
| 150.00 | 34.54 | 13.75 |
| 200.00 | 23.29 | 11.89 |
| 250.00 | 18.86 | 8.44 |
| 500.00 | 13.14 | 1.89 |

***Figure 4*** *- Dose-dependent precipitating effect of Bradykinin induced by PGG. A) PGG dose-dependently reduces the relative abundance of the ion at m/z 530.9 refers to bradykinin* $[M+2H]^{2+}$ *in respect to the abundance of the ion at m/z 950.5 attributed to the internal standard (LVNEVTEF). TA concentrations: 0 μM (a), 10 μM (b), 50 μM (c), 100 μM (d), 150 μM (e), 200 μM (f), 250 μM (g), 500 μM (h). B) Plot showing the residual bradykinin in respect to TA concentration. Values are mean ± SD of three replicates. C) Mean % of residual bradykinin for each concentration tested.*

To confirm the presence of bradykinin in the precipitates, the pellet obtained by precipitation was dissolved in $H_2O/CH_3CN/HCOOH$ (70/30/0.1, % v/v) and analysed by direct infusion in a LTQ-Orbitrap XL mass spectrometer. *Figures 5* and *6* show the presence of $[M+3H]^{3+}$ and $[M+2H]^{2+}$ ions of bradykinin without any covalent adduct with TA and PGG, as can be appreciated by the deconvoluted spectra.

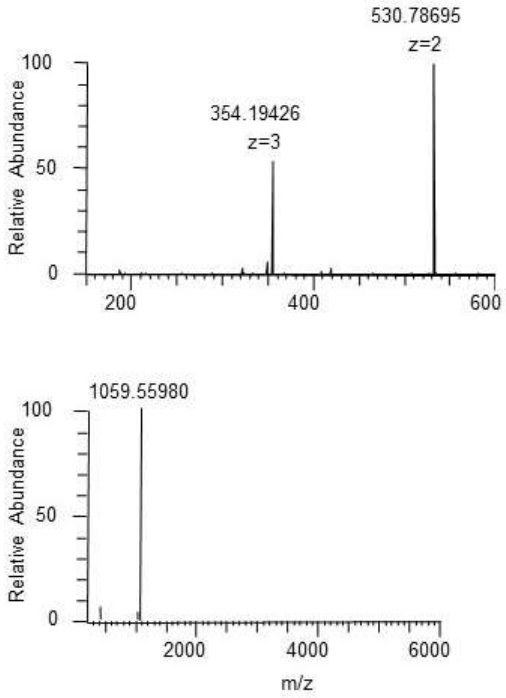


***Figure 5*** *– Analysis of the precipitate occurred between TA and bradykinin: in the upper panel the spectrum of* $[M+3H]^{3+}$ *and* $[M+2H]^{2+}$ *bradykinin ions; in the lower panel the deconvoluted spectrum obtained with MagTran confirms the identity of bradykinin*

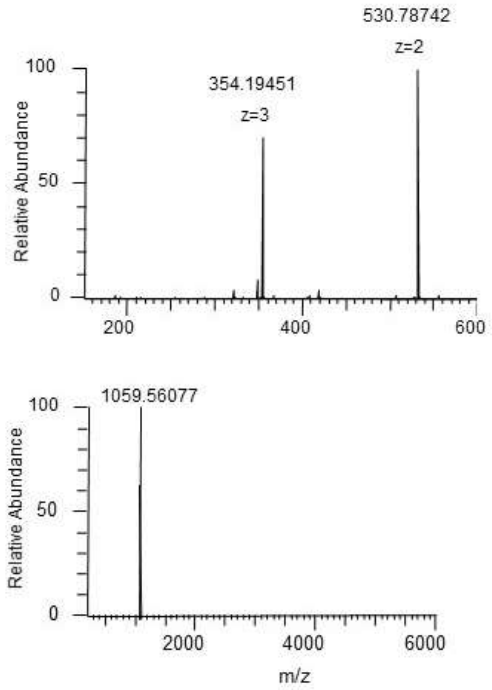


***Figure 6*** *- Analysis of the precipitate occurred between PGG and bradykinin: in the upper panel the spectrum of* $[M+3H]^{3+}$ *and* $[M+2H]^{2+}$ *bradykinin; in the lower panel the deconvoluted spectrum obtained with MagTran confirms the identity of bradykinin.*

### *3.2 Study of the involvement of proline residues in bradykinin precipitation*

In order to understand the involvement of Pro residues in bradykinin precipitation an analogue peptide (RR-9) where the Pro residues are replaced by Gly was tested. *Figure 7* shows the MS spectrum of RR-9 characterized by the ions at *m/z* 470.7 and 940.2 which represent the $[M+H]^+$ and $[M+2H]^{2+}$ ions, respectively. PGG was then selected as precipitating tannin. As shown in *Figure 8* PGG did not induce any significant precipitating effect up to 250 μM while only a weak effect was observed at 500 μM.

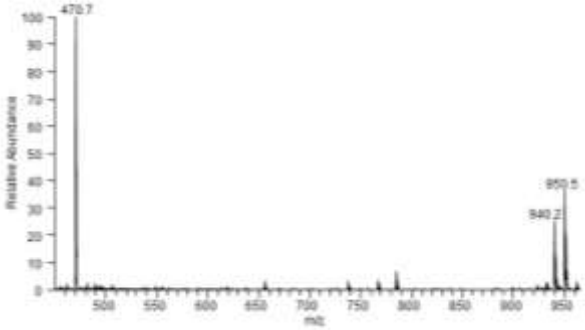


***Figure 7*** *- ESI-MS spectrum of a solution of RR-9 (10 μM) spiked with the IS. Ions at 470.7 m/z and 940.2 m/z are the $[M+2H]^{2+}$ and $[M+H]^{+}$ of RR-9, respectively. The ion at 950.5 m/z refers to the $[M+H]^{+}$ of the internal standard*

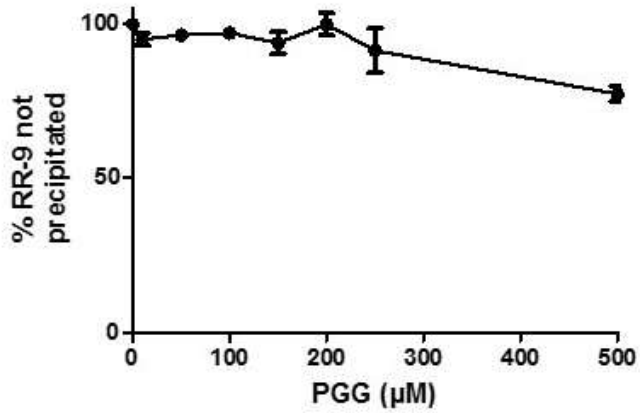


***Figure 8*** *- Profile of RR-9 reduction in the supernatant by PGG increasing concentration*

## 4. Discussion

Several methods have been set-up to measure the protein precipitation effect of tannins and the most popular are those based on BSA as protein target and colorimetric assays to measure the unbound protein fraction in the supernatant or tannins in the precipitated protein-tannin fraction. Makkar HP et al. [12] determined the precipitated BSA by ninhydrin assay and Haruo Kawamoto et al. [13] quantified the precipitated BSA by HPLC-UV. Two methods were based on the use of filter disk and membrane after tannin fractions or plant extract immobilization on these kind of surface: the extent of the interaction was determined as reduction of the BSA diffusion [14] or by gamma counting of BSA $^{125}$I-labelled adsorbed [15]. Scott H. et al. reported a miniaturized method [16] which aimed to reduce the amount of volume in the assay by using a microplate to measure the unprecipited BSA by the Bradford assay. On the other hand, some methods were based on the analysis of tannin co-precipitated fraction after solubilization of the precipitate by reaction with ferric chloride followed by quantification of the total absorbance (510 nm) [17, 18].

However, such methods are not suitable for the measurement of the precipitation of target peptides when used at micromolar level and contained in small sample volumes (not higher one than hundred microliters). Such conditions are required when using bioactive peptides which are expensive or difficult to synthesize and/or isolate. The method here reported fulfills these requirements since the volume of the samples is in the order of hundreds of

microliters and the concentration of the target peptides is in a micromolar range, depending on the MS analyzer used. In the present work, by using triple quadrupole, which is a quite common instrument, the peptide was used at a final concentration of 100 micromolar but the concentration could be further reduced when more sensitive analyzers, such as qTOF or orbitraps, are available. Moreover, the sample volumes can be further reduced if micro-wells are used and in this case a high throughput method can also be adapted. Despite the fact that the triple quadrupole mass spectrometer is not the best instrument in terms of sensitivity when used in full MS acquisition mode, good reliability and precision can be reached and better results can be obtained if compared to colorimetric assays.

## 5. Conclusions

In conclusion, an *in vitro* method was set-up for the quantitative determination of the tannin precipitation effect of proteins and proline rich peptides. The method could be useful to test the ability of tannin to precipitate and hence inactivate damaging peptides and also to evaluate the selectivity of the precipitation effect. Some proline rich peptides can be considered as potential targets of tannins such as bradykinin, an inflammatory mediator, and wheat-derived peptidic fractions which contain a high content of proline residues and which are responsible for the onset of celiac disease. The method could be applied to isolated compounds as well as to complex matrices such as plant

derivatives and fractions. The precision of the method was found satisfactory since the CV% was always lower than 20% for all the concentrations tested. Finally, the method is time efficient thus permitting the rapid screening of several plant extracts and compounds able to complex and precipitate damaging target peptides.

**Abbreviations:** TA, tannic acid; PGG, penta-O-galloyl-β-D-glucose; PRPs, proline rich proteins; BSA, bovine serum albumin.

## References

[1] J. Serrano, R. Puupponen-Pimiä, A. Dauer, A.M. Aura, F. Saura-Calixto, Tannins: current knowledge of food sources, intake, bioavailability and biological effects, Mol Nutr Food Res 53 Suppl 2 (2009) S310-29.
[2] K.T. Chung, T.Y. Wong, C.I. Wei, Y.W. Huang, Y. Lin, Tannins and human health: a review, Crit Rev Food Sci Nutr 38(6) (1998) 421-64.
[3] H. Mehansho, L.G. Butler, D.M. Carlson, Dietary tannins and salivary proline-rich proteins: interactions, induction, and defense mechanisms, Annu Rev Nutr 7 (1987) 423-40.
[4] E. Haslam, Vegetable tannins - lessons of a phytochemical lifetime, Phytochemistry 68(22-24) (2007) 2713-21.
[5] Y. Qin, J.B. Wang, W.J. Kong, Y.L. Zhao, H.Y. Yang, C.M. Dai, F. Fang, L. Zhang, B.C. Li, C. Jin, X.H. Xiao, The diarrhoeogenic and antidiarrhoeal bidirectional effects of rhubarb and its potential mechanism, J Ethnopharmacol 133(3) (2011) 1096-102.
[6] R.S. CARSON, A.W. FRISCH, The inactivation of influenza viruses by tannic acid and related compounds, J Bacteriol 66(5) (1953) 572-5.
[7] G. Liu, S. Xiong, Y.F. Xiang, C.W. Guo, F. Ge, C.R. Yang, Y.J. Zhang, Y.F. Wang, K. Kitazato, Antiviral activity and possible mechanisms of action of pentagalloylglucose (PGG) against influenza A virus, Arch Virol 156(8) (2011) 1359-69.

[8] H. Akiyama, K. Fujii, O. Yamasaki, T. Oono, K. Iwatsuki, Antibacterial action of several tannins against Staphylococcus aureus, J Antimicrob Chemother 48(4) (2001) 487-91.
[9] T. Hatano, M. Kusuda, K. Inada, T.O. Ogawa, S. Shiota, T. Tsuchiya, T. Yoshida, Effects of tannins and related polyphenols on methicillin-resistant Staphylococcus aureus, Phytochemistry 66(17) (2005) 2047-55.
[10] K. Funatogawa, S. Hayashi, H. Shimomura, T. Yoshida, T. Hatano, H. Ito, Y. Hirai, Antibacterial activity of hydrolyzable tannins derived from medicinal plants against Helicobacter pylori, Microbiol Immunol 48(4) (2004) 251-61.
[11] L.H. Vale, M.M. Mendes, A. Hamaguchi, A.M. Soares, V.M. Rodrigues, M.I. Homsi-Brandeburgo, Neutralization of pharmacological and toxic activities of bothrops snake venoms by Schizolobium parahyba (Fabaceae) aqueous extract and its fractions, Basic Clin Pharmacol Toxicol 103(1) (2008) 104-7.
[12] H.P. Makkar, R.K. Dawra, B. Singh, Protein precipitation assay for quantitation of tannins: determination of protein in tannin-protein complex, Anal Biochem 166(2) (1987) 435-9.
[13] H. Kawamoto, F. Nakatsubo, K. Murakami, Stoichiometric studies of tannin-protein co-precipitation, Phytochemistry 41(5) (1996) 1427-31.
[14] E. Obreque-Slier, C. Mateluna, A. Peña-Neira, R. López-Solís, Quantitative determination of interactions between tannic acid and a model protein using diffusion and precipitation assays on cellulose membranes, J Agric Food Chem 58(14) (2010) 8375-9.
[15] G.L. Henson, L. Niemeyer, G. Ansong, R. Forkner, H.P. Makkar, A.E. Hagerman, A modified method for determining protein binding capacity of plant polyphenolics using radiolabelled protein, Phytochem Anal 15(3) (2004) 159-63.
[16] S.H. McArt, D.E. Spalinger, J.M. Kennish, W.B. Collins, A modified method for determining tannin-protein precipitation capacity using accelerated solvent extraction (ASE) and microplate gel filtration, J Chem Ecol 32(6) (2006) 1367-77.
[17] J.F. Harbertson, R.L. Kilmister, M.A. Kelm, M.O. Downey, Impact of condensed tannin size as individual and mixed polymers on bovine serum albumin precipitation, Food Chem 160 (2014) 16-21.
[18] R. Molinari, M.G. Buonomenna, A. Cassano, E. Drioli, Rapid determination of tannins in tanning baths by adaptation of BSA method, Ann Chim 91(5-6) (2001) 255-63.

# IV

# MS methods for the study of the ADME profiles of standardized cranberry and bilberry extracts

# Study 1

**Profiling *Vaccinium Macrocarpon* components and metabolites in human urine and urine *ex-vivo* effect on the reduction of *C. Albicans* adhesion**

**Abstract**

*C. albicans* is one of the causes of nosocomial urinary tract infections (UTIs). Cranberry (*V. Macrocarpon*) is a natural source of polyphenols widely used for the treatment of some diseases including UTIs. Nevertheless, there are many conflicting results regarding the active component and this is due to the use of different dosages and non-standardized Cranberry treatments. The purpose of this work was to fully profile the components and metabolites in human urine after ingestion of a standardized Cranberry extract (Anthocran™) at a dosage which was found effective in human studies. An HPLC-MS/MS method was set up to characterize the profile of cranberry components and metabolites in human urine collected from four female volunteers after 7 days of Anthocran™ assumption. Two different strategies were adopted for the data analysis: an on target and an off target approach. CFM-ID (competitive fragmentation modeling for metabolite identification) was used for the identification of the unknown ions. These strategies allowed the identification of 35 analytes including Cranberry components, known metabolites and also metabolites hitherto unreported in the literature. Urine collected at different time ranges (1, 2, 4, 6, 10, 12, 24 hours) after the last dosage of Anthocran™ were *ex-vivo* tested on the reduction of *C. Albicans* adhesion. Fractions collected after 1 and 12 hours were found effective, reducing significantly reduce the adhesion compared to the control ($p < 0.001$). Purified Anthocran™ components and metabolites identified in the two active urine fractions will be tested.

## 1. Introduction

*Candida albicans* is one of the few fungal pathogens that can cause infections in humans [1] and it is one of the most frequently isolated pathogen in nosocomial urinary tract infections (UTIs) [2]. Urological devices, urological procedures, diabetes and being female are the main factors linked to candiduria [3]. Catheters, which are used in up to 20% of hospitalized subjects [4], are good adhesion substrates for microorganisms as well as biofilms proliferation surfaces. The most important feature of biofilms is their resistance to antimicrobial therapies [5]. Therefore, the search for new antifungal agents is necessary and it should be focused on plants active compounds.

Cranberry (*Vaccinium macrocarpon*) is a rich source of polyphenols, which possess beneficial properties towards pathogenic infections including urinary tract infections (UTIs), dental caries and stomach ulcers [6]. Moreover berry phenolics showed antioxidant, anti-inflammatory and anticancer properties [7, 8]. A synergy of all the phytochemicals could explain the great cranberry health benefits reported in *in vitro* studies [9-11]. Despite all these potential applications, cranberry based products are commonly used in the prevention of UTIs [12]. The major constituents of cranberry are flavonols, anthocyanins, PACs, flavan-3-ols and phenolic acids and derivatives [13]. Several *in vitro* studies supported the hypothesis that the antiadhesive properties of cranberry are due to PACs, and in particular to the A-type [14]. However, controversial results regarding their presence in human urine are reported: many *in vivo* studies have demonstrated that they are not detected after cranberry intake

[15-18], but two works have shown their presence in urine at a very low concentration [19, 20]. The use of different dosages and non-standardized cranberry products could explain these controversial results. The purpose of the present work is to profile the components and metabolites in human urine after ingestion of a standardized cranberry extract (Anthocran™, Indena S.p.A.) at a dosage which has been found effective in human studies [21, 22]. Furthermore, an evaluation of the activity of urine samples after cranberry intake on *C. albicans* adhesion was performed in order to isolate the bioactive molecules.

## 2. Materials and Methods

### *2.1 Reagents*

Formic acid, orthophosphoric acid, ammonium acetate, ethyl gallate, LC–MS grade solvents and β-glucuronidase from *Helix Pomatia* (Type HP-2, ≥ 100,000 units/mL) were purchased from Sigma–Aldrich (Milan, Italy). LC-grade $H_2O$ (18 MΩ cm) was prepared with a Milli-Q $H_2O$ purification system (Millipore, Bedford, MA, USA). SPE Hypersep C18 column (100 mg/mL) were from Thermo Scientific (Milan, Italy). Standardized cranberry extract (*V. Macrocarpon*) and the capsules containing 36 mg PACs/capsule (Anthocran™) were generously donated by Indena S.p.A (Milan, Italy).

*2.2 Study design on healthy volunteers*

Four young healthy female volunteers were recruited for the study: mean age 25 years, mean body weight 55 kg, non-smoker, not subjected to pharmacological treatments. They followed a diet low in polyphenols for 72 hours before the treatment and during the assumption of cranberry supplement. The diet excluded: fruits and vegetables rich in polyphenols, chocolate and some beverages such as coffee, tea, wine and fruit juice. The aim was to reduce as much as possible the concentration of polyphenols in biological fluids. The subjects assumed 2 capsules Anthocran™/day for 7 days. Urine samples were collected before and after the following time-point: 1, 2, 4, 6, 10, 12, 24 hours. Ethyl gallate 10 µM was added as internal standard and all the samples were stored at -80°C until analysis.

*2.3 Sample preparation*

1.5 mL of a pool of the 4 subject urines were treated with β-glucuronidase from *Helix Pomatia* (5000 U/1.5mL urines) in 100 mM pH 5 acetate buffer, for 18 hours at 37°C. The hydrolysis was stopped by adding orthophosphoric acid until pH 2 was reached. The samples were then centrifuged at 10000 xg for 5 minutes and the supernatant was extracted on the SPE column, working at 1 mL/min. Salts were removed with water and then all the compounds retained were eluted with 1 mL 100% acetonitrile. The fractions collected were dried under vacuum and then solubilized in 100 µL $H_2O/CH_3OH$/ HCOOH (90/10/0,1 % v/v).

*2.4 Chromatographic conditions*

Cranberry components and urine metabolites separations were performed on a reversed-phase Agilent Zorbax SB-C18 column (150 x 2.1 mm, i.d. 3.5 µm, CPS analitica, Milan, Italy), protected by an Agilent Zorbax guard column, kept at 40°C, by an UltiMate 3000 system (Dionex) equipped with an autosampler kept at 4°C working at a constant flow rate (200 µL/min). 10 µL of sample was injected into the column and both cranberry components and urine metabolites were eluted with a 80 min multistep gradient of phase A $H_2O$/HCOOH (100/0.1 % v/v) and phase B $CH_3CN$/HCOOH (100/0.1 % v/v): 0-45 min, from 10% B to 20% B; 45-65 min, from 20% B to 60% B; 65-66 min, from 60% B to 90% B; 66-70 min, isocratic of 90% B; 70-71 min, from 90% B to 10 % B, and then 71-80 min of isocratic 10% B.

*2.5 Polyphenol class identification by HPLC-UV analysis*

The identification of polyphenol classes was carried out by HPLC-UV analysis on a HPLC Surveyor LC system (Thermo Fisher Scientific, Milan, Italy) equipped with a quaternary pump, UV-VIS detector (PDA) and an autosampler. The scan range was set from 200 nm to 600 nm. A solution of 4 mg/mL of cranberry extract in $H_2O$/$CH_3OH$/HCOOH (90/10/0.1 % v/v) was used for the analysis.

### 2.6 Cranberry component profiling and urine metabolites characterization by high resolution mass spectrometry

10 µL of each sample was injected into the RP column as previously described: the cranberry extract was analyzed at a concentration of 4 mg/mL in $H_2O/CH_3OH/HCOOH$ (90/10/0.1 % v/v), while the urine samples were analyzed after the treatment described in *par. 2.3*. The analyses were performed on a LTQ-Orbitrap XL mass spectrometer using an ESI source. Mass spectra were acquired in positive and in negative ion mode. A list of 20 background ions was adopted as lock mass values for real time mass calibration [23]. The source parameters used for the positive mode are: spray voltage 4 kV, capillary temperature 300 °C, capillary voltage 30 V, tube lens offset 90 V; for the negative ion mode: spray voltage 4 kV, capillary temperature 300 °C, capillary voltage -23 V, tube lens offset -140 V. The instrument was set up to work in a data-dependent scan mode to acquire both full MS and MS/MS spectra. Full MS spectra were acquired in profile mode by the FT analyzer in a scan range of 100-1200 *m/z*, using AGC scan target 5 x $10^5$ and resolution 30000 FWHM at 400 *m/z*. Tandem mass spectra were acquired by the linear ion trap (LTQ) which was set up to fragment the 3 most intense ions exceeding 1 x $10^4$ counts. Mass acquisition settings were: centroid mode, AGC scan target 5 x $10^4$, precursor ion isolation width of 3 *m/z*, and collision energy (CID) of 35 eV. Dynamic exclusion was enabled to reduce redundant spectra acquisition: 2 repeat counts, 20 sec repeat duration, 30 sec of exclusion duration. Moreover, only singly and unassigned charged ions

were fragmented. Instrument control and spectra analysis were provided by the software Xcalibur 2.0.7 and Chromeleon Xpress 6.80.

### *2.7 On target and off target analyses of cranberry components and metabolites in human urine*

An in-house database was created for the on target analysis by adding all the cranberry extract components characterized as well as known cranberry metabolites identified in other studies and cranberry components deriving from other cranberry sources even if not present in the extract under investigation, in order to have a bigger dataset. The identification was carried out on the QualBrowser tool of Xcalibur 2.0.7 by using the exact mass and the isotopic and fragmentation patterns.

The off target analysis consisted of searching for all the ions present in the urine samples collected after the cranberry assumption that were not present or present at intensity relative to noise ($< 5*10^2$) in the pre-treatment sample. The research was carried out on the QualBrowser tool of Xcalibur 2.0.7 by screening the full MS spectra acquired in negative ion mode in ranges of 5 m/z and 10 minutes for each sample. Each ion detected with those filters was exported with the relative MS/MS spectrum, if present. The identification was performed by following two different approaches based on the exact mass and isotopic and fragmentation patterns. The first approach consists of giving the precursor ion and the MS/MS spectrum list as inputs in the Compound Identification tool of CFM-ID (http://cfmid.wishartlab.com/identify), using as

mass tolerance error 5 ppm for the precursor ion and 0.3 Da for the fragments. CFM-ID searches for candidates in available databases (HMDB and KEGG) based on the exact mass, then generating *in-silico* MS/MS spectra of all the candidates and then comparing the experimental data with those obtained *in-silico*. The top candidates were ranked (Jaccard Score) according to how closely they matched and returned to a list. The second approach was initially focused on the calculation of the elemental composition performed on the Elemental Composition page of Xcalibur 2.0.7 by using the following parameters: mass tolerance 5 ppm, charge -1, no use of Nitrogen Rule, C H O N P S as elements in use. The top 5 formulae were searched in PubChem in order to obtain a list of candidates. Next, the Peak Assignment tool of CFM-ID was used to predict the MS/MS spectra of the putative identified compounds and compare the *in-silico* spectra obtained with the experimental spectra.

### *2.8 Candida albicans adhesion ex-vivo assay*

*C. albicans* biofilm-forming ability was evaluated on polystyrene 96-well plates using the reference strain *C. albicans* SC5413 [24]. Prior to experiments, *C. albicans* was grown overnight in yeast extract, peptone, dextrose (1% w/v yeast extract, 2% w/v peptone, 2% w/v dextrose) liquid medium (YPD) at 30°C in an orbital shaker. Cells were then washed with cold phosphate-buffered saline (PBS). A standard inoculum of 5 x $10^5$ cells/mL was prepared in Roswell Park Memorial Institute 1640 medium (RPMI – 1640) and added or not with

urine fractions as well as Anthocran™ 0.1 mg/mL. 100 µL/well of the inoculum was firstly incubated at 37°C for 1 hour to promote adhesion. Non-adherent cells were removed and wells washed with PBS; medium was replaced and the plate further incubated for 24 hours. Biofilm-forming ability was quantified by crystal violet (CV) staining for total biomass measurement. Two independent experiments were carried out with six replicates for each condition. Urine samples were lyophilized, reconstituted in RPMI – 1640 and diluted 1:2 in the same medium.

## 3. Results

### *3.1 Characterization of Anthocran™ components*

Polyphenols classes of the cranberry extract were characterized by HPLC-UV analysis at typical wavelength: 310 nm for phenolic acids, 365 nm for flavonols, 520 nm for anthocyanins, 278 nm for benzoic acids, flavanols and PACs (*Figure 1*). The identification of each compound in the extract was then obtained on the basis of the exact mass and of the isotopic and the fragmentation patterns, by acquiring the mass spectra in positive and in negative ion mode. All compounds identified are reported in *Table 1, Table 2* and *Table 3.*

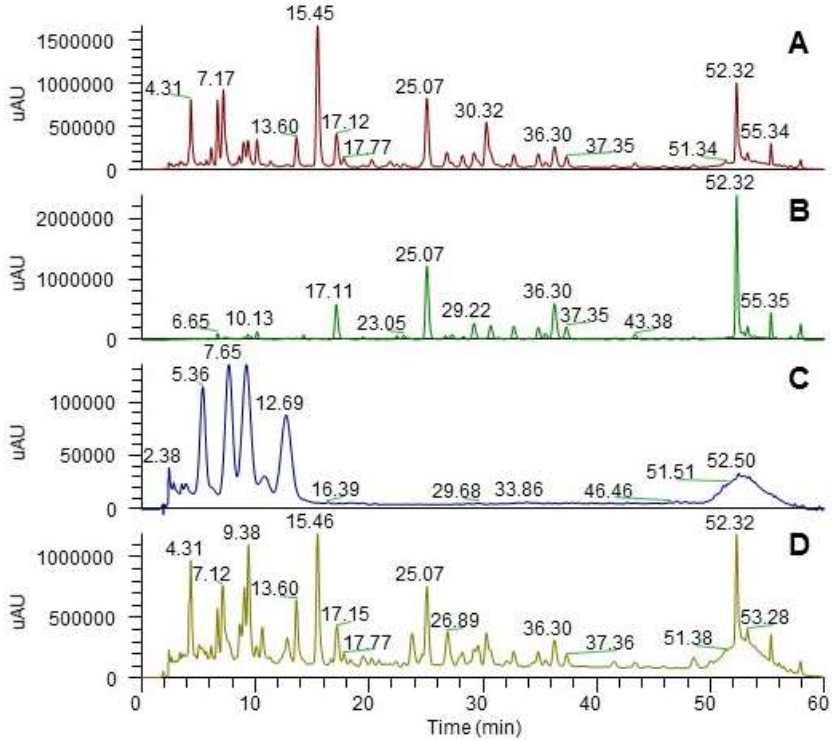


***Figure 1*** *- Characterization of cranberry extract constituents by HPLC-UV : A) phenolic acids, 310 nm ; B) flavonols, 365 nm ; C) anthocyanins, 320 nm ; D) benzoic acids, flavanols and PACs, 278 nm.*

| *Positive ion mode* | Name | RT (min) | $[M]^+$ | Fragments |
|---|---|---|---|---|
| | *Anthocyanins* | | | |
| | Cyanidin | 19 | 287.05556 | 259+255+251+245+242+125 |
| | Peonidin | 24 | 301.07121 | 268+258+230+177+151 |
| | Cyanidin-3-O-arabinoside | 6.2 | 419.09782 | 287 |
| | Peonidin-3-O-arabinoside | 10 | 433.11347 | 301 |
| | Cyanidin-3-O-galactoside | 4.15 | 449.10838 | 287 |
| | Cyanidin-3-O-glucoside | 4.6 | 449.10838 | 287 |
| | Petunidin-3-O-arabinoside | 5 | 449.10838 | 317 |
| | Peonidin-3-O-galactoside | 7.3 | 463.12403 | 301 |
| | Peonidin 3-O-glucoside | 7.6 | 463.12403 | 301 |
| | Malvidin-3-O-galactoside | 8 | 493.13460 | 331 |
| | Malvidin-3-O-glucoside | 8.4 | 493.13460 | 331 |

***Table 1*** *– Anthocyanins composition in Cranberry extract*

| *Negative ion mode* | Name | RT (min) | *m/z* | Fragments |
|---|---|---|---|---|
| | *Phenolic and benzoic acids* | | | |
| | Benzoic acid | 8.3 | 121.02896 | 77 |
| | Protocatechuic acid | 4 | 153.01879 | 109 |
| | *p*-Coumaric acid | 13.6 | 163.03952 | 119 |
| | Gallic acid | 2.5 | 169.01370 | 125 |
| | Caffeic acid | 7.9 | 179.03444 | 135 |
| | Ferulic acid | 4.9 | 193.05009 | 149+134 |
| | Sinapinic acid | 6.2 | 223.06065 | 179+164+149+135 |
| | Caffeoyl glucose | 5 | 341.08726 | 179+135 |
| | Chlorogenic acid | 6 | 353.08727 | 191+179+161 |

***Table 2*** *– Phenolic and benzoic acids in Cranberry extract*

| *Positive and negative ion mode* | Name | RT (min) | $[M+H]^+$ | Fragments | $[M-H]^-$ | Fragments |
|---|---|---|---|---|---|---|
| | *Flavonols, Flavanols, PACs* | | | | | |
| | Coumarin | 14 | 147.04460 | 119+91 | 145.02896 | - |
| | Scopoletin | 17.8 | 193.05008 | 165+152+133+119+105 | 191.03444 | - |
| | Kaempferol | 55 | 287.05556 | 259+251+241+231+ 213+165+ 153+137+121 | 285.03992 | - |
| | Epicatechin | 5.7 | 291.08685 | 169+165+151+147+139+ 123 | 289.07121 | 245+205+179+161+ 151+ 137+125+109 |
| | Catechin | 9 | 291.08686 | 169+165+151+147+139+ 123 | 289.07122 | 245+205+179+161+ 151+ 137+125+109 |
| | Quercetin | 48.5 | 303.05047 | 257+247+229+165+ 153+ 149+ 137+121 | 301.03483 | 273+257+229+179+ 151+ 121+107 |
| | Epigallocatechin | 4.4 | 307.08177 | - | 305.06613 | 261+221+219+179+ 137+125 |
| | Gallocatechin | 3.1 | 307.08177 | - | 305.06613 | 261+221+219+179+ 137+125 |
| | Isorhamnetin | 55.8 | 317.06612 | 299+285+281+274+ 257+ 165+ 153+139 | 315.05048 | 287+271+259+243+ 203+163+151 |
| | Myricetin | 32 | 319.04539 | 290+273+255+245+ 165+ 153+ 137 | 317.02975 | 255+227+193+179+ 151+137+107 |
| | 3'-O-methylmyricetin | 50 | 333.06104 | 301+287+277+273+ 245+193+165+153+ 139 | 331.04540 | 287+271+263+179+ 151 |
| | Syringetin | 55.8 | 347.07669 | 315+291+287+269+ 181+165+153+139 | 345.06104 | 315 |

| *Positive and negative ion mode* | Name | RT (min) | $[M+H]^+$ | Fragments | $[M-H]^-$ | Fragments |
|---|---|---|---|---|---|---|
| | *Flavonols, Flavanols, PACs* | | | | | |
| | Quercetin-3-O-arabinofuranoside | 25.2 | 435.0927 | 303 | 433.0771 | 301 |
| | Quercetin-3-O-arabinopyranoside | 28.4 | 435.0927 | 303 | 433.0771 | 301 |
| | Quercetin-3-O-xylopyranoside | 26.6 | 435.0927 | 303 | 433.0771 | 301 |
| | Catechin-3-O-gallate | 16.6 | 443.0978 | 291+273+151+139 | 441.0822 | 315+297+289+ 161+ 153 |
| | Epicatechin-3-O-gallate | 20 | 443.0978 | 291+273+151+139 | 441.0822 | 330+305+289+ 161+ 139 |
| | Kaempferol-7-O-glucoside | 27.2 | 449.1084 | 287 | 447.0927 | 284 |
| | Isorhamnetin-3-O-arabinofuranoside | 37 | 449.1084 | 317 | 447.0927 | 314 |
| | Isorhamnetin-3-O-xylopyranoside | 38,5 | 449,10838 | 317 | 447,09274 | 314 |
| | Isorhamnetin-3-O-arabinopyranoside | 41 | 449,10838 | 317 | 447,09274 | 314 |
| | Quercetin-3-O-rhamnoside | 30,5 | 449,10839 | 303 | 447,09275 | 301 |
| | Myricetin-3-O-arabinofuranoside | 16,6 | 451,08765 | 319 | 449,07201 | 317 |
| | Myricetin-3-O-arabinopyranoside | 19,6 | 451,08765 | 319 | 449,07201 | 317 |
| | Myricetin-3-O-xylopyranoside | 19 | 451,08765 | 319 | 449,07201 | 317 |

| Positive and negative ion mode | Name | RT (min) | $[M+H]^+$ | Fragments | $[M-H]^-$ | Fragments |
|---|---|---|---|---|---|---|
| | *Flavonols, Flavanols, PACs* | | | | | |
| | Quercetin 3-O-glucoside | 22,4 | 465,10329 | 303 | 463,08765 | 301 |
| | Quercetin-3-O-galactoside | 21,5 | 465,10330 | 303 | 463,08766 | 301 |
| | Isorhamnetin-3-O-glucopyranoside | 34,5 | 479,11894 | 317 | 477,10330 | 315 |
| | Isorhamnetin-3-O-glucofuranoside | 32,8 | 479,11894 | 317 | 477,10330 | 315 |
| | Isorhamnetin-3-O-galactoside | 31,1 | 479,11894 | 317 | 477,10330 | 315 |
| | Syringetin-3-O-arabinofuranoside | 38,8 | 479,11894 | 347 | 477,10330 | 345 |
| | Syringetin-3-O-xylopyranoside | 39,8 | 479,11894 | 347 | 477,10330 | 345 |
| | Syringetin-3-O-arabinopyranoside | 43,5 | 479,11894 | 347 | 477,10330 | 345 |
| | Myricetin-3-O-glucoside | 15,1 | 481,09820 | 319 | 479,08256 | 317 |
| | Myricetin-3-O-galactoside | 14,5 | 481,09821 | 319 | 479,08257 | 317 |
| | Syringetin-3-O-rhamnoside | 43,8 | 493,13460 | 347 | 491,11896 | - |
| | Proanthocyanidin A-type dimer | 17/23 | 577,13457 | 437+425+397+287 | 575,11893 | 425+289+287 |
| | Proanthocyanidin B-type dimer | 22,6 | 579,15022 | 453+439+427+409+301+291 | 577,13458 | 425+407+289 |
| | Proanthocyanidin A-type trimer | 16/25 /27.3 | 865,19796 | 713+577+425+287 | 863,18232 | 575+423+289 |
| | Proanthocyanidin B-type trimer | 11.5/ 14.3/ 24 | 867,21361 | 579+427+409+291 | 865,19797 | 577+425+407+287 |

***Table 3*** *– Flavonols, Flavonols and PACs in Cranberry extract*

*3.2 On target analysis of human urine after cranberry extract intake*

The on target analysis was based on the use of the database reported in the *Table S1* of Supplementary materials, composed of the cranberry extract components characterized and by cranberry compounds and metabolites characterized in other studies [15, 16, 19, 20, 25-28]. The identification was performed on Xcalibur 2.0.7 by using the exact mass, the isotopic and fragmentation patterns and the retention time. The last feature was only used for cranberry extract components, thus permitting the identification of compounds not intense enough to be fragmented, such as gallic acid, kaempferol, quercetin, isorhamnetin, syringetin, quercetin-3-O-arabinofuranoside, isorhamnetin-3-o-arabinopyranoside, quercetin 3-O-rhamnoside and quercetin-3-O-galactoside. The fragmentation pattern however was fundamental for the identification of the metabolites described in other studies as well as for the confirmation of the identity of some cranberry components. In *Figure 2* are reported the single ion chromatograms and the MS/MS spectra of some identified compounds : *Figure 2A* showed the chromatograms of protocatechuic acid (4.1 min), 2,5-dihydroxybenzoic acid (6.9 min), 2,4-dihydroxybenzoic acid (8.6 min) and 2,3-dihydroxybenzoic acid (9.3 min) and their MS/MS spectrum which is characterized by the 109 *m/z* fragment deriving from the loss of $CO_2$ ; *Figure 2B* showed the chromatogram and the MS/MS spectrum of *p*-coumaric acid, which give 119 *m/z* as fragment ion that derives from the loss of $CO_2$ ; in *Figure 2C* are reported sinapinic acid chromatogram and MS/MS spectrum, which is characterized by the fragment

deriving from the loss of $CO_2$ (179 *m/z*) and those from the loss of the two methyl groups (164 *m/z* and 149 *m/z*) ; *Figure 2D* showed the chromatogram and the MS/MS spectrum of hippuric acid, which give 134 *m/z* as fragment ion that derives from the loss of $CO_2$ ; in *Figure 2E* are reported the chromatograms of two isomers (3.7 and 4.5 min) of hydroxyhippuric acid and the MS/MS spectrum, which is characterized by the fragment deriving from the loss of $CO_2$ (150 *m/z*) and that at 100 *m/z* which comes from the fragmentation of the aromatic ring . The identification was mainly carried out using the negative ion mode : in *Table 4* are reported all the compounds and metabolites identified with the m/z, RT and fragments where available.

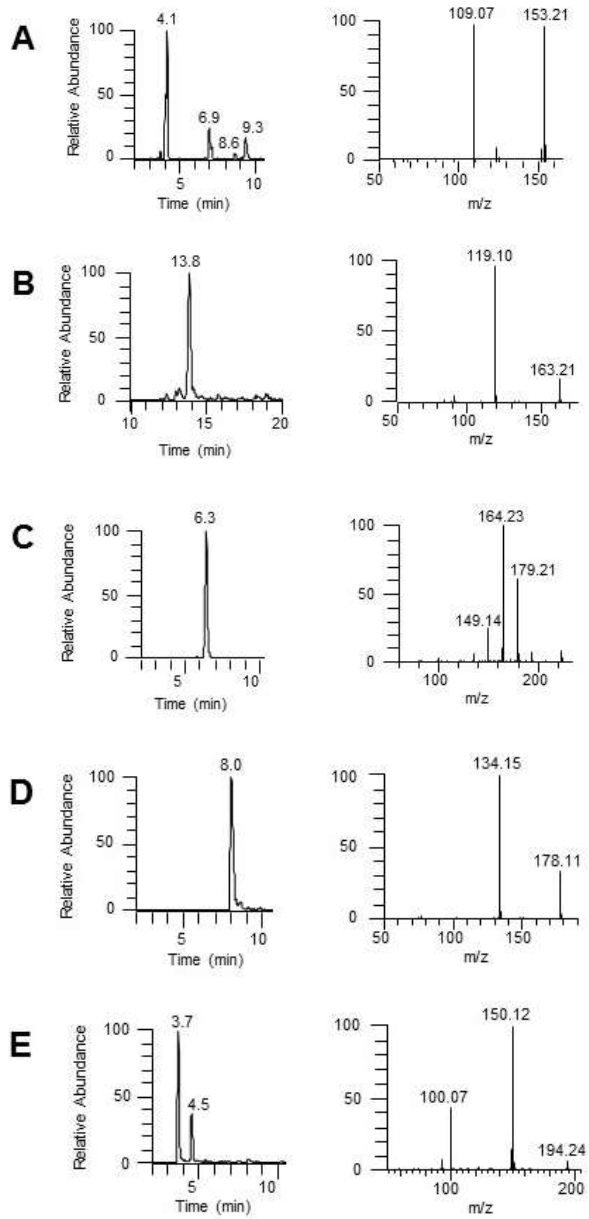


***Figure 2*** *– Single ion chromatograms and MS/MS spectra of some cranberry components and metabolites identified using the on target analysis : A) Dihydroxybenzoic acids ; B) p-Coumaric acid ; C) Sinapinic acid ; D) Hippuric acid ; E) Hydroxyhippuric acid isomers 1 and 2.*

| Name | $[M-H]^-$ | RT | MS/MS Fragments |
|---|---|---|---|
| *Cranberry extract components* | | | |
| Protocatechuic acid | 153.01879 | 4.1 | 109 |
| *p*-Coumaric acid | 163.03952 | 13.8 | 119 |
| Gallic acid | 169.01370 | 2.5 | - |
| Sinapinic acid | 223.06065 | 6.3 | 179+164+135 |
| Kaempferol | 285.03992 | 55 | - |
| Quercetin | 301.03483 | 48.5 | - |
| Isorhamnetin | 315.05048 | 55.8 | - |
| Syringetin | 345.06104 | 55.8 | - |
| Quercetin-3-O-arabinofuranoside | 433.07709 | 25.2 | - |
| Isorhamnetin-3-o-arabinopyranoside | 447.09274 | 41 | - |
| Quercetin 3-O-rhamnoside | 447.09275 | 30.5 | - |
| Quercetin-3-O-galactoside | 463.08766 | 21.5 | - |
| *Cranberry metabolites characterized in other studies* | | | |
| 2-Hydroxybenzoic acid | 137.02387 | 6.6 | 93 |
| Cinnamic acid | 147.04461 | 14.6 | 103 |
| 2,3-dihydroxybenzoic acid | 153.01879 | 9.3 | 109 |
| 2,5-dihydroxybenzoic acid | 153.01879 | 6.9 | 109 |
| 2,4-dihydroxybenzoic acid | 153.01879 | 8.6 | 109 |
| 3-(4-hydroxyphenyl)-propionic acid | 165.05516 | 14.8 | 147+121+103 |
| Vanillic acid | 167.03444 | 8.5 | 123+108 |
| 3,4-Dihydroxyphenylacetic acid | 167.03444 | 3.5 | 123 |
| Hippuric acid | 178.05042 | 8 | 134 |
| 3,4-Dihydroxyhydrocinnamic acid | 181.04991 | 5.1 | 121 |
| Hydroxyhippuric acid isomer 1 | 194.04562 | 3.7 | 150+100+93 |
| Hydroxyhippuric acid isomer 2 | 194.04562 | 4.5 | 150+100+93 |

***Table 4*** *– Cranberry components and metabolites identified using the on target analysis*

*3.3 Off target analysis of human urine after cranberry extract intake*

The metabolites identified through the off target analysis are reported in *Table 5*. In *Figure 3* are reported, as examples, the single ion chromatograms of quinic acid (*Figure 3B*) and 5'-(3',4'-dihydroxyphenyl)-gamma-valerolactone (*Figure 3E*) in the urine fraction in which they reached their maximum concentration (1 h for quinic acid and 12 h for 5'-(3',4'-dihydroxyphenyl)-gamma-valerolactone), while in the control sample (*Figure 3A* and *Figure 3D* respectively) they were not present. The analysis was performed using the negative ion mode because all the compounds identified using the on target analysis were mainly detected in this polarity mode. As the interesting compounds were those whose identification can be hypothesized, other unidentified compounds, or those recognized as coming from the human basal metabolism (e.g. aminoacids), were not included on the list. In *Figure 3C* and *Figure 3F* are reported the experimental MS/MS spectra used as input for the Compound Identification tool of CFM-ID that gave as best matched results quinic acid and 5'-(3',4'-dihydroxyphenyl)-gamma-valerolactone respectively : quinic acid MS/MS spectrum is characterized by the ions 145, 129 and 101 *m/z* and 5'-(3',4'-dihydroxyphenyl)-gamma-valerolactone MS/MS spectrum is composed by the ions 163 and 122 *m/z*. The structures reported for each fragment ion were predicted by the software.

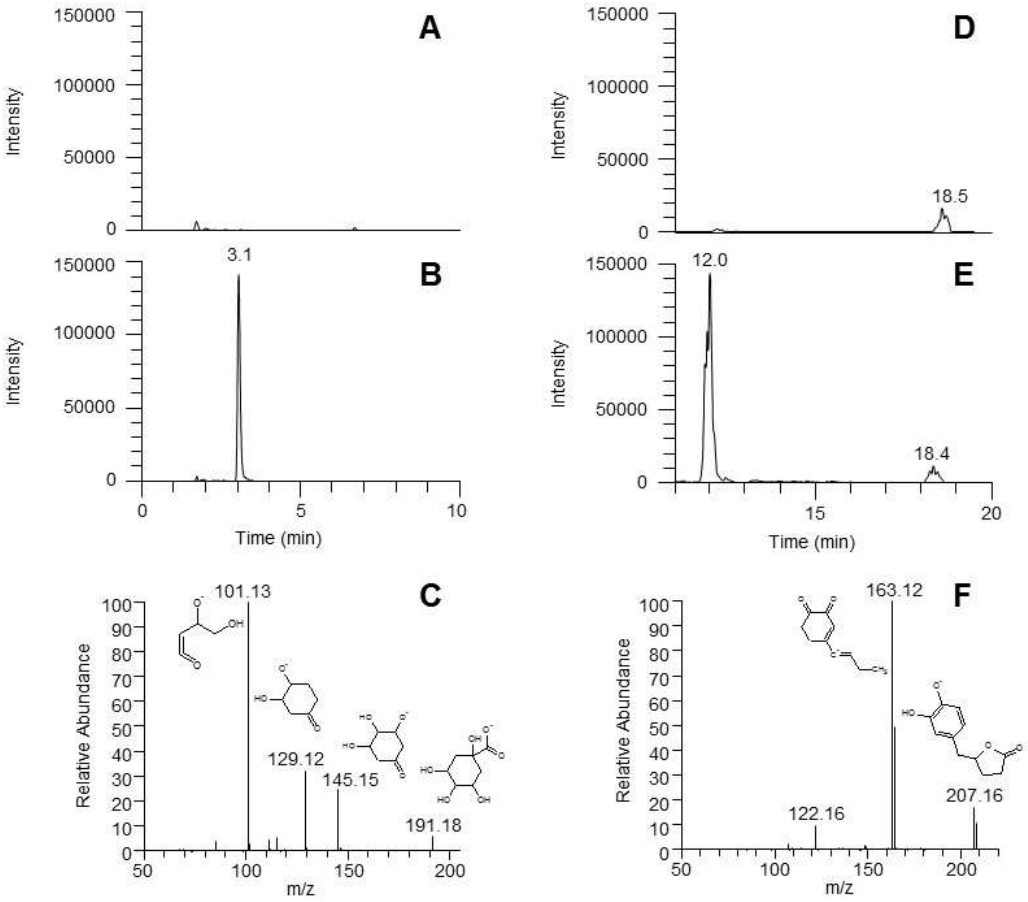


***Figure 3*** *– The peak of quinic acid (A) and 5'-(3',4'-hydroxyphenyl)-gamma-valerolactone (D) in the control sample were not present. Single ion chromatogram of quinic acid (B) in the urine sample at 1 h and 5'-(3',4'-hydroxyphenyl)-gamma-valerolactone (E) in the urine sample at 12 h. MS/MS spectra of quinic acid (C) and 5'-(3',4'-hydroxyphenyl)-gamma-valerolactone (F) with the predicted structure for each fragments assigned by the Compound Identification tool of CFM-ID .*

| *m/z* | MS/MS Fragments | Formula | Delta ppm | Name | Database |
|---|---|---|---|---|---|
| 181.04991 | 121 | $C_9H_{10}O_4$ | -3.989 | 3,4-Dihydroxyhydrocinnamic acid | HMDB |
| 191.05536 | 145+129+101 | $C_7H_{12}O_6$ | -3.934 | Quinic acid | HMDB |
| 192.06700 | 157+131+111+74 | $C_{10}H_{11}NO_3$ | 1.996 | 2-Methylhippuric acid | HMDB |
| 194.04562 | 150+100+93 | $C_9H_9NO_4$ | -1.346 | (4-)Hydroxyhippuric acid | HMDB |
| 194.04562 | 150+100+93 | $C_9H_9NO_4$ | -1.346 | (2-)Hydroxyhippuric acid | HMDB |
| 207.0657 | 163+122 | $C_{11}H_{12}O_4$ | -2.812 | 5-(3' ,4' -dihydroxyphenyl)-gamma-valerolactone | HMDB |
| 223.0606 | 193+179+164+149 | $C_{11}H_{12}O_5$ | -2.587 | Sinapinic acid | HMDB |
| 285.0406 | 252+241+223+205+199 +175+163+151 | $C_{15}H_{10}O_6$ | 0.451 | 2'-Hydroxygenistein | HMDB |
| 287.0225 | 207+163 | $C_{11}H_{12}SO_7$ | -2.084 | 5-(4' -hydroxyphenyl) -gamma-valerolactone-3' -O-sulphate | HMDB |
| 287.0225 | 207+163 | $C_{11}H_{12}SO_7$ | -2.084 | 5-(3' -hydroxyphenyl) - gamma-valerolactone-4' -O-sulphate | HMDB |
| 303.018 | 259+223+179 | $C_{11}H_{12}SO_8$ | 0.090 | 5-(3',4',5'-Trihydroxyphenyl) -gamma-valerolactone-3'-O-sulphate | HMDB |
| 305.0339 | 225+208+179+162 | $C_{11}H_{14}SO_8$ | 0.909 | 4-Hydroxy-5-(dihydroxyphenyl)-valeric acid-O-sulphate | HMDB |
| 370.0783 | 325+194+166+138+ 123+113 | $C_{15}H_{17}NO_{10}$ | 1.001 | Salicyluric glucuronide | CFM-ID |
| 383.0445 | 303+285+259+244+ 217+153+137+123 | $C_{16}H_{16}SO_9$ | 0.790 | 3-O-Methylcatechin-sulphate | CFM-ID |

***Table 5*** *– Metabolites identified using the off target analysis*

*3.4 Ex-vivo inhibition of Candida albicans adhesion by urine fractions*

Anthocran™ 0.1 mg/mL, urine before Anthocran™ intake and urine fractions (1h, 2h, 4h, 6h, 10h, 12h and 24h) collected after the treatment were tested to investigate the potential ability to reduce *C. albicans* adhesion on polystyrene 96-well plates. The results are reported in *Figure 4*. Urine samples before the treatment were shown to be inactive, while it is evident that Anthocran™ was able to strongly reduce adhesion and biofilm formation ($p < 0.001$). Considering urine after Anthocran™ assumption, two fractions were shown to significantly reduce the adhesion

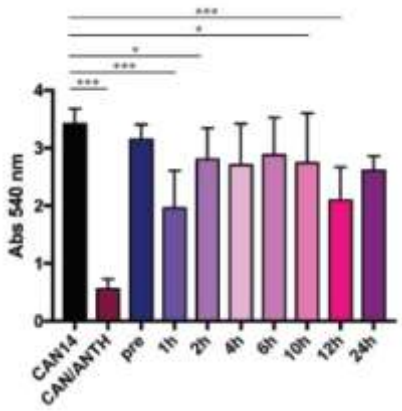


***Figure 4*** *– Activity of Anthocran™ (0.1 mg/mL), urine before Anthocran™ intake and urinary fractions after the treatment. Significant differences are indicated by *p < 0.05, ***p < 0.001, Mann-Whitney test.*

compared to the control ($p < 0.001$) : 1 hours and 12 hours after the last capsule intake. A lower activity was observed for the 2 hours and 10 hours fractions compared to the control ($p < 0.05$).

*3.5 Possible bioactive components present in urine fractions*

The area under the curve of the selected ion chromatogram of each compound identified with the on target and off target approach were extracted and normalized to that of the internal standard (ethyl gallate) in order to obtain semiquantitative ratios of the compounds present in each urine fraction. A selection was then made by picking those metabolites which were present at their maximum relative concentration in the two most active urine fractions (1 h and 12 h after the last capsule intake). As examples, in *Figure 5* are shown two compounds which reached the maximum relative abundance in the active fractions and two compounds that reached it in other urine fractions : *Figure 5A* is relative to 5-(3' -hydroxyphenyl)- gamma-valerolactone-4' -O-sulphate, which Tmax was 1 h ; in *Figure 5B* shows the excretion profile of quercetin, which Tmax was 12 h ; *Figure 5C* is relative *p*-coumaric acid, which Tmax was 2 h ; in *Figure 5D* shows the excretion profile of 3-O-methylcatechin sulphate, which Tmax was 4 h. The list of the possible bioactive components contains both cranberry components and metabolites (*Table 6*).

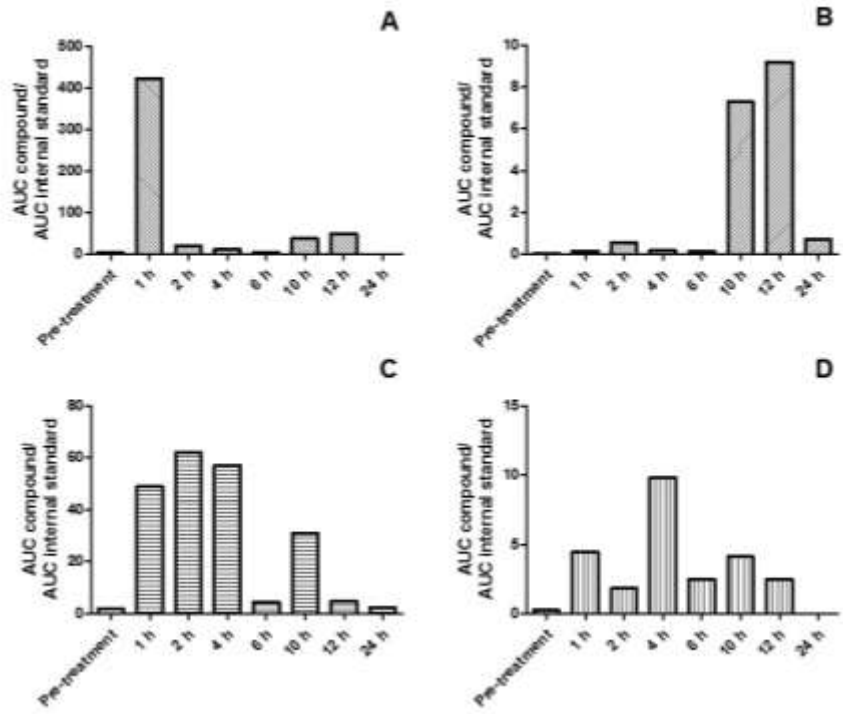


***Figure 5*** *– Excretion profiles of 5-(3' -hydroxyphenyl)- gamma-valerolactone-4' -O-sulphate (A), quercetin (B), p-coumaric acid (C) and 3-O-methylcatechin sulphate (D)*

| NAME | $T_{MAX}$ | IDENTIFICATION APPROACH |
|---|---|---|
| 2-Hydroxybenzoic | 1h | On Target |
| Cinnamic acid | 1h | On Target |
| 2,3-Dihydroxybenzoic acid | 1h | On Target |
| Hydroxyhippuric acid isomer 1 | 1h | On Target/Off Target |
| Hydroxyhippuric acid isomer 2 | 1h | On Target/Off Target |
| 2,5-Dihydroxybenzoic acid | 1h | On Target |
| 3,4-Dihydroxyphenylacetic acid | 1h | On Target/Off Target |
| Kaempferol | 12h | On Target |
| Quercetin | 12h | On Target |
| Isorhamnetin | 12h | On Target |
| Syringetin | 12h | On Target |
| Quinic acid | 1h | Off Target |
| 2'-Hydroxygenistein | 1h | Off Target |
| 4-Hydroxy-5-(dihydroxyphenyl)-valeric acid-O-sulphate | 1h | Off Target |
| Salyciluric glucuronide | 1h | Off Target |
| 5-(3' -hydroxyphenyl)- gamma-valerolactone-4' -O-sulphate | 1h | Off Target |
| 5-(3' ,4' -dihydroxyphenyl)-gamma-valerolactone | 12h | Off Target |

***Table 6*** *– Cranberry components and metabolites that have the highest relative content in the active urine fractions.*

## 4. Discussion

### *4.1 Compounds identified using the on target analysis*

The on target analysis allowed the identification of several cranberry components already present in the extract as well as some known metabolites. The results reported are based on the acquisition in negative ion mode, since the positive mode didn't show more information. In fact, anthocyanins, which are the main components well ionized in positive acquisition mode, were not detected at all. The reason of their absence in urine could be that they have low bioavailability, but also because they can be catabolised by the colonic microflora into small phenolic compounds, such as protocatechuic acid, phloroglucinaldehyde, ferulic acid, syringic acid, gallic acid and vanillic acid [29-31]. In the present study we detected protocatechuic acid, ferulic acid, gallic acid and vanillic acid. Some flavonols were found as well as some of their glicosilated forms : kaempferol, quercetin and traces of its glicosides (quercetin-3-O-arabinofuranoside, quercetin 3-O-rhamnoside and quercetin-3-O-galactoside), syringetin and isorhamnetin with traces of isorhamnetin-3-O-arabinopyranoside. The low abundance of the glicosilated forms is due to the enzymatic hydrolysis by cellular and bacterial β-glucosidases in the intestine into the relative aglycones [32]. The aglycones can undergo phase-II metabolism or methylation and they can be transformed by microbiota in the intestinal tract into phenolic acids by C-ring cleavage [33]. Studies performed on quercetin (the most representative flavonol) and related

glicoside metabolisms in the intestine showed that the main metabolites are represented by hydroxyphenylacetic acid catabolites [34, 35]. Having performed β-glucuronidase hydrolysis, we were able to detect the aglycon of quercetin, kaempferol, syringetin and isorhamnetin as free form. The last one can derive from the isorhamnetin derivatives present in the extract or from the methylation of quercetin. Moreover, 3,4-dihydroxyphenylacetic acid was found in urine as possible metabolite of flavonols deriving from intestinal microbiota metabolism. Proanthocyanidins present in the extract (procyanidins A-type and B-type) were not detected in urine in the present study. Controversial results have been obtained on this class of polyphenols in previous studies, in particular concerning procyanidin A2 to which several studies attributed the activity of cranberry products in UTIs prevention. In most cases they weren't found in human urine [15-18] as in our study. By contrast, two works reported PACs in human urine : one work was performed on men and postmenopausal women of 50–70 years who assumed a single dose of 237 mL of cranberry juice (PACs content in the juice was not reported) [19]; in the second study, performed by the same research group, five young women (20-30 years) consumed 237 mL/day of cranberry juice (140 mg of PACs) according to a weekly schedule for 7 weeks [20]. The results that they obtained were very low levels of PAC-A2 quantified in human urine (Cmax = 24 ng/mg creatinine) and they concluded that PAC-A2 cannot be used as biomarker of cranberry intake since there was not correlation with the amount of juice consumed. Taking into consideration all these results, it is commonly accepted that PACs

have a very low bioavailability, which decreases as the degree of their polymerization increases [27]. Moreover, it is reported that human microbiota degrades PACs in the colon into phenolic compounds : phenylacetic acids and phenylpropionic acids as metabolites of procyanidins A2, B2, catechin and epicatechin ; for procyanidin B2, catechin and epicatechin also valerolactones and valeric acids derivatives [36, 37]. In the present study, we detected 3,4-dihydroxyphenylacetic acid and 3-(4-hydroxyphenyl)-propionic acid, but also dihydroxybenzoic acids, hydroxybenzoic acid and hydroxyhippuric acids which are metabolites deriving from phenylpropionic acids [38]. The main class of polyphenols identified was the one of phenolic acids : protocatechuic acid, *p*-coumaric acid, gallic acid and sinapinic acid were already found in the extract, but they can also derive from the metabolism of other polyphenols as mentioned above ; 3,4-dihydroxyhydrocinnamic acid and cinnamic acid probably derived from the metabolism of chlorogenic acid [16], while hydroxybenzoic acid, dihydroxybenzoic acids, hippuric acid and hydroxyhippuric acids can derived from the metabolism of all the other flavonoid components [38].

*4.2 Compounds identified using the off target analysis*

In the off target analysis several metabolites were identified. Some of them had already been identified using the on target analysis, confirming the reliability of this second approach. *Figure 6* shows an overview of all the

compounds which have been identified in the present study with the on target (red circle) and off target (blue circle) analyses.

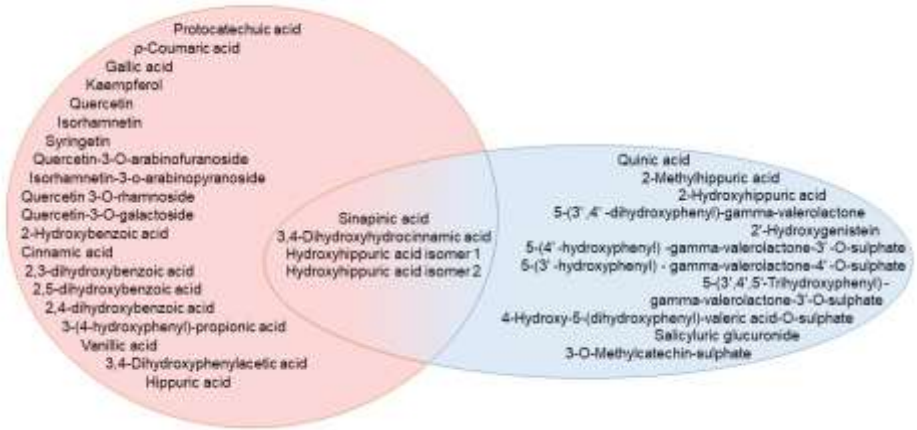


***Figure 6*** *– Venn diagram reporting all the compounds identified with the on target (red circle) and off target (blue circle) analyses.*

Compounds already identified were : 3,4-dihydroxyhydrocinnamic acid, sinapinic acid and the two hydroxyhippuric acid isomers, which were annotated by CFM-ID as 4- and 2-hydroxyhippuric acids. However standards will be used to confirm the correct identities of this two isomers. Most of the other compounds were putatively identified with CFM-ID as the best match (given by the highest Jaccard score), but the identities of the top 5 candidates were manually verified in order to give an annotation that could also have a biological meaning. Two acids were identified : quinic acid, which can derive from chlorogenic acid, and 2-methylhippuric acid, a methyl derivative of hippuric acid. 2'-hydroxygenistein was found as first candidate for the ion 285.0406 m/z, but it cannot derive from cranberry intake since it is not present

in the extract and cannot be a product of metabolism. Other possible candidates returned by CFM-ID are other isoflavones (3'-Hydroxygenistein), some aurones (Cernuine, Maritimetin), one flavone (Luteolin) and one flavonol (Kaempferol, excluded because the retention time was different from that characterized in the extract), but none of them could derive from the extract or from the metabolism of extract components. In this case to obtain an identification, further studies are needed (e.g. the use of standard). Different valerolactones and one valeric acid derivative were identified : 5-(3' ,4' -dihydroxyphenyl)-gamma-valerolactone, 5-(4' -hydroxyphenyl) -gamma-valerolactone-3'-O-sulphate, 5-(3' -hydroxyphenyl) - gamma-valerolactone-4' -O-sulphate, 5-(3',4',5'-Trihydroxyphenyl) -gamma-valerolactone-3'-O-sulphate, 4-Hydroxy-5-(dihydroxyphenyl)-valeric acid-O-sulphate. Among those metabolites, 5-(3' -hydroxyphenyl) - gamma-valerolactone-4' -O-sulphate had been identified in previous studies [16, 18] and it was not included in the database used for the on target research because of the sulphate conjugation (not considered because of the β-glucuronidase hydrolysis, which also has sulphatase activity). In a very recent study, which reported other valerolactone derivatives, also 5-(3' ,4' -dihydroxyphenyl)-gamma-valerolactone was detected [39]. None of the other valerolactones here described were previously identified in urine after cranberry intake, but they are known to be PACs metabolites [37]. All the metabolites reported thus far were identified with the first approach of the off target analysis. While salicyluric glucuronide and 3-O-methylcatechin-sulphate were identified with

the second approach, which was itself shown to be less precise because it doesn't give a similarity score but it verified only the presence of overlapping fragments, so further investigation is needed. Since all these compounds have been identified by using the exact mass and the isotopic and the fragmentation pattern in comparison with *in silico* MS/MS spectra, a higher level of identification could be obtained by using standards of those components, so that the retention time can be used to confirm the identity. The results of all the studies performed on metabolites characterization in human urine after cranberry intake are reported in *Table 7* and compared to that obtained in the present study. As already discussed above, PACs were detected only in two studies [19, 20] but one of such [19] didn't report the amount of PACs in the cranberry product. Moreover, PACs metabolites described were only phenolic acids and no valerolactone derivatives were detected. The study performed by Valentova et al. [15] didn't report in details all the compounds identified, but no valerolactones were present. All the other studies [16-18, 39] were based on a single-dose treatment constituted by a high content of PACs. Feliciano et al. [16,18] were able to identify a huge number of metabolites by using standards, but they detected only one valerolactone derivative. Peron et al. [39] identified a lower amount of metabolites but a higher number of valerolactone derivatives, two of which were detected also in our study.

| | PRESENT STUDY | VALENTOVA ET AL. [15] | MCKAY ET AL. [19] | WALSH ET AL. [20] | ISWALDI ET AL [17] | FELICIANO ET AL. [16,18] | PERON ET AL. [39] |
|---|---|---|---|---|---|---|---|
| **CRANBERRY TREATMENT** | 2 capsules/day standardized cranberry extract | 1200 mg/day of dried cranberry juice | 237 mL cranberry juice cocktail | 237 mL/day cranberry juice cocktail | 0.6 mL/kg of cranberry syrup | 450 mL of a single-strength cranberry juice beverage | 360 mg of cranberry extract |
| **PACS CONTENT** | 36 mg/capsule | 14.4 mg | NA | 140 mg | 0.71% (w/v) | 710 mg | 42.6% w/w of PAC-A/14.6% w/w of PAC-B |
| **TREATMENT TIME** | 7 days | 8 weeks | Single dose (24h) | 7 weeks | Single dose (24h) | Single dose (24h) | Single dose (24h) |
| **NUMBER OF METABOLITES** | 35 | NA | 26 | 19 | 32 | 57 | 14 |
| **PACS PRESENCE** | no | no | yes | yes | no | no | no |
| **N PACS METABOLITES (N VALEROLACTONES)** | 14 (5) | NA | 8 (0) | 7 (0) | 3 (0) | 17 (1) | 12 (6) |

***Table 7*** *– Results of known studies on metabolite characterization after cranberry products intake. The comparison regards: cranberry treatment, PACs content in the cranberry product used, the time of the treatment, the number of cranberry metabolites identidfied, the eventual presence of PACs and the number of known PACs metabolites including phenolic acid and valerolactone derivatives.*

### 4.3 Reduction of C. albicans adhesion and biomass production by urine fractions and putative bioactive components of the active fractions

The antiadhesive properties of cranberry, both *in vitro* and *in vivo*, have long been reported [40-43] mainly with regard to *E. coli*, which is the principal uropathogen that causes UTIs. An *in vitro* study showed that cranberry PACs prevent *C. albicans* biofilm formation in artificial urine [44]. In the present work we demonstrate for the first time that cranberry extract as well as some urine fractions after one week of cranberry treatment are able not only to reduce *C. albicans* adhesion but also its biomass production. Since the assay showed that fractions at 1 hour and 12 hours after the last capsule assumption were the most active, we focused attention on the components which reached their highest concentration in these fractions. The fraction at 1 hour contains mainly phenolic acids all deriving from the metabolism of cranberry polyphenols (identified with the on target analysis), but also one valerolactone and one valeric acid deriving from PACs metabolism. Among the phenolic acids selected, 3,4-dihydroxyphenylacetic acid was previously reported to have anti-adhesive activity, in an *in vitro* assay, against *E. coli* [45]. Moreover, a recent *in vitro* study [46] demonstrates that valerolactones derivatives have anti-adhesive activity against *E. coli*, confirming that the activity *in vivo* is not due to intact PACs but to their metabolites. The components found with the highest concentration in the 12 hours urine fraction are kaempferol, quercetin, syringetin, isorhamnetin and 5-(3' ,4' -dihydroxyphenyl)-gamma-

valerolactone. Considering the flavonol aglycones, they probably all derived from β-glucuronidase hydrolysis of the respective glucuronides or sulphates, but among those phenolics only quercetin was reported to have *in vitro* anti-adhesive properties [47]. However, the *in vitro* activity reported for these compounds is related to *E. coli*, so we cannot exclude all the others putative bioactive components.

## 5. Conclusions

The HR-MS method developed allowed the identification of several cranberry components and metabolites in human urine after a standardized cranberry extract assumption. PACs were not detected as reported by previous studies, but several metabolites deriving from their catabolism operated by the gut microflora and hereto not found *in vivo* were identified. The crude extract and these two urine fractions collected after cranberry intake were found to be active against *C. albicans* adhesion *ex-vivo*. Among the metabolites that reached their highest concentration in these fractions there are also two known metabolites of PACs, 4-Hydroxy-5-(dihydroxyphenyl)-valeric acid-O-sulphate and 5-(3' -hydroxyphenyl)- gamma-valerolactone-4' -O-sulphate. To our knowledge this is the first work which demonstrates an *ex-vivo* inhibition of *C. albicans* adhesion by human urine after cranberry intake. We are now working on understanding whether the activity is related to one or more

components or to a synergy of such. Moreover the study will be performed on a huge number of subjects in order to evaluate the inter-individual variability.

**Abbreviations:** UTIs, urinary tract infections; PACs, proanthocyanidins; CFM-ID, competitive fragmentation modeling for metabolite identification.

**Acknowledgments**

We gratefully acknowledge financial support from Indena S.p.A.

## References

[1] C.J. Nobile, A.D. Johnson, Candida albicans Biofilms and Human Disease, Annu Rev Microbiol 69 (2015) 71-92.
[2] J.M. Achkar, B.C. Fries, Candida infections of the genitourinary tract, Clin Microbiol Rev 23(2) (2010) 253-73.
[3] C.A. Kauffman, Diagnosis and management of fungal urinary tract infection, Infect Dis Clin North Am 28(1) (2014) 61-74.
[4] S. Saint, J. Wiese, J.K. Amory, M.L. Bernstein, U.D. Patel, J.K. Zemencuk, S.J. Bernstein, B.A. Lipsky, T.P. Hofer, Are physicians aware of which of their patients have indwelling urinary catheters?, Am J Med 109(6) (2000) 476-80.
[5] S. Tobudic, C. Kratzer, A. Lassnigg, E. Presterl, Antifungal susceptibility of Candida albicans in biofilms, Mycoses 55(3) (2012) 199-204.
[6] M. Heinonen, Antioxidant activity and antimicrobial effect of berry phenolics--a Finnish perspective, Mol Nutr Food Res 51(6) (2007) 684-91.
[7] S.H. Nile, S.W. Park, Edible berries: bioactive components and their effect on human health, Nutrition 30(2) (2014) 134-44.
[8] S. Skrovankova, D. Sumczynski, J. Mlcek, T. Jurikova, J. Sochor, Bioactive Compounds and Antioxidant Activity in Different Types of Berries, Int J Mol Sci 16(10) (2015) 24673-706.
[9] N.P. Seeram, L.S. Adams, M.L. Hardy, D. Heber, Total cranberry extract versus its phytochemical constituents: antiproliferative and synergistic effects against human tumor cell lines, J Agric Food Chem 52(9) (2004) 2512-7.
[10] X. Yan, B.T. Murphy, G.B. Hammond, J.A. Vinson, C.C. Neto, Antioxidant activities and antitumor screening of extracts from cranberry fruit (Vaccinium macrocarpon), J Agric Food Chem 50(21) (2002) 5844-9.
[11] C. Bodet, F. Chandad, D. Grenier, Cranberry components inhibit interleukin-6, interleukin-8, and prostaglandin E production by

lipopolysaccharide-activated gingival fibroblasts, Eur J Oral Sci 115(1) (2007) 64-70.
[12] I. Vasileiou, A. Katsargyris, S. Theocharis, C. Giaginis, Current clinical status on the preventive effects of cranberry consumption against urinary tract infections, Nutr Res 33(8) (2013) 595-607.
[13] E. Pappas, K.M. Schaich, Phytochemicals of cranberries and cranberry products: characterization, potential health effects, and processing stability, Crit Rev Food Sci Nutr 49(9) (2009) 741-81.
[14] A.B. Howell, J.D. Reed, C.G. Krueger, R. Winterbottom, D.G. Cunningham, M. Leahy, A-type cranberry proanthocyanidins and uropathogenic bacterial anti-adhesion activity, Phytochemistry 66(18) (2005) 2281-91.
[15] K. Valentova, D. Stejskal, P. Bednar, J. Vostalova, C. Cíhalík, R. Vecerova, D. Koukalova, M. Kolar, R. Reichenbach, L. Sknouril, J. Ulrichova, V. Simanek, Biosafety, antioxidant status, and metabolites in urine after consumption of dried cranberry juice in healthy women: a pilot double-blind placebo-controlled trial, J Agric Food Chem 55(8) (2007) 3217-24.
[16] R.P. Feliciano, A. Boeres, L. Massacessi, G. Istas, M.R. Ventura, C. Nunes Dos Santos, C. Heiss, A. Rodriguez-Mateos, Identification and quantification of novel cranberry-derived plasma and urinary (poly)phenols, Arch Biochem Biophys 599 (2016) 31-41.
[17] I. Iswaldi, D. Arráez-Román, A.M. Gómez-Caravaca, M.e.M. Contreras, J. Uberos, A. Segura-Carretero, A. Fernández-Gutiérrez, Identification of polyphenols and their metabolites in human urine after cranberry-syrup consumption, Food Chem Toxicol 55 (2013) 484-92.
[18] R.P. Feliciano, E. Mecha, M.R. Bronze, A. Rodriguez-Mateos, Development and validation of a high-throughput micro solid-phase extraction method coupled with ultra-high-performance liquid chromatography-quadrupole time-of-flight mass spectrometry for rapid identification and quantification of phenolic metabolites in human plasma and urine, J Chromatogr A 1464 (2016) 21-31.
[19] D.L. McKay, C.Y. Chen, C.A. Zampariello, J.B. Blumberg, Flavonoids and phenolic acids from cranberry juice are bioavailable and bioactive in healthy older adults, Food Chem 168 (2015) 233-40.
[20] J.M. Walsh, X. Ren, C. Zampariello, D.A. Polasky, D.L. McKay, J.B. Blumberg, C.Y. Chen, Liquid chromatography with tandem mass spectrometry quantification of urinary proanthocyanin A2 dimer and its potential use as a biomarker of cranberry intake, J Sep Sci 39(2) (2016) 342-9.
[21] A. Ledda, G. Belcaro, M. Dugall, B. Feragalli, A. Riva, S. Togni, L. Giacomelli, Supplementation with high titer cranberry extract (Anthocran®) for the prevention of recurrent urinary tract infections in elderly men suffering from moderate prostatic hyperplasia: a pilot study, Eur Rev Med Pharmacol Sci 20(24) (2016) 5205-5209.

[22] A. Ledda, G. Belcaro, M. Dugall, A. Riva, S. Togni, R. Eggenhoffner, L. Giacomelli, Highly standardized cranberry extract supplementation (Anthocran®) as prophylaxis in young healthy subjects with recurrent urinary tract infections, Eur Rev Med Pharmacol Sci 21(2) (2017) 389-393.
[23] B.O. Keller, J. Sui, A.B. Young, R.M. Whittal, Interferences and contaminants encountered in modern mass spectrometry, Anal Chim Acta 627(1) (2008) 71-81.
[24] C.G. Pierce, P. Uppuluri, A.R. Tristan, F.L. Wormley, E. Mowat, G. Ramage, J.L. Lopez-Ribot, A simple and reproducible 96-well plate-based method for the formation of fungal biofilms and its application to antifungal susceptibility testing, Nat Protoc 3(9) (2008) 1494-500.
[25] I. Iswaldi, A.M. Gómez-Caravaca, D. Arráez-Román, J. Uberos, M. Lardón, A. Segura-Carretero, A. Fernández-Gutiérrez, Characterization by high-performance liquid chromatography with diode-array detection coupled to time-of-flight mass spectrometry of the phenolic fraction in a cranberry syrup used to prevent urinary tract diseases, together with a study of its antibacterial activity, J Pharm Biomed Anal 58 (2012) 34-41.
[26] R. Rajbhandari, N. Peng, R. Moore, A. Arabshahi, J.M. Wyss, S. Barnes, J.K. Prasain, Determination of cranberry phenolic metabolites in rats by liquid chromatography-tandem mass spectrometry, J Agric Food Chem 59(12) (2011) 6682-8.
[27] R.P. Feliciano, C.G. Krueger, J.D. Reed, Methods to determine effects of cranberry proanthocyanidins on extraintestinal infections: Relevance for urinary tract health, Mol Nutr Food Res 59(7) (2015) 1292-306.
[28] R. Ohnishi, H. Ito, N. Kasajima, M. Kaneda, R. Kariyama, H. Kumon, T. Hatano, T. Yoshida, Urinary excretion of anthocyanins in humans after cranberry juice ingestion, Biosci Biotechnol Biochem 70(7) (2006) 1681-7.
[29] R.M. de Ferrars, C. Czank, Q. Zhang, N.P. Botting, P.A. Kroon, A. Cassidy, C.D. Kay, The pharmacokinetics of anthocyanins and their metabolites in humans, Br J Pharmacol 171(13) (2014) 3268-82.
[30] S.C. Forester, A.L. Waterhouse, Identification of Cabernet Sauvignon anthocyanin gut microflora metabolites, J Agric Food Chem 56(19) (2008) 9299-304.
[31] A. Rodriguez-Mateos, D. Vauzour, C.G. Krueger, D. Shanmuganayagam, J. Reed, L. Calani, P. Mena, D. Del Rio, A. Crozier, Bioavailability, bioactivity and impact on health of dietary flavonoids and related compounds: an update, Arch Toxicol 88(10) (2014) 1803-53.
[32] A. Scalbert, G. Williamson, Dietary intake and bioavailability of polyphenols, J Nutr 130(8S Suppl) (2000) 2073S-85S.
[33] K. Kawabata, R. Mukai, A. Ishisaka, Quercetin and related polyphenols: new insights and implications for their bioactivity and bioavailability, Food Funct 6(5) (2015) 1399-417.

[34] I.B. Jaganath, W. Mullen, C.A. Edwards, A. Crozier, The relative contribution of the small and large intestine to the absorption and metabolism of rutin in man, Free Radic Res 40(10) (2006) 1035-46.
[35] H. Schneider, A. Schwiertz, M.D. Collins, M. Blaut, Anaerobic transformation of quercetin-3-glucoside by bacteria from the human intestinal tract, Arch Microbiol 171(2) (1999) 81-91.
[36] K. Ou, P. Sarnoski, K.R. Schneider, K. Song, C. Khoo, L. Gu, Microbial catabolism of procyanidins by human gut microbiota, Mol Nutr Food Res 58(11) (2014) 2196-205.
[37] M. Monagas, M. Urpi-Sarda, F. Sánchez-Patán, R. Llorach, I. Garrido, C. Gómez-Cordovés, C. Andres-Lacueva, B. Bartolomé, Insights into the metabolism and microbial biotransformation of dietary flavan-3-ols and the bioactivity of their metabolites, Food Funct 1(3) (2010) 233-53.
[38] D. Del Rio, A. Rodriguez-Mateos, J.P. Spencer, M. Tognolini, G. Borges, A. Crozier, Dietary (poly)phenolics in human health: structures, bioavailability, and evidence of protective effects against chronic diseases, Antioxid Redox Signal 18(14) (2013) 1818-92.
[39] G. Peron, S. Sut, A. Pellizzaro, P. Brun, D. Voinovich, I. Castagliuolo, S. Dall'Acqua, The antiadhesive activity of cranberry phytocomplex studied by metabolomics: Intestinal PAC-A metabolites but not intact PAC-A are identified as markers in active urines against uropathogenic Escherichia coli, Fitoterapia 122 (2017) 67-75.
[40] G. Ermel, S. Georgeault, C. Inisan, M. Besnard, Inhibition of adhesion of uropathogenic Escherichia coli bacteria to uroepithelial cells by extracts from cranberry, J Med Food 15(2) (2012) 126-34.
[41] J.P. Lavigne, G. Bourg, C. Combescure, H. Botto, A. Sotto, In-vitro and in-vivo evidence of dose-dependent decrease of uropathogenic Escherichia coli virulence after consumption of commercial Vaccinium macrocarpon (cranberry) capsules, Clin Microbiol Infect 14(4) (2008) 350-5.
[42] K. Gupta, M.Y. Chou, A. Howell, C. Wobbe, R. Grady, A.E. Stapleton, Cranberry products inhibit adherence of p-fimbriated Escherichia coli to primary cultured bladder and vaginal epithelial cells, J Urol 177(6) (2007) 2357-60.
[43] A. Turner, S.N. Chen, M.K. Joike, S.L. Pendland, G.F. Pauli, N.R. Farnsworth, Inhibition of uropathogenic Escherichia coli by cranberry juice: a new antiadherence assay, J Agric Food Chem 53(23) (2005) 8940-7.
[44] M.L. Porter, C.G. Krueger, D.A. Wiebe, D.G. Cunningham, J.D. Reed, Cranberry proanthocyanidins associate with low-density lipoprotein and inhibit in vitro Cu2+-induced oxidation., Journal of Science of Food and Agricolture (2001).
[45] D.G. de Llano, A. Esteban-Fernández, F. Sánchez-Patán, P.J. Martínlvarez, M.V. Moreno-Arribas, B. Bartolomé, Anti-Adhesive Activity of Cranberry Phenolic Compounds and Their Microbial-Derived Metabolites

against Uropathogenic Escherichia coli in Bladder Epithelial Cell Cultures, Int J Mol Sci 16(6) (2015) 12119-30.
[46] P. Mena, D. Gonzalez de Llano, N. Brindani, A. Esteban-Fernandez, C. Curti, M.V. Moreno-Arribas, D. Del Rio, 5-(3′,4′-Dihydroxyphenyl)-γ-valerolactone and its sulphate conjugates, representative circulating metabolites of flavan-3-ols, exhibit anti-adhesive activity against uropathogenic Escherichia coli in bladder epithelial cells, Journal of Functional Food 29 (2017) 275-280.
[47] C. Rodríguez-Pérez, R. Quirantes-Piné, J. Uberos, C. Jiménez-Sánchez, A. Peña, A. Segura-Carretero, Antibacterial activity of isolated phenolic compounds from cranberry (Vaccinium macrocarpon) against Escherichia coli, Food Funct 7(3) (2016) 1564-73.

**Table S1 – Database used for the on target analysis**

| Name | $[M]^+$ | Source |
|---|---|---|
| Cyanidin | 287.05556 | Cranberry extract |
| Peonidin | 301.07121 | Cranberry extract |
| Pelargonidin-3-O-arabinoside | 403.10290 | [28] |
| Cyanidin-3-O-arabinoside | 419.09782 | Cranberry extract |
| Peonidin-3-O-arabinoside | 433.11347 | Cranberry extract |
| Pelargonidin-3-O-galactoside | 433.11347 | [28] |
| Delphinidin-3-O-arabinoside | 435.09273 | [15,28] |
| Cyanidin-3-O-galactoside | 449.10838 | Cranberry extract |
| Cyanidin-3-O-glucoside | 449.10838 | Cranberry extract |
| Petunidin-3-O-arabinoside | 449.10838 | Cranberry extract |
| Peonidin-3-O-galactoside | 463.12403 | Cranberry extract |
| Peonidin 3-O-glucoside | 463.12403 | Cranberry extract |
| Malvidin-3-O-arabinoside | 463.12403 | [28] |
| Petunidin-3-O-galactoside | 479.11895 | [28] |
| Malvidin-3-O-galactoside | 493.13460 | Cranberry extract |
| Malvidin-3-O-glucoside | 493.13460 | Cranberry extract |

| Name | $[M+H]^+$ | $[M-H]^-$ | Source |
|---|---|---|---|
| Coumarin | 147.0446 | 145.02896 | Cranberry extract |
| Scopoletin | 193.05008 | 191.03444 | Cranberry extract |
| Methyl-scopoletin | 208.07355 | 206.0579 | [17] |
| Apigenin | 271.06064 | 269.04499 | [15] |
| Kaempferol | 287.05556 | 285.03992 | Cranberry extract |
| Dihydrocatechin | 288.06338 | 286.04773 | [17] |
| Epicatechin | 291.08685 | 289.07121 | Cranberry extract |
| Catechin | 291.08686 | 289.07122 | Cranberry extract |
| Quercetin | 303.05047 | 301.03483 | Cranberry extract |
| Epigallocatechin | 307.08177 | 305.06613 | Cranberry extract |
| Gallocatechin | 307.08177 | 305.06613 | Cranberry extract |
| Methyl-quercetin | 316.0583 | 314.04265 | [17,29] |
| Isorhamnetin | 317.06612 | 315.05048 | Cranberry extract |
| Myricetin | 319.04539 | 317.02975 | Cranberry extract |
| 3'-O-methyl-myricetin | 333.06104 | 331.0454 | Cranberry extract |
| Syringetin | 347.07669 | 345.06104 | Cranberry extract |
| Quercetin-3-O-arabinofuranoside | 435.09273 | 433.07709 | Cranberry extract |
| Quercetin-3-O-arabinopyranoside | 435.09273 | 433.07709 | Cranberry extract |
| Quercetin-3-O-xylopyranoside | 435.09273 | 433.07709 | Cranberry extract |
| Catechin-3-O-gallate | 443.09782 | 441.08218 | Cranberry extract |
| Epicatechin-3-O-gallate | 443.09782 | 441.08218 | Cranberry extract |
| Kaempferol-7-O-glucoside | 449.10838 | 447.09274 | Cranberry extract |
| Isorhamnetin-3-O-arabinofuranoside | 449.10838 | 447.09274 | Cranberry extract |
| Isorhamnetin-3-O-xylopyranoside | 449.10838 | 447.09274 | Cranberry extract |
| Isorhamnetin-3-O-arabinopyranoside | 449.10838 | 447.09274 | Cranberry extract |

| Name | $[M+H]^+$ | $[M-H]^-$ | Source |
|---|---|---|---|
| Quercetin-3-O-rhamnoside | 449.10839 | 447.09275 | Cranberry extract |
| Myricetin-3-O-arabinofuranoside | 451.08765 | 449.07201 | Cranberry extract |
| Myricetin-3-O-arabinopiranoside | 451.08765 | 449.07201 | Cranberry extract |
| Myricetin-3-O-xylopyranoside | 451.08765 | 449.07201 | Cranberry extract |
| Quercetin 3-O-glucoside | 465.10329 | 463.08765 | Cranberry extract |
| Quercetin-3-O-galactoside | 465.1033 | 463.08766 | Cranberry extract |
| Methoxyquercetin 3-O-galactoside | 479.11894 | 477.10329 | [17] |
| Isorhamnetin-3-O-glucopyranoside | 479.11894 | 477.1033 | Cranberry extract |
| Isorhamnetin-3-O-glucofuranoside | 479.11894 | 477.1033 | Cranberry extract |
| Isorhamnetin-3-O-galactoside | 479.11894 | 477.1033 | Cranberry extract |
| Syringetin-3-O-arabinofuranoside | 479.11894 | 477.1033 | Cranberry extract |
| Syringetin-3-O-xylopyranoside | 479.11894 | 477.1033 | Cranberry extract |
| Syringetin-3-O-arabinopyranoside | 479.11894 | 477.1033 | Cranberry extract |
| Myricetin-3-O-glucoside | 481.0982 | 479.08256 | Cranberry extract |
| Myricetin-3-β-O-galactoside | 481.09821 | 479.08257 | Cranberry extract |
| Methoxyquercetin-3-O-galactoside + OH | 494.10603 | 492.09038 | [17] |
| Syringetin-3-O-rhamnoside | 493.1346 | 491.11896 | Cranberry extract |
| Proanthocyanidin A-Type dimer | 577.13457 | 575.11893 | Cranberry extract |
| Proanthocianidin B-Type dimer | 579.15022 | 577.13458 | Cranberry extract |
| Proanthocyanidin A-Type trimer | 865.19796 | 863.18232 | Cranberry extract |
| Proanthocyanidin B-Type trimer | 867.21361 | 865.19797 | Cranberry extract |

| Name | $[M-H]^-$ | Source |
|---|---|---|
| Benzoic acid | 121.02896 | Cranberry extract |
| 4-Hydroxyibenzaldehyde | 121.02895 | [18] |
| Phenylacetic acid | 135.04460 | [16,18] |
| 2-Hydroxybenzoic acid | 137.02387 | [16,18] |
| 3-Hydroxybenzoic acid | 137.02387 | [18-20] |
| 4-Hydroxybenzoic acid | 137.02387 | [18-20] |
| Cinnamic acid | 147.04461 | [16,18] |
| 4-Hydroxyphenylacetic acid | 153.03951 | [18-20] |
| Phloroglucinaldehyde | 153.03879 | [29] |
| 2,3-Dihydroxybenzoic acid | 153.01879 | [15] |
| 2,4-Dihydroxybenzoic acid | 153.01879 | [15] |
| 2,5-Dihydroxybenzoic acid | 153.01879 | [15] |
| Protocatechuic acid | 153.01879 | Cranberry extract |
| *p*-Coumaric acid | 163.03952 | Cranberry extract |
| 3-(4-hydroxyphenyl)-propionic acid | 165.05516 | [18] |
| Vanillic acid | 167.03444 | [16,18-20] |
| 3,4-Dihydroxyphenylacetic acid | 167.03444 | [18-20] |
| Gallic acid | 169.01370 | Cranberry extract |

| Name | $[M-H]^-$ | Source |
|---|---|---|
| Hippuric acid | 178.05042 | [15,17] |
| Caffeic acid | 179.03444 | Cranberry extract |
| 2-(4-hydroxyphenoxy)-propionic acid | 181.05008 | [16] |
| Homovanillic acid | 181.05008 | [16,18-20] |
| 3,4-Dihydroxyhydrocinnamic acid (Dihydrocaffeic acid) | 181.05008 | Cranberry extract |
| Ferulic acid | 193.05009 | Cranberry extract |
| Citric acid | 193.03482 | [15] |
| 4-hydroxyhippuric acid | 194.04533 | [16,18] |
| 3-hydroxyhippuric acid | 194.04533 | [16,18] |
| 2-hydroxyhippuric acid | 194.04533 | [16,18-20] |
| Dihydroferulic acid | 195.06573 | [16,18] |
| Syringic acid | 197.04550 | [16,18] |
| Sinapinic acid | 223.06065 | Cranberry extract |
| Coumaroyl-hexose (Formic Acid Adduct) | 325.09235 (371.09783) | Cranberry extract |
| Caffeoyl glucose $-H_2$ | 339.07160 | [17] |
| Caffeoyl glucose | 341.08726 | Cranberry extract |
| Chlorogenic acid | 353.08727 | Cranberry extract |
| Sinapoyl-hexose | 385.11348 | Cranberry extract |

# Study 2

**Pharmacokinetic profile of bilberry anthocyanins in rats and the role of glucose transporters: LC-MS/MS and computational studies**

**Abstract**

The aim of the present investigation was to better understand the pharmacokinetic profile of bilberry (*Vaccinium Myrtillus*) anthocyanins and the role of glucose transporters (sGLT1 and GLUT2) on their absorption. In particular, the absorption of 15 different anthocyanins contained in a standardized bilberry extract (Mirtoselect®) was measured in rats by a validated LC-ESI-MS/MS approach. The plasma concentration peak (C*max*) of 11.1 ng/mL was reached after 30 minutes and fasting condition significantly increased the bioavailability of anthocyanins by more than 7 fold in respect to fed rats. Glucose co-administration did not interfere with the overall anthocyanin uptake.

Bioavailability of each anthocyanin was then estimated by comparing the relative content in plasma *vs* extract. The 15 anthocyanins behaved differently in term of bioavailability and both the aglycone and the sugar moiety were found to affect the absorption. For instance, arabinoside moiety was detrimental while cyanidin enhanced bioavailability. Computational studies permitted to rationalize such results, highlighting the role of glucose transporters (sGLT1 and GLUT2) in anthocyanins absorption. In particular a significant correlation was found for the 15 anthocyanins between sGLT1 and GLUT2 recognition and absorption.

## 1. Introduction

Anthocyanins (from Greek anthos = flower and kyanos = blue) are water-soluble pigments, widely present in plants and belonging to the flavonoid class. They are responsible for the distinctive colours of plant tissues like blue, purple and red [1]. Their basic structure is composed of two aromatic rings (A and B) that are linked together by three carbon atoms forming a heterocycle with an oxygen atom (ring C). This basic structure, named anthocyanidin, is characterized by several hydroxyl groups to which are bound one or more sugar moieties, leading to a high number of possible compounds. The principal anthocyanidins present in nature are six, namely cyanidin (Cya), peonidin (Peo), petunidin (Pet), delphinidin (Del), malvidin (Mal) and pelargonidin (Pel). The glycosidic bond occurs mostly at C3 position but a second glycosylation frequently occurs on the C5 or C7: the sugars involved are mainly hexoses (glucose and galactose) or pentoses (arabinose, rhamnose and xylose) [2].

Several studies report the health benefits of anthocyanins, such as antioxidant [3], anti-inflammatory [4] and anticarcenogenic properties [5], leading to a potential use of these molecules in several oxidative-based diseases. Moreover, epidemiological evidence suggests that the consumption of anthocyanins decreases the risk of cardiovascular diseases, cancer growth and chronic degenerative diseases [6-8].

Bioavailability of anthocyanins was believed to be low [9], less than 2% [10], but then, using a stable isotopically labelled anthocyanin, it was found that it is comparable to that of other flavonoids; in particular bioavailability of cyanidin-3-glucoside was estimated to be at least 12 % [11]. Several studies have shown that anthocyanins are rapidly absorbed as such in the stomach and small intestine [12-15]. After ingestion, anthocyanins appear to permeate the stomach mucosa; proposed mechanisms include a bilitranslocase carrier and a saturable transporter, GLUT1 [16-18]. More recently, computational studies have shown at molecular level that anthocyanins can bind to glucose transporters such as GLUT1 thus underlining the importance of such a transporter for anthocyanin bioavailability [18]. However more studies are needed to study the role of gastric GLUT1 on anthocyanin absorption, also considering that little is known on the distribution of GLUT1 in the stomach tissue. Nevertheless, the majority of absorption and transformation occurs in the small intestine where anthocyanins are hypothesized to undergo a glucose dependent absorption which is mediated by sGLT1 and GLUT2, the latter providing a basolateral exit [19]. An elegant in vitro confirmation of such an absorption mechanism has been reported by Zou et al [20] who by using human intestinal epithelial (Caco-2) cells have found that cyanidin-3-O-β-glucoside absorption is dependent on the activities of sGLT1 and GLUT2.

Based on these premises, the aim of the present investigation is to better understand the role of glucose transporters and in particular of sLGT1 and GLUT2 on anthocyanin absorption. To do this, the absorption of 15 different

anthocyanins contained in a standardized bilberry extract (Mirtoselect®, 36% anthocyanins, Indena) (*Table 1*) was measured by a validated LC-ESI-MS/MS approach; the role of sGLT1 and GLUT2 in modulating the yield of absorption of each anthocyanin was then investigated by docking studies which provided a better understanding of the molecular recognition of anthocyanins as well as the effects of sugar and the aglycone moieties. Finally, the effects of fasting and glucose co-ingestion on anthocyanin bioavailability was evaluated.

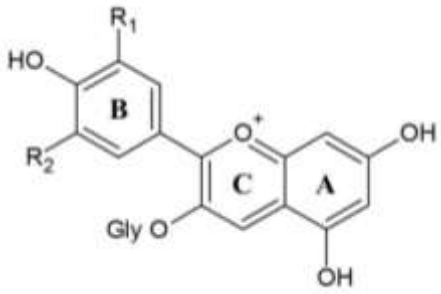


| *Anthocyanins* | $R_1$ | $R_2$ | *Gly* | *MW* |
|---|---|---|---|---|
| Cyanidin-3-O-arabinoside | OH | H | Arabinose | 419 |
| Peonidin-3-O-arabinoside | $OCH_3$ | H | Arabinose | 433 |
| Delphinidin-3-O-arabinoside | OH | OH | Arabinose | 435 |
| Cyanidin-3-O-galactoside | OH | H | Galactose | 449 |
| Cyanidin-3-O-glucoside | OH | H | Glucose | 449 |
| Petunidin-3-O-arabinoside | $OCH_3$ | OH | Arabinose | 449 |
| Peonidin-3-O-galactoside | $OCH_3$ | H | Galactose | 463 |
| Peonidin-3-O-glucoside | $OCH_3$ | H | Glucose | 463 |
| Malvidin-3-O-arabinoside | $OCH_3$ | $OCH_3$ | Arabinose | 463 |
| Delphinidin-3-O-galactoside | OH | OH | Galactose | 465 |
| Delphinidin-3-O-glucoside | OH | OH | Glucose | 465 |
| Petunidin-3-O-galactoside | $OCH_3$ | OH | Galactose | 479 |
| Petunidin-3-O-glucoside | $OCH_3$ | OH | Glucose | 479 |
| Malvidin-3-O-galactoside | $OCH_3$ | $OCH_3$ | Galactose | 493 |
| Malvidin-3-O-glucoside | $OCH_3$ | $OCH_3$ | Glucose | 493 |

***Table 1*** *– Anthocyanins contained in a standardized bilberry extract (Mirtoselect®)*

## 2. Materials and Methods

### *2.1 Reagents*

Formic acid, trichloroacetic acid (TCA) and LC–MS grade solvents were purchased from Sigma–Aldrich (Milan, Italy). LC-grade $H_2O$ (18 MΩ cm) was prepared with a Milli-Q $H_2O$ purification system (Millipore, Bedford, MA, USA). Naringenin-7-O-glucoside used as internal standard was from Extrasynthese (Genay, France). Standardized bilberry extract (*V. Myrtillus*) containing 36% anthocyanins (Mirtoselect®) was generously donated by Indena S.p.A (Milan, Italy).

### *2.2 Chromatographic condition*

The analyses were performed on a reversed-phase Agilent Zorbax SB-C18 (150 x 2.1 mm, i.d. 3.5µm, CPS analitica, Milan, Italy) protected by an Agilent Zorbax guard column, kept at 35°C, by a Surveyor system (ThermoFinnigan Italy, Milan, Italy) equipped with an autosampler kept at 4°C working at a constant flow rate (250 µL/min). 20 µL of sample were injected and the anthocyanins were eluted with a 38 min multistep gradient of phase A $H_2O$/HCOOH (100/1 % v/v) and phase B $CH_3CN$/$CH_3OH$/HCOOH (50/50/1 % v/v): 0-3 minutes, isocratic of 5% B; 3-8 minutes, from 5% B to 15 % B; 8-13 minutes, from 15% B to 28% B; 13-25.5 minutes, from 28% B to 32% B; 25.5-28 minutes, from 32% B to 50% B; 28-33 minutes, isocratic of 50% B; 33-34 minutes from 50% B to 5% B and then 34-38 minutes of isocratic 5% B.

*2.3 Qualitative profile of Mirtoselect® anthocyanins*

The qualitative analysis of the fifteen anthocyanins was performed on a LTQ-Orbitrap XL mass spectrometer using an ESI source (Thermo Scientific, Milan, Italy). Mirtoselect® 50 µg/mL, corresponding to 18 µg/mL of total anthocyanins, was analyzed working in full scan mode. Source parameters: spray voltage 4.5 kV, capillary temperature 270°C, capillary voltage 38 V, tube lens offset 110 V. A list of 20 background ions was adopted as lock mass values for real time mass calibration [24]. Mass spectra were acquired by the Orbitrap analyzer in positive ion mode using: profile mode, scan range *m/z* 100-700, AGC target 5 × 105, maximum inject time 1000 ms, resolving power 100000 (FWHM at *m/z* 400). The identification was obtained by using the exact mass.

*2.4 Characterization of MS/MS product ions for Multiple Reaction Monitoring analyses*

A multiple reaction monitoring (MRM) method was set up for the quantitative analyses. Mirtoselect® (50 µg/mL corresponding to 18 µg/mL of total anthocyanins) and the internal standard (1 µg/mL) dissolved in phase A were infused into the mass spectrometer at a flow rate of 10 µL/min to characterize the product ions of each compound. The fragmentation was performed in CID mode. The MS/MS analyses were performed with a TSQ Quantum Triple Quadrupole (Thermo Finnigan Italy, Milan, Italy) mass spectrometer fitted with an electrospray (ESI) interface operating in positive ion mode and with the

following source parameters: capillary temperature, 270°C; spray voltage 4.5 kV; capillary voltage, 35 V; and tube lens voltage 106 V. The parameters influencing the transitions were optimized as follows: argon gas pressure in the collision Q2, 1.0 mtorr; peak full width at half-maximum (fwhm), 0.50 *m/z* at Q1 and Q3; scan width for all MRM channels, 0.5 *m/z*; and scan rate (dwell time), 0.05 s/scan.

*2.5 Preparation of calibration curve and QC samples*

Sample preparation was optimized starting from that reported by Morazzoni et al. [25]. Samples for calibration curves were obtained by spiking a water solution of Mirtoselect® in blank plasma in order to reach the following final concentrations of anthocyanins: 3.6, 9.0, 18.0, 36.0, 90.0, 180.0, 360.0, 720.0 ng/mL. Samples were then spiked with the internal standard to reach a final concentration of 2.5 μM. After adding trichloroacetic acid (TCA, 5% as final concentration), samples were centrifuged at 8000 rpm for 10 minutes at 4°C and filtered on 0.45 μm Millex-LH filters (Millipore, Milan, Italy). The calibration curves (five replicates) were built by plotting the ratios (analyte/IS) between the sum of the areas under the peak of the fifteen anthocyanins and the the internal standard versus the nominal concentrations using a linearly weighted (1/x2) least squares regression. Data processing was performed by Xcalibur 2.0 software. QC samples used in the validation were prepared as calibration samples at three different anthocyanin concentrations: 3.6, 36.0, and 720.0 ng/mL.

*2.6 Method validation*

Method validation was performed based on US FDA guidelines for bioanalytical method validation (http://www.fda.gov/downloads/Drugs/Guidance/ucm070107.pdf) . The parameters evaluated were: selectivity, linearity and LLOQ, precision, accuracy, stability and carry-over effect.

2.7 *Pharmacokinetic study*

28 male Sprague Dawley rats (6 weeks old, 220 g of average body weight) were housed in cages (two animals/cage) at 21.5 ± 1.5° C under a 12 h light/dark cycle. All the animal procedures (including housing, health monitoring, restraint, dosing, etc) and ethical revision were performed according to the current Italian legislation (Legislative Decree March 4th, 2014 n. 26) enforcing the 2010/63/UE Directive on the protection of animals used for biomedical research. The rats were divided into four groups: the first group was not subject to a particular diet or starvation (they were allowed to eat 4RF21 GLP pellets *ad libitum*, supplied by Mucedola), the other groups were allowed only to drink water *ad libitum* for 18 hours before the treatment. All the groups were orally treated by gavage with the relative formulation (Mirtoselect® dry extract dissolved in water or in water plus glucose or only water plus glucose) prepared extemporaneously on the basis of the rat's weight. The fed rats were treated with 100 mg/kg Mirtoselect® (Group 1). The three groups of fasted rats underwent the following treatments: one group was

treated with 100 mg/kg Mirtoselect® (Group 2), one group was treated with 100 mg/kg Mirtoselect® and 1 g/kg glucose (Group 3) and the last group was treated only with 1 g/kg glucose (Group 4) as a control group of Group 3. Blood sample aliquots were withdrawn from the retro orbital sinus under anesthesia (isoflurane) before administration and after 5 min and 0.25, 0.5, 1, 2, 3, 6, 24 hours of the single oral dose.

Blood was put in heparinized tubes and within 30 minutes centrifuged at 10000g for 3 minutes at 4°C and plasma samples stored at -80°C until analysis. Plasma samples were prepared by adding 50 µL of 10% TCA and the internal standard to 50 µL of plasma samples, then centrifuged at 8000 rpm for 10 minutes at 4°C and filtered on 0.45 µm Millex-LH filters (Millipore, Milan, Italy). The pharmacokinetic parameters were calculated with PK solver add-in program for Microsoft Excel. Animal studies were conducted by Accelera Srl (Nerviano, Italy) (study numbers: 2016-0087, 2016-0169, 2016-0329).

### *2.8 Modelling studies*

By considering the known transporters responsible for the glucose absorption at the gastro-intestinal level, computational studies involved homology modelling and docking simulations on the human glucose transporters sGLT1 and GLUT2 [26]. Thus, the primary sequence of sGLT1 (P13866 SC5A1_HUMAN) and GLUT2 (P11168 GTR2_HUMAN) was retrieved from

Uniprot and submitted to SwissModel server to search reliable templates and to build the corresponding homology models. With regard to sGLT1, SwissModel proposed 11 possible templates among which the mutated form of the Na+/glucose cotransporter from *Vibrio parahaemolyticus* was selected since it covers 75% of the sequence with an identity of 30%. Again, 50 templates were proposed to model GLUT2 and the resolved structure of human GLUT1 was selected given its high coverage (90%) and identity (57.2%). The corresponding models were generated, refined and checked as described elsewhere.

Given their acid-base equilibria, anthocyanins were simulated in their neutral state (quinoidal base) considering the three well-known tautomeric forms (A1, 2-phenyl-5H-chromen-5-one; A2, 2-phenyl-7H-chromen-7-one; A3, 4-(2H-chromen-2-ylidene)cyclohexa-2,5-dien-1-one) plus the corresponding hemiketal form in both resulting enantiomers. For simplicity's sake, only the anionic form corresponding to A1 base was simulated, while the corresponding flavylium species were not investigated since they are stable only at very acidic pH ranges. Their conformational profile was investigated through MonteCarlo simulations and the so generated lowest energy structures were finally optimized by semi-empirical PM7 calculations using MOPAC2012. Docking simulations were performed by using PLANTS focusing the search within a 10 Å radius sphere around Gln314 for GLUT2 and Asp161 for sGLT1. The poses were ranked by using the ChemPLP function with a speed equal to 1. The generated best complexes were then

minimized and rescored by using ReScore+ [27]. The computed scores were finally utilized in correlative studies as performed by the Vega suite of programs [28]. The reported equations were generated by including at most two independent and non collinear (i.e. VIF < 5) variables which were selected by exhaustively combining all computed scores.

## 3. Results

### *3.1 Optimization of HPLC–MS/MS and HPLC-orbitrap method*

MS detection was performed in positive ion mode in both an orbitrap and triple quadrupole MS analyzers. MS parameters of collision energy (CE), spray voltage, capillary voltage and tube lens voltage were optimized in both the instruments by infusing a standard solution of Mirtoselect® to achieve maximum responses of precursor and product ions. To achieve good chromatographic behaviours and high responses of analytes, methanol and acetonitrile were tested as organic phase, and a higher chromatographic peak response was obtained when choosing a mixture of methanol and acetonitrile. We also investigated one additive, formic acid for the enhancement of ionization at two different percentages: 0.1% and 1% and the latter was found to be the suitable percentage.

### *3.2 Development of sample preparation procedure*

Two different protein precipitation methods were investigated: precipitation with solvent and with acid. When samples were pre-treated with acetonitrile,

recovery was low and a strong matrix interference was observed. The solvent precipitation was performed according to Morazzoni P et al. [25] which consisted of treating 0.5 mL of plasma with 0.5 mL 10% TCA and, after centrifugation, the precipitates were washed with 1 mL 5% TCA. We found that by eliminating the last step (washing procedure) the recovery was improved without impacting selectivity and matrix effects. Moreover the acid conditions permitted the maintenance of anthocyanins in the stable flavylium cation form.

### *3.3 Profiling plasma anthocyanins and metabolites by LC-ESI-orbitrap*

Identification of anthocyanins in rats treated with Mirtoselect® was firstly carried out by using an orbitrap as mass analyzer. Identification of the analytes was obtained by accurate mass and on the basis of the isotopic and fragmentation pattern, analyzing 0.25 and 0.5 h time point samples. As an example, in *Figure 1* is reported the identification of Cya-3-O-ara in a plasma sample withdrawn after 0.25 h Mirtoselect® ingestion. Anthocyanins were finally identified by comparing the relative retention time with that of the

standard components contained in Mirtoselect®. *Table 2* summarizes the analytes identified with the relative retention times.

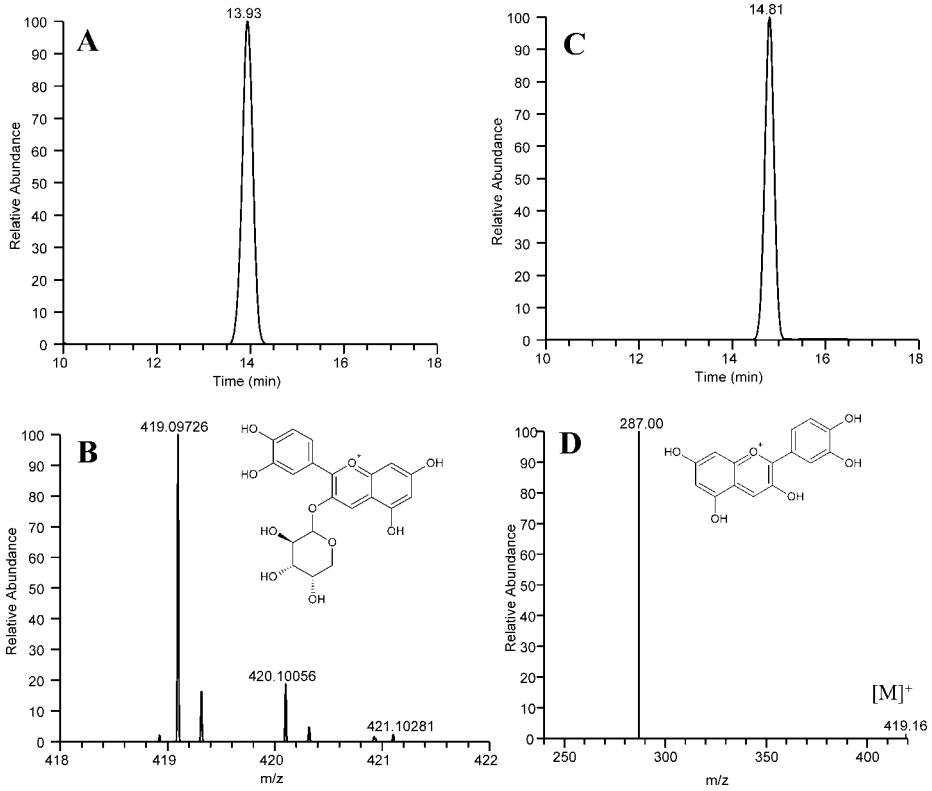


***Figure 1*** *– Identification of Cya-3-O-ara in a plasma sample withdrawn after 0.25 h Mirtoselect® ingestion. LC-ESI-MS analysis by using an orbitrap as MS analyzer: (A) Single ion chromatogram at m/z 419.09782; panel (B) shows the full MS spectrum reporting the experimental m/z value at 419.09726 (Δ ppm= -0.033) and the relative isotopic pattern; LC-ESI-MS analysis by using a triple quadrupole as MS analyzer: (C) MRM ion chromatogram using the transition m/z 419 → 287; (D) product ion MS spectrum setting the ion at m/z 419 as parent ion.*

| Anthocyanin | Calculated $[M]^+$ | Experimental $[M]^+$ | Δ ppm | Formula | RT min (RSD%) |
|---|---|---|---|---|---|
| Cya-3-O-ara | 419.09782 | 419.09726 | -0.033 | $C_{20}H_{19}O_{10}^+$ | 13.72 (0.94) |
| Peo-3-O-ara | 433.11347 | 433.11322 | 0.684 | $C_{21}H_{21}O_{10}^+$ | 16.53 (1.34) |
| Del-3-O-ara | 435.09273 | 435.09219 | 0.004 | $C_{20}H_{19}O_{11}^+$ | 12.27 (1.11) |
| Cya-3-O-gal | 449.10838 | 449.10788 | -0.041 | $C_{21}H_{21}O_{11}^+$ | 12.17 (1.00) |
| Cya-3-O-glu | 449.10838 | 449.10788 | -0.041 | $C_{21}H_{21}O_{11}^+$ | 12.88 (1.02) |
| Pet-3-O-ara | 449.10838 | 449.10788 | -0.041 | $C_{21}H_{21}O_{11}^+$ | 14.81 (1.47) |
| Peo-3-O-gal | 463.12403 | 463.12335 | -0.299 | $C_{22}H_{23}O_{11}^+$ | 14.62 (1.24) |
| Peo-3-O-glu | 463.12403 | 463.12335 | -0.299 | $C_{22}H_{23}O_{11}^+$ | 15.48 (1.03) |
| Mal-3-O-ara | 463.12403 | 463.12335 | -0.299 | $C_{22}H_{23}O_{11}^+$ | 17.30 (1.62) |
| Del-3-O-gal | 465.10330 | 465.10266 | -0.200 | $C_{21}H_{21}O_{12}^+$ | 10.96 (0.84) |
| Del-3-O-glu | 465.10330 | 465.10266 | -0.200 | $C_{21}H_{21}O_{12}^+$ | 11.46 (0.89) |
| Pet-3-O-gal | 479.11895 | 479.11838 | -0.048 | $C_{22}H_{23}O_{12}^+$ | 13.15 (1.36) |
| Pet-3-O-glu | 479.11895 | 479.11838 | -0.048 | $C_{22}H_{23}O_{12}^+$ | 13.77 (0.95) |
| Mal-3-O-gal | 493.13460 | 493.13388 | -0.351 | $C_{23}H_{25}O_{12}^+$ | 15.41 (0.76) |
| Mal-3-O-glu | 493.13460 | 493.13388 | -0.351 | $C_{23}H_{25}O_{12}^+$ | 16.16 (0.85) |

***Table 2*** *– Anthocyanins identified in plasma samples of rats after 0.25 h the oral administration of 100 mg/Kg of Mirtoselect®. Identification was achieved by LC-ESI-MS and using an orbitrap as mass analyzer.*

### *3.4 Quantitative analysis of anthocyanins in plasma*

Quantitative analysis of anthocyanins was then carried out by using an HPLC connected with a triple quadrupole set in MRM mode. The retention time of each anthocyanin as determined by HPLC-ESI orbitrap and HPLC-ESI-TSQ showed a minimum shift because of the different HPLC void volumes. *Table 3* summarizes the transitions used. Calibration curves were built by spiking Mirtoselect® to plasma samples and plotting the concentration versus the ratio between the sum of the area of each anthocyanin and the IS.

This method permits the determination of the overall plasma concentration of anthocyanins but not their individual absolute content. The amount of each anthocyanin was determined as a relative percentage in respect to the overall content of anthocyanins.

| Name | Parent ion (m/z) | Product ion (m/z) | Collision energy (V) |
|---|---|---|---|
| Cya-3-O-ara | 419 | 287 | 20 |
| Peo-3-O-ara | 433 | 301 | 20 |
| Del-3-O-ara | 435 | 303 | 20 |
| Cya-3-O-gal | 449 | 287 | 20 |
| Cya-3-O-glu | 449 | 287 | 20 |
| Pet-3-O-ara | 449 | 317 | 20 |
| Peo-3-O-gal | 463 | 301 | 20 |
| Peo-3-O-glu | 463 | 301 | 20 |
| Mal-3-O-ara | 463 | 331 | 20 |
| Del-3-O-gal | 465 | 303 | 20 |
| Del-3-O-glu | 465 | 303 | 20 |
| Pet-3-O-gal | 479 | 317 | 20 |
| Pet-3-O-glu | 479 | 317 | 20 |
| Mal-3-O-gal | 493 | 331 | 20 |
| Mal-3-O-glu | 493 | 331 | 20 |
| Naringenin-7-O-glucoside | 435 | 273 | 15 |

***Table 3*** *– Precursor and product ion pairs for MRM analysis of anthocyanins and Naringenin-7-O-glucoside chosen as internal standard.*

Anthocyanins, as well as the internal standard, are characterized by the loss of the sugar moiety as a neutral loss. The major product ion is the aglycone,

detected as $[M]^+$ ions for anthocyanins (*Figure 2*) and as $[M+H]^+$ for the internal standard.

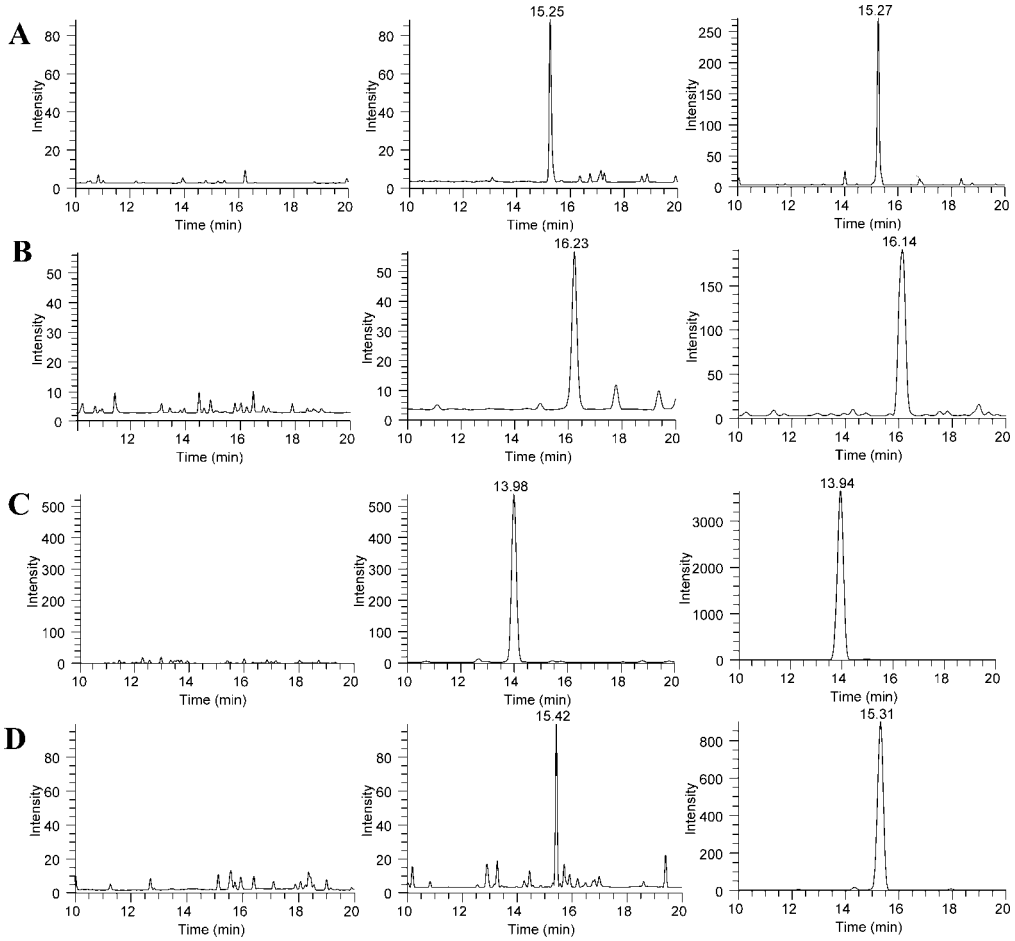


***Figure 2*** *– Representative MRM chromatograms of anthocyanin arabinosides in blank plasma (left panel), blank plasma spiked with Mirtoselect® at LLOQ (middle panel) and plasma sample collected after 0.25 h of Mirtoselect® administration (right panel). (A) Cya-3-o-ara, (B) Peo-3-O-ara, (C) Del-3-O-ara, (E) Pet-3-O-ara. Please note that the RT of the analytes identified by the LC-ESI-triple quadrupole are slight different in respect to the values determined by LC-ESI-orbitrap due to different void volumes.*

### *3.4.1. Selectivity*

Typical MRM chromatograms relative to the anthocyanin arabinosides and obtained from a blank sample, a spiked plasma sample with Mirtoselect® (at LLOQ) and IS, and a plasma sample after 0.25 h of the administration of Mirtoselect® 100 mg/kg are shown in *Figure 2*. No interference of endogenous peaks were exhibited in blank plasma samples collected from 7 different rats thus indicating the high selectivity of the method.

### *3.4.2. Linearity and LLOQ*

The method was validated over a range of 3.6-720.0 ng/mL of total anthocyanins. The $r^2$ values of the five calibration curves were > 0.997. The R.S.D. values on the slope were below 15%. Mean regression parameters are: y = 4.419 (± 0.06234) x - 0.04810 (± 0.01726). The LLOQ was 3.6 ng/mL with a R.S.D. < 5% and a bias < 18%.

### *3.4.3. Precision and accuracy*

The intra- and inter-day precision and accuracy obtained by QC samples are listed in *Table 4*. The RSD values of all analytes were less than 15.67% and the accuracy ranged from -19.3% to 14.82% (bias%). The results indicated that this method is reliable and reproducible enough for further pharmacokinetic studies.

| Anthocyanins concentration ng/mL | Intra-day (n=5) | | Inter-day (n=15) | |
|---|---|---|---|---|
| | Precision (RSD, %) | Accuracy (Bias %) | Precision (RSD, %) | Accuracy (Bias %) |
| 3.60 | 15.67 | -19.30 | 4.94 | 14.82 |
| 36.00 | 5.23 | -4.86 | 9.42 | 8.29 |
| 720.00 | 2.92 | 0.81 | 2.37 | 1.57 |

***Table 4*** *–Intra-day and inter-day precision and accuracy of the method.*

### *3.4.4 Stability*

Samples were tested only for two cycles of freeze-thaw. After one cycle of freeze-thaw anthocyanins were stable (±13%) while after two cycles they were no longer stable (loss > 50%). Anthocyanin concentration after 18 hours at 4°C fell within the ±15% range and so can be considered stable for the time analyses.

### *3.4.5 Carry-over effect*

Carry-over of all analytes in blank sample following the high concentration standard (ULOQ) was not greater than the 20% of the LLOQ and 5% for the IS.

## *3.5 Pharmacokinetic study*

The quantitative method was then applied to measure the concentrations of total anthocyanins in plasma samples of Groups 1, 2 and 3 at different time points (*Figure 3*). In *Table 5* are reported the relative pharmacokinetic parameters AUC, $T_{MAX}$ and $C_{MAX}$, calculated with PK solver add-in program for

Microsoft Excel. The plasma concentration peak was reached after 0.25 h for Group 2, while for the other two groups the peak was at 0.5 h.

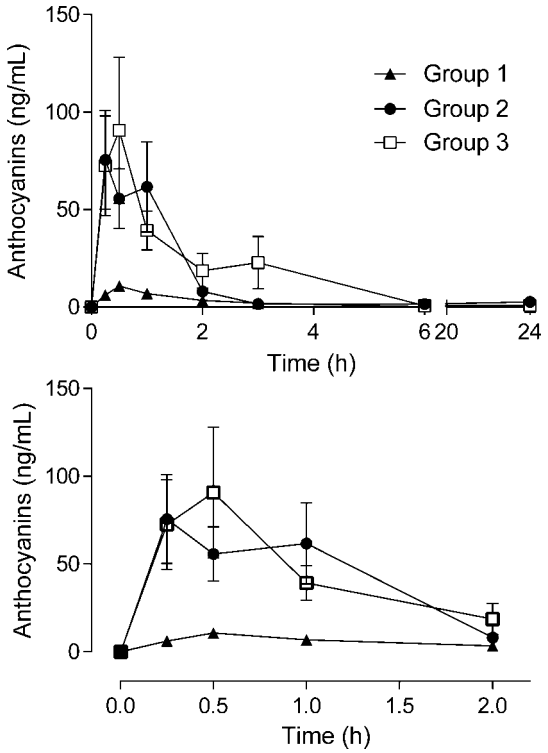


***Figure 3*** *- Plasma profile of anthocyanins in Group 1 (Fed rats treated with 100 mg/kg Mirtoselect®), Group 2 (Fasted rats treated with 100 mg/kg Mirtoselect®) and Group 3 (Fasted rats treated with 100 mg/kg Mirtoselect® and 1g/kg glucose). The lower graph is a blow-up of the 0-2 hours.*

| | AUC 0-t (ng/mL*h) | Tmax (h) | Cmax (ng/mL) |
|---|---|---|---|
| ***Group 1*** | 18.67 (0.90) | 0.50 (0.00) | 10.79 (1.02) |
| ***Group 2*** | 139.05 (33.75) | 0.25 (0.00) | 75.60 (23.14) |
| ***Group 3*** | 160.79 (21.26) | 0.50 (0.00) | 90.73 (32.92) |

***Table 5*** *– Mean and SEM of pharmacokinetic parameters of anthocyainis following 100 mg/Kg dose of Mirtoselect®*

The data well indicate that the fasting condition significantly increases the bioavailability of anthocyanins by more than 7 fold in respect to fed rats. Several reasons could explain the effect of food intake in reducing anthocyanin availability, such as the matrix effect and the interaction of anthocyanins with food components (proteins and lipids) and the effect of fasting on GLUT expression. We then used fasting rats to understand the effect of glucose intake on anthocyanin PK. The AUCs of anthocyanins given as such or with glucose were found superimposable and not significantly different, thus suggesting that glucose does not interfere with the overall anthocyanin uptake. The difference between the two curves can be found in the $T_{MAX}$ which was shifted by 15 min when glucose was added to anthocyanins thus indicating that glucose co-administration affects the kinetic but not the overall amount of absorbed anthocyanins. By contrast, it has been found by others in *in vitro* and *ex vivo* conditions [10, 22, 30] that anthocyanins inhibit glucose absorption thus indicating that the binding constant of anthocyanins and glucose towards GLUT transporters should be quite different.

The plasma content of each anthocyanin was then determined as a relative percentage in respect to the total amount of anthocyanins. Then, to compare the different bioavailability of anthocyanins, the relative plasma content of each anthocyanin was compared to that determined in Mirtoselect®. Based on this comparison, an anthocyanin better absorbed in respect to the others

contained in the mixture would be characterized by a relative content in plasma higher in respect to its relative content in the mixture. Therefore, the fifteen constituents can be divided into three classes: A) anthocyanins showing a relative abundance in plasma higher in respect to extract (more absorbed, *Figure 4A*); B) anthocyanins with no significant difference of relative abundance between plasma and extract (*Figure 4B*); C) anthocyanins with a plasma relative abundance lower in respect to that determined in the extract (less absorbed, *Figure 4C*). By comparing the anthocyanins characterized by the same anthocyanidin moiety but with the variable sugar moiety, the following rank could be considered: Cya-3-O-gal > glu >> ara; Peo-3-O-gal > glu >> ara; Del-3-O-gal > glu > ara; Mal-3-O-gal ~ glu > ara; Pet-3-O-gal > glu > ara.

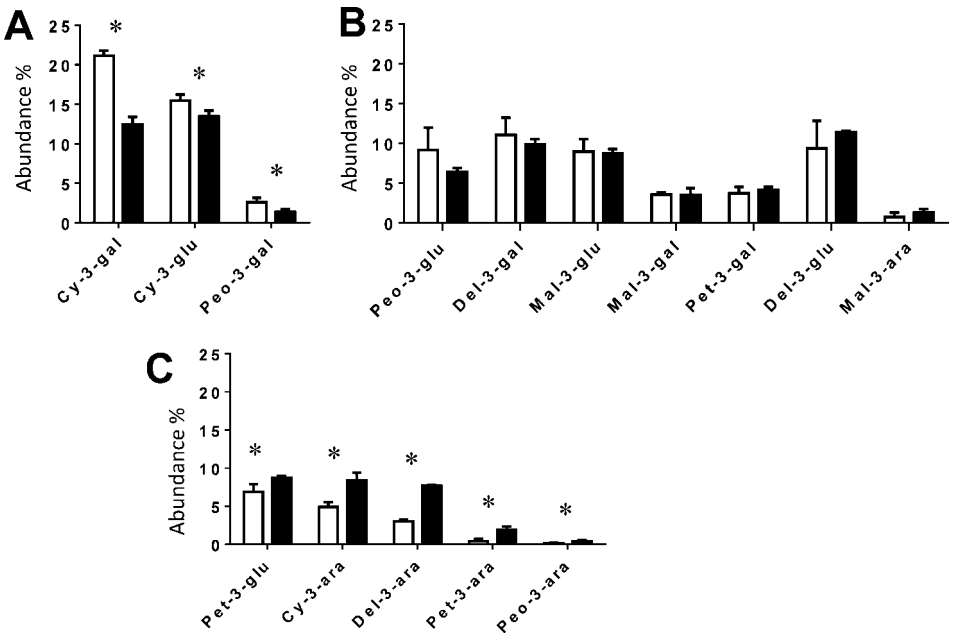


***Figure 4*** *– Relative abundance of Mirtoselect® anthocyanins in plasma in respect to the extract. Based on the difference in relative abundances, the 15 anthocyanins were divided into three groups: A) anthocyanins showing a relative abundance significantly higher in plasma in respect to extract and hence more absorbed; B) anthocyanins with no significant difference of relative abundance between plasma and extract; C) anthocyanins with a plasma relative abundance lower in respect to that determined in the extract and hence less absorbed. Empty bar: relative abundance in plasma; Filled bar: relative abundance in Mirtoselect®; * = p<0.05*

It is quite clear that the sugar moiety greatly affects absorption and that gal and glu, at least for Cya and Peo, significantly favour the absorption while ara, for all the anthocyanins, is detrimental. These results are in line with those reported by Ichiyanagi, T.  et al. [31]

The aglycone moiety too was found to affect absorption. This is well evident for glucoside since of the four anthocyanins containing the glu moiety,

Cyanidin-3-O-glucoside was significantly more absorbed in respect to the other glucosides, suggesting that Cyanidin moiety enhances bioavailability (*Table 6*).

| Anthocyanins | Variation (%) |
|---|---|
| Cya-3-O-gal | 70.16 |
| Cya-3-O-glu | 14.68 |
| Peo-3-O-gal | 88.46 |
| Peo-3-O-glu | 42.27 |
| Del-3-O-gal | 11.96 |
| Mal-3-O-glu | 2.04 |
| Mal-3-O-gal | 0.37 |
| Pet-3-O-gal | -11.26 |
| Del-3-O-glu | -18.06 |
| Mal-3-O-ara | -44.65 |
| Pet-3-O-glu | -21.03 |
| Cya-3-O-ara | -41.52 |
| Del-3-O-ara | -60.54 |
| Pet-3-O-ara | -77.70 |
| Peo-3-O-ara | -63.14 |

***Table 6*** *– Relative absorption of anthocyanins deteremined as follows: (%plasma-%Mirtoselect®)/%Mirtoselect®)x100 where %plasma is the relative content of anthocyanin in plasma determined at the Tmax and %Mirtoselect® is the relative content in the standardized extract given to rats by gavage. Relative absorption was used as dependent variable in correlative analyses.*

### *3.6 Computational analyses*

As mentioned in the Introduction, computational studies were performed i) to better elucidate the molecular recognition between anthocyanins and GLUT2 and sGLT1; ii) to understand their role on anthocyanin absorption and in

particular to understand which transporter better explains the different absorption found among the 15 anthocyanins as determined in the PK studies, iii) to investigate which electrical form is involved in the transport process. Moreover, the simulations were focused on the GLUT2 isoform which is principally expressed at the intestinal level even though the obtained results might be extended to the other GLUT isoforms due to the high homology degree between them.

With regard to GLUT2, *Figure 5* compares the putative complexes computed for highly transported (i.e. cyanidin-3-O-galactoside, 5A) and poorly transported (i.e. petunidin-3-O-arabinoside, 5B) ligands as simulated in their most effective quinodal base (A1, see statistics in *Table 7*). In detail, *Figure 5A* reveals a very rich interaction pattern which can be roughly subdivided into three parts: (a) almost all sugar hydroxyl functions are engaged in a network of H-bonds involving Gln314, Gln315, Asn320 and Asn443; (b) the 5H-chromen-5-one ring is involved in an extended π-π stacking with Trp420 plus H-bonds with Ser169 and Gln193; (c) the 3,4-dihydroxyphenyl moiety elicits H-bonds with Glu412. As evidenced in *Figure 5B*, such an interaction network can clearly explain the poor recognition of peonidin-3-O-arabinoside which loses an H-bond involving the sugar moiety, while the 3 methoxyl group bumps against Gln193 and Pro417 weakening the interactions stabilized by the aglycone moiety. Nevertheless it should be noted that the replacement of a hydroxyl function by a methoxy group is not necessarily detrimental to the

overall transport as evidenced by peonidin-3-O-galactoside which shows a relative absorption even better than cyanidin-3-O-galactoside. As detailed below, a fine balance between polar and apolar contacts has a clearly beneficial role on the transport by both proteins. The other two neutral tautomers show similar interaction patterns apart from the A1 base which shows a slightly translated pose of the quinone ring to minimize the possible repulsion between carbonyl oxygen atom and Glu412. Such a shift induces a slight worsening of all monitored interactions.

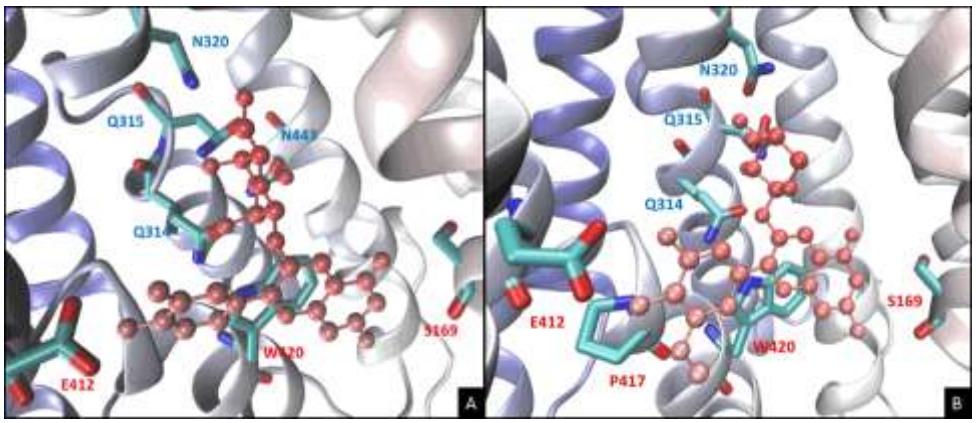


***Figure 5*** *- Major interactions stabilizing the putative of Cyanidin-3-O-galactoside (5A) and Petunidin-3-O-arabinoside (5B) with GLUT2. Residues interacting with sugar moiety are labeled in blue, residues interacting with the aglycone in red.*

| Transporter | N | Form | R2 | Q2 | Equation |
|---|---|---|---|---|---|
| GLUT2 | 1 | Base_A1 | 0.71 | 0.55 | −0.72 − 1.47 $MLP_{InS}$_2 − 0.011 Elect |
| | 2 | Base_A2 | 0.47 | 0.24 | −16.51 + 4.16 XScore + 21.42 $Contacts_{H}$ |
| | 3 | Base_A3 | 0.58 | 0.34 | −0.13 − 9.02 $MLP_{InS}$ + 0.027 Elect |
| | 4 | Anion_A- | 0.62 | 0.42 | −25.35 + 0.19 Elect + 3.93 $XScore_{HM}$ |
| | 5 | Hemiketal | 0.44 | 0.24 | 7.46 − 0.11 MLPInS + 2.07 $PLP95_{H}$ |
| | 6 | Base_Mean | 0.77 | 0.61 | 11.57 − 31.17 $MLP_{InS}$ + 0.18 CHEMPLP |
| sGLT1 | 7 | Base_A1 | 0.67 | 0.51 | −15.09 + 2.44 $XScore_{HP}$ − 2.16 $MLP_{InS}$ |
| | 8 | Base_A2 | 0.66 | 0.49 | 0.69 − 0.099 $MLP_{InS}$ + 0.047 Elect |
| | 9 | Base_A3 | 0.58 | 0.39 | 9.24 − 0.15 $MLP_{InS}$ − 0.08 PLP95 |
| | 10 | Anion_A- | 0.7 | 0.5 | −0.82 − 0.10 $MLP_{InS}$ + 0.032 Elect |
| | 11 | Hemiketal | 0.57 | 0.45 | −6.71 + 3.71 $PLP95_{H}$ + 3.25 $XScore_{HS}$ |
| | 12 | Base_all | 0.76 | 0.62 | −1.89 + 247.52 $Contacts_{W}$A1 − 0.17 PLPA2 |
| | 13 | Base_mean | 0.78 | 0.65 | −0.52 − 0.17 $MLP_{InS}$ + 0.032 Elect |
| | 14 | Base_mean + Anion | 0.82 | 0.7 | −2.49 − 0.19 MLPInS_A- + 0.042 Elect_mean |

*Table 7. Predictive equations as generated for GLUT2 and sGLT1 transporters by considering separately each simulated form (Eqs 1–5 and 7–11), by including the score averages for the three neutral tautomers (Eqs. 6 and 13) by considering simultaneously the scores of the neutral species (Eq. 12) or combining he score averages for the three neutral tautomers with the scores of the anionic form (Eq. 14). Notice that the corresponding Eqs 12 and 14 for GLUT2 are not reported since they did not give satisfactory results. The models for hemiketals (Eqs. 5 and 11) were generated by averaging the scores for the two resulting enantiomers.*

Again, the hemiketal forms yield complexes similar to those shown in *Figure 5A* with the added hydroxyl group which contacts Gln193 and Gln314 in the (*R*) and (*S*) isomers, respectively. Due to the above mentioned electrostatic repulsion with Glu412, the simulated anionic form assumes a substantially

different pose in which the sugar ring approaches Ser169 and Ser112 and the aromatic system loses several key contacts.

Similarly to *Figure 5* and with regard to sGLT1, *Figure 6* compares the complexes computed for highly (i.e. cyanidin-3-O-galactoside, 6A) and poorly transported (i.e. petunidin-3-O-arabinoside, 6B) ligands as simulated in their most effective neutral tautomer (A1, see below). Also here, the numerous interactions stabilized by cyanidin-3-O-galactoside can be subdivided in three groups: (a) the sugar hydroxyl functions elicit H-bonds with His83, Asp161, Tyr290, Ser393; (b) the 5H-chromen-5-one ring elicits a π-π stacking interaction with Tyr290 plus H-bonds with Thr460 and to a minor extent with Lys157; (c) the 3,4-dihydroxyphenyl moiety is engaged in π-π stacking interactions with Phe101 and Trp291 while the hydroxyl functions are involved in a rich network of H-bonds with Asn78, Glu102 and Lys321. Similarly to what was observed for GLUT2, Figure 6B shows that the sugar moiety of petunidin-3-O-arabinoside loses the H-bond with Tyr290, while the phenyl moiety is constrained to assume a slightly different arrangement where the 4-hydroxy functions interact with the above mentioned polar residues, while the methoxyl group approaches Leu87. The A2 neutral tautomers provide interaction patterns almost superimposable on A1 bases, while the A1 forms reveal overturned poses in which the 5H-chromen-5-one ring stabilizes H-bonds with Asp161 and the quinone ring contacts Thr460 and Gln457 (complexes not shown). Finally, the putative complex between sGLT1 and cyanidin-3-O-

galactoside in the simulated anionic form reveals a slightly different pose which appears to be vastly stabilized by the ion-pair between the negatively charged chromene ring and Lys157. When comparing the poses assumed in the two transporters by the simulated forms, one may notice a greater versatility of sGLT1 compared to GLUT2. Indeed, while GLUT2 conveniently accommodates the neutral A1 tautomer, sGLT1 appears to be able to accommodate almost all simulated species which assume slightly different poses which mostly differ in the arrangement of the aglycone while the sugar moiety acts as a pivot by stabilizing roughly constant interactions. Such a key difference in the interaction pattern between the two simulated transporters is ascribable to the different role of the ionized residues. The molecular recognition by GLUT2 is indeed heavily influenced by the only charged residue lining the GLUT2 binding cavity, namely Glu412, the negative charge of which renders the pocket highly selective and prevents a proper accommodation of both some neutral tautomers (i.e., A3) and the anionic species. In contrast, the binding cavity of sGLT1 is flanked by more positively and negatively charged residues (i.e. Glu102 and Lys321) which variously participate in the substrate recognition and increase the versatility of the cavity which is thus able to conveniently harbour almost all simulated ligand forms.

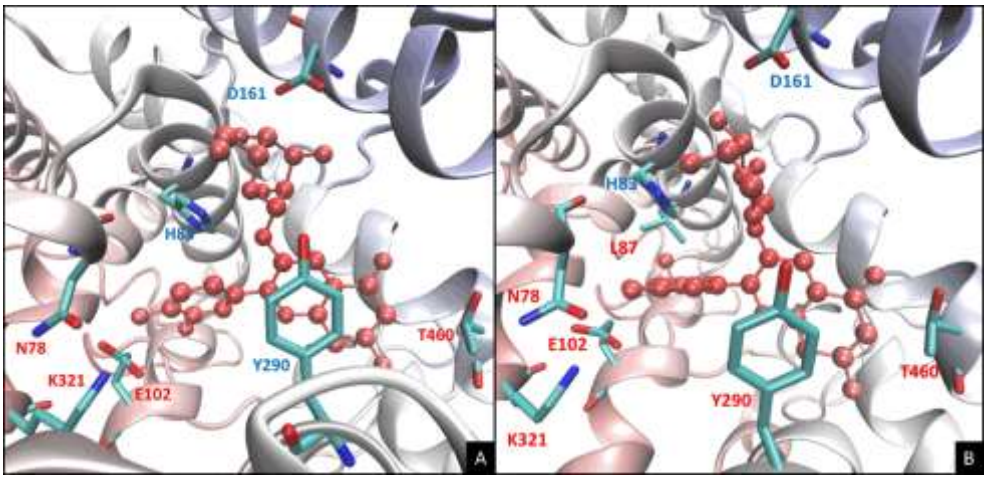


***Figure 6*** *– Major interactions stabilizing the putative of Cyanidin-3-O-galactoside (5A) and Petunidin-3-O-arabinoside (5B) with sGLT1. Residues interacting with sugar moiety are labeled in blue, residues interacting with the aglycone in red.*

The different versatility of the two transporters is reflected in the correlative models reported in *Table 7* 2GV1. Indeed, the correlative equations developed for the three neutral tautomers in GLUT2 (*Eqs. 1-3*) clearly differ in their statistical reliability with only the A1 forms yielding a satisfactory model (see *Eq. 3*). Again hemiketal and anionic species do not offer relevant equations (*Eqs 4-5*), while equations obtained combining or averaging the docking scores of more simulated species reveal limited synergistic effects and only the model including the score averages of the three quinodal bases (*Eq. 6*) evidences a modest improvement compared to the *Eq. 3*.

In contrast, the equations developed for sGLT1 show limited differences with both A1 and A2 tautomers yielding similarly satisfactory models (*Eq. 8-9*) as well as the anionic species (*Eq. 10*). Again, combinations and averaging of

more docking scores provides here more interesting results and the best model (*Eq. 14*) is developed by combining the average scores for the three neutral forms with the score for anionic ligands.

Collectively, the reported models allow for some key considerations. First, the two simulated transporters yield roughly comparable models which suggest that both proteins might be similarly involved in the transport of anthocyanins and thus responsible for the observed differences in their absorption. Second and as detailed above, the key difference between GLUT2 and sGLT1 involves the greater flexibility of the latter which seems to be able to recognize almost all simulated forms while the former shows a clear preference for a specific neutral tautomer (A1). Third and while avoiding a systematic description of all included docking scores, the generated equations emphasize that a good substrate has to stabilize a balanced set of polar and hydrophobic interactions. Surprisingly, the score encoding for ionic contacts is often included with a positive sign (see the best *Eq. 14*) thus suggesting that ligands stabilizing too strong polar contacts can remain trapped within the binding pocket thus acting as transport blockers. In contrast, ligands stabilizing a proper set of polar and apolar contacts are suitably recognized without hampering the transport turn-over.

## 4. Conclusions

By using a validated LC-ESI-MS method we found that 15 bilberry anthocyanins behave differently in term of bioavailability and that both the aglycone and the sugar moiety significantly affect the PK profile. Such different behaviour can be well explained by considering the involvement of glucose transporters as supported by computational studies which have found a significant correlation between the relative absorption of each anthocyanin and their GLUT2 and sGLT1 molecular recognition.

Finally, although modelling and docking simulations were performed on human glucose transporters sGLT1 and GLUT2, the results of this study cannot be easily transposed to humans, due to the fact that bioavailability and metabolism of flavonoids is species specific. Hence an intervention study in humans should be performed in order to confirm the involvement of glucose transporters in anthocyanin absorption. We believe that the study here reported can help the realization of this future study, having defined the analytical and computational approaches which can be easily transferred to the human study.

**Abbreviations:** Cya, Cyanidin; Peo, Peonidin; Pet, Petunidin; Del, Delphinidin; Mal, Malvidin; Ara, arabinoside; Gal, Galactoside; Glu, Glucoside.

**Acknowledgments**

We gratefully acknowledge financial support from Indena S.p.A.

## References

[1] F. Pina, M.J. Melo, C.A. Laia, A.J. Parola, J.C. Lima, Chemistry and applications of flavylium compounds: a handful of colours, Chem Soc Rev 41(2) (2012) 869-908.
[2] A. Smeriglio, D. Barreca, E. Bellocco, D. Trombetta, Chemistry, Pharmacology and Health Benefits of Anthocyanins, Phytother Res 30(8) (2016) 1265-86.
[3] S. Zafra-Stone, T. Yasmin, M. Bagchi, A. Chatterjee, J.A. Vinson, D. Bagchi, Berry anthocyanins as novel antioxidants in human health and disease prevention, Mol Nutr Food Res 51(6) (2007) 675-83.
[4] S.V. Joseph, I. Edirisinghe, B.M. Burton-Freeman, Berries: anti-inflammatory effects in humans, J Agric Food Chem 62(18) (2014) 3886-903.
[5] B.W. Lin, C.C. Gong, H.F. Song, Y.Y. Cui, Effects of anthocyanins on the prevention and treatment of cancer, Br J Pharmacol (2016).
[6] A. Cassidy, M. Bertoia, S. Chiuve, A. Flint, J. Forman, E.B. Rimm, Habitual intake of anthocyanins and flavanones and risk of cardiovascular disease in men, Am J Clin Nutr 104(3) (2016) 587-94.
[7] C. Cerletti, A. de Curtis, F. Bracone, C. Digesù, A.G. Morganti, L. Iacoviello, G. de Gaetano, M.B. Donati, Dietary anthocyanins and health: data from FLORA and ATHENA EU projects, Br J Clin Pharmacol (2016).
[8] M. Iriti, E.M. Varoni, Chemopreventive potential of flavonoids in oral squamous cell carcinoma in human studies, Nutrients 5(7) (2013) 2564-76.
[9] C. Felgines, O. Texier, C. Besson, D. Fraisse, J.L. Lamaison, C. Rémésy, Blackberry anthocyanins are slightly bioavailable in rats, J Nutr 132(6) (2002) 1249-53.
[10] M.L. Castro-Acosta, G.N. Lenihan-Geels, C.P. Corpe, W.L. Hall, Berries and anthocyanins: promising functional food ingredients with postprandial glycaemia-lowering effects, Proc Nutr Soc 75(3) (2016) 342-55.
[11] C. Czank, A. Cassidy, Q. Zhang, D.J. Morrison, T. Preston, P.A. Kroon, N.P. Botting, C.D. Kay, Human metabolism and elimination of the anthocyanin, cyanidin-3-glucoside: a (13)C-tracer study, Am J Clin Nutr 97(5) (2013) 995-1003.

[12] J. He, T.C. Wallace, K.E. Keatley, M.L. Failla, M.M. Giusti, Stability of black raspberry anthocyanins in the digestive tract lumen and transport efficiency into gastric and small intestinal tissues in the rat, J Agric Food Chem 57(8) (2009) 3141-8.
[13] T.K. McGhie, M.C. Walton, The bioavailability and absorption of anthocyanins: towards a better understanding, Mol Nutr Food Res 51(6) (2007) 702-13.
[14] S. Talavéra, C. Felgines, O. Texier, C. Besson, C. Manach, J.L. Lamaison, C. Rémésy, Anthocyanins are efficiently absorbed from the small intestine in rats, J Nutr 134(9) (2004) 2275-9.
[15] J. Fang, Bioavailability of anthocyanins, Drug Metab Rev 46(4) (2014) 508-20.
[16] S. Passamonti, U. Vrhovsek, F. Mattivi, The interaction of anthocyanins with bilitranslocase, Biochem Biophys Res Commun 296(3) (2002) 631-6.
[17] I. Fernandes, V. de Freitas, C. Reis, N. Mateus, A new approach on the gastric absorption of anthocyanins, Food Funct 3(5) (2012) 508-16.
[18] H. Oliveira, I. Fernandes, N.F. Brás, A. Faria, V. De Freitas, C. Calhau, N. Mateus, Experimental and Theoretical Data on the Mechanism by Which Red Wine Anthocyanins Are Transported through a Human MKN-28 Gastric Cell Model, J Agric Food Chem 63(35) (2015) 7685-92.
[19] P.V. Röder, K.E. Geillinger, T.S. Zietek, B. Thorens, H. Koepsell, H. Daniel, The role of SGLT1 and GLUT2 in intestinal glucose transport and sensing, PLoS One 9(2) (2014) e89977.
[20] T.B. Zou, D. Feng, G. Song, H.W. Li, H.W. Tang, W.H. Ling, The role of sodium-dependent glucose transporter 1 and glucose transporter 2 in the absorption of cyanidin-3-o-β-glucoside in Caco-2 cells, Nutrients 6(10) (2014) 4165-77.
[21] S.M. Boue, K.W. Daigle, M.H. Chen, H. Cao, M.L. Heiman, Antidiabetic Potential of Purple and Red Rice (Oryza sativa L.) Bran Extracts, J Agric Food Chem 64(26) (2016) 5345-53.
[22] A. Faria, D. Pestana, J. Azevedo, F. Martel, V. de Freitas, I. Azevedo, N. Mateus, C. Calhau, Absorption of anthocyanins through intestinal epithelial cells - Putative involvement of GLUT2, Mol Nutr Food Res 53(11) (2009) 1430-7.
[23] S. Vendrame, C. Del Bo', S. Ciappellano, P. Riso, D. Klimis-Zacas, Berry Fruit Consumption and Metabolic Syndrome, Antioxidants (Basel) 5(4) (2016).
[24] B.O. Keller, J. Sui, A.B. Young, R.M. Whittal, Interferences and contaminants encountered in modern mass spectrometry, Anal Chim Acta 627(1) (2008) 71-81.
[25] P. Morazzoni, S. Livio, A. Scilingo, S. Malandrino, Vaccinium myrtillus anthocyanosides pharmacokinetics in rats, Arzneimittelforschung 41(2) (1991) 128-31.
[26] D. Deng, C. Xu, P. Sun, J. Wu, C. Yan, M. Hu, N. Yan, Crystal structure of the human glucose transporter GLUT1, Nature 510(7503) (2014) 121-5.

[27] A. Pedretti, C. Granito, A. Mazzolari, G. Vistoli, Structural Effects of Some Relevant Missense Mutations on the MECP2-DNA Binding: A MD Study Analyzed by Rescore+, a Versatile Rescoring Tool of the VEGA ZZ Program, Mol Inform 35(8-9) (2016) 424-33.
[28] A. Pedretti, L. Villa, G. Vistoli, VEGA: a versatile program to convert, handle and visualize molecular structure on Windows-based PCs, Journal of Molecular Graphics & Modelling 21(1) (2002) 47-49.
[29] C. Lammi, C. Zanoni, A. Arnoldi, G. Vistoli, Two Peptides from Soy β-Conglycinin Induce a Hypocholesterolemic Effect in HepG2 Cells by a Statin-Like Mechanism: Comparative in Vitro and in Silico Modeling Studies, J Agric Food Chem 63(36) (2015) 7945-51.
[30] N. Hoggard, M. Cruickshank, K.M. Moar, C. Bestwick, J.J. Holst, W. Russell, G. Horgan, A single supplement of a standardised bilberry (Vaccinium myrtillus L.) extract (36 % wet weight anthocyanins) modifies glycaemic response in individuals with type 2 diabetes controlled by diet and lifestyle, J Nutr Sci 2 (2013) e22.
[31] T. Ichiyanagi, Y. Shida, M.M. Rahman, Y. Hatano, T. Konishi, Bioavailability and tissue distribution of anthocyanins in bilberry (Vaccinium myrtillus L.) extract in rats, J Agric Food Chem 54(18) (2006) 6578-87.

# V

# General conclusions

Plants are a rich source of bioactive compounds and their use as therapeutic agents dates back since ancient times. However, the complexity of their composition still limits the complete characterization of the bioactive compounds, their mechanisms of action and ADME profiles. These limitations are due to the lack of suitable analytical methods and leading to a reduced application of plant based products, which have a great potential in the treatment of several pathologies. In light of all these considerations, the aim of this Ph.D thesis was to set up high resolution mass spectrometric and selective MS/MS methods to characterize and identify bioactive molecules present in plant extracts and to understand their mechanisms of action and their bioavailability in human and in rodents. The results reported in the present Ph.D thesis demonstrate how novel mass spectrometric strategies can be applied to obtain the same information as that obtained for pure compounds in the discovery stage.

In particular, MS strategies were applied to investigate the ability of plant extracts to act as a) sequestering agents of reactive carbonyl species, toxic lipid peroxidation products involved in the pathogenetic mechanisms of several inflammatory based disorders and b) as protein precipitation agents (tannin effect) using bradykinin, a pro-inflammatory mediator, as protein target; and to study the ADME profiles of a) a standardized cranberry extract in humans and b) a standardized bilberry extract in rodents.

The activity of different rice extracts to inhibit protein carbonylation was tested by using a HRMS method. The screening analysis showed that black rice with giant germ extract was the most active. A novel MS strategy based on a specific isotopic labelling was then applied to identify the active compounds, which are represented by some anthocyanidins and aminoacids.

Tannin protein precipitation extent was quantified by a fast and reliable LC-MS method, which was developed by using tannic acid and penta-O-galloyl-β-D-glucose as tannin agents and bradykinin as a peptide model. The method allowed us to get easily quantitative data, so it can be used as an *in vitro* screening of several plant extracts and compounds able to complex and precipitate damaging target peptides.

The controversial results present in the literature on the bioactive compounds of cranberry, used in the prevention of urinary tract infections, are mainly due to different dosages and non-standardized treatments. The activity was associated with PACs by several *in vitro* studies, but *in vivo* they seemed to be absent in urine. Moreover some *in vivo* studies are limited to the research in human urine of known compounds and metabolites. The use of a standardized extract and a dosage found effective in human studies associated with a HRMS method and the on target and off target data analyses adopted in the present Ph.D thesis, aimed to overcome these limits. 35 metabolites were identified and some of them are PACs metabolites. The ex-vivo study performed on the inhibition of *C. albicans* adhesion by urine

fractions allowed attention to be focused on the major compounds present in the active fractions.

Anthocyanins health benefits, related to their antioxidant, anti-inflammatory and anticarcinogenic properties, have long been reported but less is known about their mechanism of absorption. Among the mechanisms proposed there is the GLUT transporters. The aim of this work was to better understand the role of GLUT transporters (GLUT2 and sGLT1) in anthocyanin absorption by applying a selective and sensitive HPLC-MS/MS method to a pharmacokinetic study in rats. Three different conditions were investigated: fed, fasting conditions and fasting conditions with glucose co-somministration. The results obtained in conjunction with those achieved by docking studies confirm the GLUT2 and sGLT1 involvement in anthocyanin absorption.

In conclusion, the development of different MS strategies has improved the knowledge of the mechanisms of action, bioactivity and bioavailability of the plant extracts investigated. The examples reported in the present thesis confirm that information usually obtained for pure compounds in the discovery stage can also be retrieved for more complex bioactive products such as plant extracts. Plant extracts which nowadays find a wide use as health products should be better characterized in terms of biological activity and pharmacokinetic, thus assuring greater efficacy and safety and the fact they are a complex matrix should not limit this information.

# VI

# Appendix

## 1. Bioactive components of plants

The molecules with a potential pharmacological interest present in plants are the secondary metabolites, which are synthesized by plants as mechanism of defence. These compounds are represented by polyphenols, terpenoids and alkaloids. In particular, a great interest was shown in polyphenols, that are the most abundant and heterogeneous class. They are reported to have several health benefits [1]: their main ability is to act as antioxidant [2-4], but they were also found to be able to interact and modulate the activity of enzymes and receptors leading to several potential applications [5]. Polyphenols are classified in different classes on the basis of the number of phenol rings and the way in which they are linked together. We can distinguish : flavonoids, phenolic acids, stilbens and lignans [6]. Among these compounds several health benefits have been related to flavonoids [7-9], which are composed by a fifteen-carbon skeleton consisting of two benzene rings (A and B) linked via a heterocyclic pyrane ring (C) (*Figure 1*) [9].

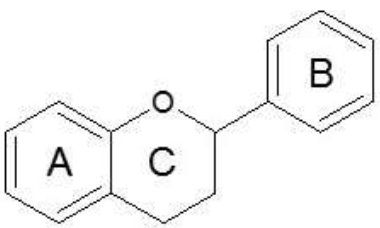


***Figure 1*** *– Basic flavonoid structure*

Depending on the level of oxidation and on the substituents on the C ring, flavonoids can be subdivided in several classes : anthocyanins, flavonols, flavanones, flavones, iso-flavones, flavan-3-ols and other minor classes. Single compounds of each class differ in the pattern of substitution of the A and B rings [10] and they can exist as aglycone, glicoside and methylated derivatives. Flavonoids activity is related to their structure.

Anthocyanins are natural pigments which give the blue, purple, red and orange colour of many fruits and vegetables [11]. The aglycone, named anthocyanidin, is characterized by several hydroxyl groups to which are bound one or more sugar moieties. The main sources of anthocyanin are red fruits, cereals, vegetables and red wine among drinks [12, 13]. Their potential applications towards oxidative-based diseases are supported by several studies reporting their antioxidant [14], anti-inflammatory [15] and anticarcenogenic properties [16].

Flavonols are the most ubiquitous flavonoid class present in foods, the main representatives are quercetin and kaempferol, and they are mainly present in glycosylated forms [6]. Some examples of foods rich in flavonols are onions, cherries, apples and broccoli [17]. *In vitro* and *in vivo* studies performed on quercetin aglycone and phase II metabolites have shown vasorelaxant and hypotensive effects [18, 19], but also anti-inflammatory properties [20]. It is also reported in an *in vitro* study that quercetin-3-O-glucuronide significantly

reduced the generation of β-amyloid peptides, but the activity can be limited by the permeability of the BEE [21].

Flavanones, such as hesperidin, naringenin and eriodictyol, are mostly found in citrus fruits [17]. They are associated to vascular benefits [22].

Apigenin and luteolin, and their glycosilated forms, are the main representative of flavone class, which are known to have neuroprotective actions [23].

Isoflavones are flavonoids having a structure similar to estrogens. This similarity conferes them the ability to bind to estrogen receptors, so they are classified as phytoestrogens. Isoflavones are found almost exclusively in leguminous plants (e.g. soya) and their assumption was related to bone beneficial effects [24].

Flavanols or flavan-3-ols, also called catechins, can exist as monomeric or oligomeric and polymeric forms having different types of linkages. The oligo/polymers are named proanthocyanidins but they are also known as condensed tannins [25]. Monomeric flavanols (catechin and epicatechin) and their derivatives are the major polyphenols present in tea leaves [26], while proanthocyanidins are present in great amount into fruits, in particular in berries such as cranberries (*Vaccinium macrocarpum*), cereals and nuts and chocolate [27]. Several studies decribed their anti-oxidant, anti-inflammatory and anticarcenogenic properties, benefits on cardiovascular and diabetic complication, and antibacterial effects [28].

## 2. Bioavailability of flavonoids

The biological fate of the dietary flavonoid glycosides has been a controversial issue over the years. Although many answers have now been provided, this issue is still far from established. Due to their chemical features, such as highly polarity, it was long believed that they could not be absorbed intact after oral ingestion, but they were hydrolyzed to their aglycones by bacterial enzymes in the lower part of the intestine [29, 30]. Further, aglycones might then be partially absorbed or may undergo a further biotransformation by bacteria. However, some scientific evidence have demonstrated that some flavonoid glycosides could be absorbed intact in the small intestine, using the sodium dependent glucose transporter 1 (SGLT1) as reported by Hollman 1995; it was verified that the efficiency of such absorption was dramatically suppressed by efflux of at least some flavonoid glycosides by the apical transporter multidrug resistance-associated protein 2 (MRP2). At the same time, a number of studies support the view that quercetin glycosides are not absorbed intact in humans or, rather, are not able to reach the systemic circulation [31, 32]. Similar findings have been observed for the intact glycosides of diosmetin [33] and luteolin [34], thus confirming the tendency of flavonoid glycosides to be hydrolyzed.

A huge scenario of bioabsorption seems to be attributed to the different classes of flavonoid glycosides. Because absorption occurs less readily in the colon than in the small intestine because of a smaller exchange area and a

lower density of transport systems, as a general rule, glycosides with rhamnose are absorbed less rapidly and less efficiently than aglycones and glucosides. This has been clearly shown in humans for quercetin glycosides: maximum absorption occurs 0.5–0.7 h after ingestion of quercetin 4'-glucoside and 6–9 h after ingestion of the same quantity of rutin (quercetin-3-rutinoside). The bioavailability of rutin is only 15–20% of that of quercetin 4'-glucoside [32, 35]. Similarly, absorption of quercetin is more rapid and efficient after ingestion of onions, which are rich in glucosides, than after ingestion of apples containing both glucosides and various other glycosides [36]. In the case of quercetin glucosides, absorption occurs in the small intestine, and the efficiency of absorption is higher than that for the aglycone itself [37, 38].

In the small intestine, cleavage of the sugar unit is mediated through the action of cytosolic β-glucosidase [39] and lactase phloridzin hydrolase (LPH), located in the brush border of epithelial cells. LPH exhibits broad specificity for flavonoid-O-β-D-glucosides, and the released aglycones can enter the epithelial cells by passive diffusion due to their increased lipophilicity [40]. Both enzymes are probably involved, but their relative contribution for the various glucosides remains to be clarified. Quercetin 3-glucoside, which is not a substrate for cytosolic-glucosidase, is certainly absorbed after hydrolysis by lactase phloridzine hydrolase, at least in rats, whereas hydrolysis of quercetin 4'-glucoside seems to involve both pathways.

The extent of absorption and bioavailability of drugs has long been known to be affected by membrane transporters, mainly efflux transporters, in addition to metabolism. The traditional efflux transporter for drugs i.e., P-glycoprotein, does not seem to be involved in the transport of flavonoids, mainly dependent on differences in chemical structures. However, other transporters have been found that may be important. This has been recognized mainly through the use of monolayers of the human intestinal Caco-2 cells or intestinal rat preparations. These transporters include the absorptive transporter SGLT1, identified in both Caco-2 cells [41] and the rat small intestine [42]. The monocarboxylate transporter (MCT), recently identified for the tea flavonoid ECG [43] was, actually, also included. MRP2, but probably also other MRP isoforms, has been demonstrated to be an important efflux transporter. This is most clearly the case for flavonoid glucuronide and sulfate conjugates [44]. Once absorbed, flavonoids and related phenolics follow the common metabolic pathway of exogenous organic substances and, like drugs and most xenobiotics, undergo phase II enzymatic metabolism. They can be conjugated with glucuronic acid, sulphate and methyl groups, in reactions catalysed by UDP-glucuronosyltransferases (UGTs), sulphotransferases (SULTs) and catechol-O-methyltransferases (COMT), respectively [45]. Phase II metabolism first occurs in the wall of the small intestine, after which metabolites pass through the portal vein to the liver, where they may undergo further conversions before entering the systemic circulation and eventually undergoing renal excretion. However, flavonoid metabolites are difficult to

quantify because only a few are commercially available as reference compounds and they are very complicated to synthesize [46].

## 3. Mass spectrometry techniques for the characterization, identification and quantification of plant extract compounds

### *3.1. MS analyzers and sources for biomolecules analysis*

Mass spectrometry has its origins around the beginning of the last century in the studies performed by J. J. Thomson [47] and F. W. Aston [48]. Today MS is the most sensitive method for the structural characterization of biomolecules.

The introduction of the soft ionization methods, such as electrospray (ESI) [49] and matrix-assisted laser-desorption- ionization (MALDI) [50], led to several improvements in biochemical MS. While MALDI is the optimum method of ionizing peptides, ESI is the most efficient method for the ionization of polar biomolecules. Focusing on ESI-MS, this technique allows to analyze compounds in aqueous or aqueous/organic solutions, establishing it as a convenient mass detector for HPLC. In fact, ESI permits MS analysis at relatively high HPLC flow rates (1.0 mL/min) and high mass accuracy (±0.01%).

In order to characterize and identify an unknown compounds the nominal mass is not enough when the compound of interest is in a complex matrix.

Thanks to the advent of high resolution mass spectrometer which possess high mass accuracy and high isotopic abundance accuracy, few molecular formula candidates can be obtained. Among the HR mass spectrometer there are time-of-flight (TOF), Fourier transform ion cyclotron resonance (FT ICR), and Orbitrap detectors. In addition to molecular weight, more details on the structure composition can be achieved by different type of fragmentation experiments. Fragmentation is usually performed by inducing ion/molecule collisions, process known as collision-induced dissociation (CID). As first one ion, called precursor, is selected by a mass analyzer and focused into a collision region preceding a second mass analyzer. In the collision region or cell product ions are generated and then detected by the second analyzer. These analyzers can be set in series either in space (triple quadrupole and hybrid instruments) or in time (ion trap instrument). Different MS/MS experiments, such as precursor ion scan, product ion scan, neutral loss scan and selected ion monitoring scan (*Figure 2*) [51], can be developed in order to reach the goal of interest (e.g. structure elucidation or quantitative analysis of selected ions in order to reach an higher selectivity and sensitivity).

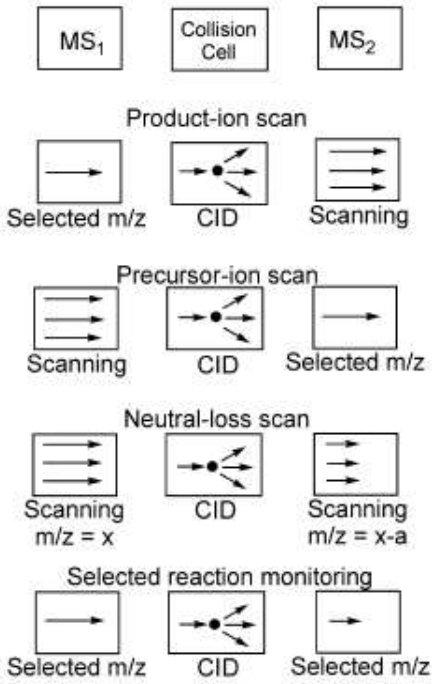


***Figure 2*** *– Scan mode used in MS/MS analyses [51].*

## *3.2 Characterization, identification and quantification of plant extract compounds*

The analysis of polyphenols in the context of their natural source or in biological matrixes is a hard challenge and the analytical strategies depends on the sample and analytes characteristics. A chomatographic separation step before MS detection in always necessary for adequate analysis. Moreover, retention time can also give structural information. Since $C_{18}$ or $C_8$-RP columns are the most used in plant extract analysis, retention times are

inversely correlated with increasing glycosylation, whereas methylation has the opposite effect. The retention time is also influenced by the position of glycosylation [52] or methylation [53]. Frequently the flow deriving from the LC is splitted into two way, the first directed to the MS and the second to a UV diod-array detector. This choice is due to the known flavonoids characteristic UV absorption [54], which can provide adding information on the class of compounds. The MS analysis can be performed both in positive and negative ion mode. The negative ion mode shows the highest sensitivity [55], which is important where concentrations are low, while more structural information are obtained with the first-order mass spectrum in the positive ion mode contains more structural information [56]. Regarding the quantitative analysis, multiple-reaction ion monitoring (MRM) methods are widely used because of the high selectivity obtained [57]. The amount of the analyte is determined by comparing the ratios of peak area of analytes to that of an internal standard.

### *3.3 Sample preparation*

Sample preparation is a very important step in the analyses of complex matrices. Considering flavonoids in their original source homogenization, liquid extraction and filtration and/or centrifugation method can be adopted. The kind and amount of flavonoids isolated are subsceptible to the conditions use, such as temperature, pH and extraction solvent [58]. Sometimes further steps, such as purification or enrichment of some fractions, are necessary to

discard interference analytes. The method of choice in this case it is represented by solid-phase extraction (SPE) [59].

When flavonoids analysis is performed onto physiological fluids, such as urine and plasma, an initial extraction may be not necessary. However an hydrolyzation step can be considered by using β-glucuronidase, sulfatase, or a mixture containing both enzymes. After the hydrolysis the sample has to be extracted using liquid–liquid extraction or solid-phase extraction (SPE). In some cases protein removal is performed, e.g. on plasma samples, by solvent or acidic precipitation, followed by centrifugation and supernatant filtration.

## References

[1] A. Scalbert, C. Manach, C. Morand, C. Rémésy, L. Jiménez, Dietary polyphenols and the prevention of diseases, Crit Rev Food Sci Nutr 45(4) (2005) 287-306.
[2] C. Rice-Evans, R. Miller, G. Paganga, Antioxidant properties of phenolic compounds, Trends in Plant Science 2 4 (1997) 152-159.
[3] L. Bravo, Polyphenols: chemistry, dietary sources, metabolism, and nutritional significance, Nutr Rev 56(11) (1998) 317-33.
[4] K.B. Pandey, S.I. Rizvi, Plant polyphenols as dietary antioxidants in human health and disease, Oxid Med Cell Longev 2(5) (2009) 270-8.
[5] E. Middleton, C. Kandaswami, T.C. Theoharides, The effects of plant flavonoids on mammalian cells: implications for inflammation, heart disease, and cancer, Pharmacol Rev 52(4) (2000) 673-751.
[6] C. Manach, A. Scalbert, C. Morand, C. Rémésy, L. Jiménez, Polyphenols: food sources and bioavailability, Am J Clin Nutr 79(5) (2004) 727-47.
[7] K.E. Heim, A.R. Tagliaferro, D.J. Bobilya, Flavonoid antioxidants: chemistry, metabolism and structure-activity relationships, J Nutr Biochem 13(10) (2002) 572-584.

[8] C. Kandaswami, C. Kanadaswami, L.T. Lee, P.P. Lee, J.J. Hwang, F.C. Ke, Y.T. Huang, M.T. Lee, The antitumor activities of flavonoids, In Vivo 19(5) (2005) 895-909.
[9] S. Kumar, A.K. Pandey, Chemistry and biological activities of flavonoids: an overview, ScientificWorldJournal 2013 (2013) 162750.
[10] E. Middleton, Effect of plant flavonoids on immune and inflammatory cell function, Adv Exp Med Biol 439 (1998) 175-82.
[11] F. Pina, M.J. Melo, C.A. Laia, A.J. Parola, J.C. Lima, Chemistry and applications of flavylium compounds: a handful of colours, Chem Soc Rev 41(2) (2012) 869-908.
[12] J.B. Harborne, The Flavonoids Advances in Research Since 1986, Chapman and Hall, London, 1993.
[13] M.T. Escribano-Bailón, C. Santos-Buelga, J.C. Rivas-Gonzalo, Anthocyanins in cereals, J Chromatogr A 1054(1-2) (2004) 129-41.
[14] S. Zafra-Stone, T. Yasmin, M. Bagchi, A. Chatterjee, J.A. Vinson, D. Bagchi, Berry anthocyanins as novel antioxidants in human health and disease prevention, Mol Nutr Food Res 51(6) (2007) 675-83.
[15] S.V. Joseph, I. Edirisinghe, B.M. Burton-Freeman, Berries: anti-inflammatory effects in humans, J Agric Food Chem 62(18) (2014) 3886-903.
[16] B.W. Lin, C.C. Gong, H.F. Song, Y.Y. Cui, Effects of anthocyanins on the prevention and treatment of cancer, Br J Pharmacol (2016).
[17] L.H. Yao, Y.M. Jiang, J. Shi, F.A. Tomás-Barberán, N. Datta, R. Singanusong, S.S. Chen, Flavonoids in food and their health benefits, Plant Foods Hum Nutr 59(3) (2004) 113-22.
[18] Y. Shen, K.D. Croft, J.M. Hodgson, R. Kyle, I.L. Lee, Y. Wang, R. Stocker, N.C. Ward, Quercetin and its metabolites improve vessel function by inducing eNOS activity via phosphorylation of AMPK, Biochem Pharmacol 84(8) (2012) 1036-44.
[19] P. Galindo, I. Rodriguez-Gómez, S. González-Manzano, M. Dueñas, R. Jiménez, C. Menéndez, F. Vargas, J. Tamargo, C. Santos-Buelga, F. Pérez-Vizcaíno, J. Duarte, Glucuronidated quercetin lowers blood pressure in spontaneously hypertensive rats via deconjugation, PLoS One 7(3) (2012) e32673.
[20] E. Derlindati, M. Dall'Asta, D. Ardigò, F. Brighenti, I. Zavaroni, A. Crozier, D. Del Rio, Quercetin-3-O-glucuronide affects the gene expression profile of M1 and M2a human macrophages exhibiting anti-inflammatory effects, Food Funct 3(11) (2012) 1144-52.
[21] L. Ho, M.G. Ferruzzi, E.M. Janle, J. Wang, B. Gong, T.Y. Chen, J. Lobo, B. Cooper, Q.L. Wu, S.T. Talcott, S.S. Percival, J.E. Simon, G.M. Pasinetti, Identification of brain-targeted bioactive dietary quercetin-3-O-glucuronide as a novel intervention for Alzheimer's disease, FASEB J 27(2) (2013) 769-81.
[22] H. Takumi, H. Nakamura, T. Simizu, R. Harada, T. Kometani, T. Nadamoto, R. Mukai, K. Murota, Y. Kawai, J. Terao, Bioavailability of orally administered water-dispersible hesperetin and its effect on peripheral

vasodilatation in human subjects: implication of endothelial functions of plasma conjugated metabolites, Food Funct 3(4) (2012) 389-98.
[23] F. Dajas, A.C. Andrés, A. Florencia, E. Carolina, R.M. Felicia, Neuroprotective actions of flavones and flavonols: mechanisms and relationship to flavonoid structural features, Cent Nerv Syst Agents Med Chem 13(1) (2013) 30-5.
[24] S.E. Putnam, A.M. Scutt, K. Bicknell, C.M. Priestley, E.M. Williamson, Natural products as alternative treatments for metabolic bone disorders and for maintenance of bone health, Phytother Res 21(2) (2007) 99-112.
[25] E. Haslam, Y. Cai, Plant polyphenols (vegetable tannins): gallic acid metabolism, Nat Prod Rep 11(1) (1994) 41-66.
[26] W. Si, J. Gong, R. Tsao, M. Kalab, R. Yang, Y. Yin, Bioassay-guided purification and identification of antimicrobial components in Chinese green tea extract, J Chromatogr A 1125(2) (2006) 204-10.
[27] L. Gu, M.A. Kelm, J.F. Hammerstone, G. Beecher, J. Holden, D. Haytowitz, S. Gebhardt, R.L. Prior, Concentrations of proanthocyanidins in common foods and estimations of normal consumption, J Nutr 134(3) (2004) 613-7.
[28] R. de la Iglesia, F.I. Milagro, J. Campión, N. Boqué, J.A. Martínez, Healthy properties of proanthocyanidins, Biofactors 36(3) (2010) 159-68.
[29] L.A. Griffiths, A. Barrow, Metabolism of flavonoid compounds in germ-free rats, Biochem J 130(4) (1972) 1161-2.
[30] V.D. Bokkenheuser, C.H. Shackleton, J. Winter, Hydrolysis of dietary flavonoid glycosides by strains of intestinal Bacteroides from humans, Biochem J 248(3) (1987) 953-6.
[31] I. Erlund, T. Kosonen, G. Alfthan, J. Mäenpää, K. Perttunen, J. Kenraali, J. Parantainen, A. Aro, Pharmacokinetics of quercetin from quercetin aglycone and rutin in healthy volunteers, Eur J Clin Pharmacol 56(8) (2000) 545-53.
[32] E.U. Graefe, J. Wittig, S. Mueller, A.K. Riethling, B. Uehleke, B. Drewelow, H. Pforte, G. Jacobasch, H. Derendorf, M. Veit, Pharmacokinetics and bioavailability of quercetin glycosides in humans, J Clin Pharmacol 41(5) (2001) 492-9.
[33] D. Cova, L. De Angelis, F. Giavarini, G. Palladini, R. Perego, Pharmacokinetics and metabolism of oral diosmin in healthy volunteers, Int J Clin Pharmacol Ther Toxicol 30(1) (1992) 29-33.
[34] K. Shimoi, H. Okada, M. Furugori, T. Goda, S. Takase, M. Suzuki, Y. Hara, H. Yamamoto, N. Kinae, Intestinal absorption of luteolin and luteolin 7-O-beta-glucoside in rats and humans, FEBS Lett 438(3) (1998) 220-4.
[35] P.C. Hollman, M.N. Bijsman, Y. van Gameren, E.P. Cnossen, J.H. de Vries, M.B. Katan, The sugar moiety is a major determinant of the absorption of dietary flavonoid glycosides in man, Free Radic Res 31(6) (1999) 569-73.
[36] P.C. Hollman, J.M. van Trijp, M.N. Buysman, M.S. van der Gaag, M.J. Mengelers, J.H. de Vries, M.B. Katan, Relative bioavailability of the

antioxidant flavonoid quercetin from various foods in man, FEBS Lett 418(1-2) (1997) 152-6.
[37] P.C. Hollman, J.H. de Vries, S.D. van Leeuwen, M.J. Mengelers, M.B. Katan, Absorption of dietary quercetin glycosides and quercetin in healthy ileostomy volunteers, Am J Clin Nutr 62(6) (1995) 1276-82.
[38] C. Morand, C. Manach, V. Crespy, C. Remesy, Quercetin 3-O-beta-glucoside is better absorbed than other quercetin forms and is not present in rat plasma, Free Radic Res 33(5) (2000) 667-76.
[39] A.J. Day, M.S. DuPont, S. Ridley, M. Rhodes, M.J.C. Rhodes, M.R.A. Morgan, G. Williamson, Deglycosylation of flavonoid and isoflavonoid glycosides by human small intestine and liver beta-glucosidase activity, Febs Letters 436(1) (1998) 71-75.
[40] A.J. Day, F.J. Cañada, J.C. Díaz, P.A. Kroon, R. Mclauchlan, C.B. Faulds, G.W. Plumb, M.R. Morgan, G. Williamson, Dietary flavonoid and isoflavone glycosides are hydrolysed by the lactase site of lactase phlorizin hydrolase, FEBS Lett 468(2-3) (2000) 166-70.
[41] R.A. Walgren, J.T. Lin, R.K. Kinne, T. Walle, Cellular uptake of dietary flavonoid quercetin 4'-beta-glucoside by sodium-dependent glucose transporter SGLT1, J Pharmacol Exp Ther 294(3) (2000) 837-43.
[42] S. Wolffram, M. Blöck, P. Ader, Quercetin-3-glucoside is transported by the glucose carrier SGLT1 across the brush border membrane of rat small intestine, J Nutr 132(4) (2002) 630-5.
[43] J.B. Vaidyanathan, T. Walle, Cellular uptake and efflux of the tea flavonoid (-)epicatechin-3-gallate in the human intestinal cell line Caco-2, J Pharmacol Exp Ther 307(2) (2003) 745-52.
[44] U.K. Walle, A. Galijatovic, T. Walle, Transport of the flavonoid chrysin and its conjugated metabolites by the human intestinal cell line Caco-2, Biochem Pharmacol 58(3) (1999) 431-8.
[45] D. Del Rio, A. Rodriguez-Mateos, J.P. Spencer, M. Tognolini, G. Borges, A. Crozier, Dietary (poly)phenolics in human health: structures, bioavailability, and evidence of protective effects against chronic diseases, Antioxid Redox Signal 18(14) (2013) 1818-92.
[46] M. Zhang, G.E. Jagdmann, M. Van Zandt, R. Sheeler, P. Beckett, H. Schroeter, Chemical synthesis and characterization of epicatechin glucuronides and sulfates: bioanalytical standards for epicatechin metabolite identification, J Nat Prod 76(2) (2013) 157-69.
[47] J.J. Thomson, Rays of positive electricity and their application to chemical analyses, London, New York [etc.] Longmans, Green and Co.1913.
[48] F.W. Aston, Mass spectra and isotopes, Edward Arnold, London, 1933.
[49] M. Yamashita, J.B. Fenn, Electrospray ion source. Another variation on the free-jet theme, Journal of Physical Chemistry 88(20) (1984) 4451-4459.
[50] M. Karas, F. Hillenkamp, Laser desorption ionization of proteins with molecular masses exceeding 10,000 daltons, Anal Chem 60(20) (1988) 2299-301.

[51] W.J. Griffiths, Y. Wang, Mass spectrometry: from proteomics to metabolomics and lipidomics, Chem Soc Rev 38(7) (2009) 1882-96.
[52] J.B. Harborne, M. Boardley, Use of high-performance liquid chromatography in the separation of flavonol glycosides and flavonol sulphates, Journal of Chromatography A 299(C) (1984) 377-385.
[53] J. Greenham, C. Williams, J.B. Harborne, Identification of lipophilic flavonols by a combination of chromatographic and spectral techniques, Phytochemical Analysis 6(4) (1995) 211-217.
[54] F. Cuyckens, M. Claeys, Optimization of a liquid chromatography method based on simultaneous electrospray ionization mass spectrometric and ultraviolet photodiode array detection for analysis of flavonoid glycosides, Rapid Commun Mass Spectrom 16(24) (2002) 2341-8.
[55] N. Fabre, I. Rustan, E. de Hoffmann, J. Quetin-Leclercq, Determination of flavone, flavonol, and flavanone aglycones by negative ion liquid chromatography electrospray ion trap mass spectrometry, J Am Soc Mass Spectrom 12(6) (2001) 707-15.
[56] F. Cuyckens, M. Claeys, Mass spectrometry in the structural analysis of flavonoids, J Mass Spectrom 39(1) (2004) 1-15.
[57] J.K. Prasain, C.C. Wang, S. Barnes, Mass spectrometric methods for the determination of flavonoids in biological samples, Free Radic Biol Med 37(9) (2004) 1324-50.
[58] Characterization of Citrus by chromatographic analysis of flavonoids., Journal of the Science of Food and Agriculture (1997).
[59] D. Tura, K. Robards, Sample handling strategies for the determination of biophenols in food and plants, J Chromatogr A 975(1) (2002) 71-93.

**Publications**

*Baron G, Altomare A, Regazzoni L, Redaelli V, Grandi S, Riva A, Morazzoni P, Mazzolari A, Carini M1, Vistoli G, Aldini G* - **Pharmacokinetic profile of bilberry anthocyanins in rats and the role of glucose transporters: LC-MS/MS and computational studies**. J Pharm Biomed Anal. **2017** Sep 10;144:112-121. doi: 10.1016

**Oral Comunications**

*G. Baron, A. Altomare, L. Regazzoni, S. G. Grandi, A. Riva, P. Morazzoni, M. Carini, G. Aldiini* - **Profiling Vaccinium Macrocarpon components and metabolites in human urine** (RDPA - Rimini September 20-23 2017)

*G., Baron.* **Mass spectrometric strategies for the study of bioavailability, bioactivity, bioactivity and mechanisms of action of plant extracts** (SSPA - Rimini, September 18 – 20 2017)

*G. Baron, M. Colzani, A. Criscuolo, YM. Lee, SI. Han, M. Carini, KJ. Yeum, G. Aldini.* **Quenching of cytotoxic reactive carbonyl species by black rice with giant embryo**. (RDPA - Perugia, June 28- July 1, 2015).

**Poster sessions**

*Baron G., Altomare A., Regazzoni L., Carini M., Aldini G.* **Development of a mass spectrometric method for the evaluation of the tannin protein precipitation effect** (RDPA – Rimini, September 20-23 2017)

*Baron, G.; Redaelli, V.; Regazzoni L; Carini M.; Vistoli G.; Riva A.; Morazzoni P. and Aldini, G.* **Development of a HPLC-MS/MS method for the simultaneous determination of 15 Vaccinium myrtillus anthocyanins and its application to a pharmacokinetic study in rats**. (XXIV National Meeting in Medicinal Chemistry – 10th Young Medicinal Chemists' Symposium)

**01/05/2017-31/10/2017** – *Université de Gèneve* – Collaboration Project: "***Evaluation and prediction of MS/MS spectra in the context of the Sigma Library***"